Department of
Industry and Resources

RECORD
2007/20

A GEOLOGICAL TRAVERSE ACROSS THE NORTHERN YILGARN CRATON — A FIELD GUIDE

compiled by S Wyche
with contributions from
S Wyche, CV Spaggiari, CJ Forbes, JA Bunting,
N Thébaud, D Hollingsworth, N Culpan, and J Vearncombe

Geological Survey of Western Australia

KALGOORLIE '07
Old Ground New Knowledge

Presented by

GEOCONFERENCES (WA) INC.

Thank you to Mercator for permission to view their mines:

MERCATOR GOLD PLC

GEOLOGICAL SURVEY OF WESTERN AUSTRALIA

Record 2007/20

A GEOLOGICAL TRAVERSE ACROSS THE NORTHERN YILGARN CRATON — A FIELD GUIDE

compiled by
S Wyche

with contributions from
S Wyche[1], CV Spaggiari[1], CJ Forbes[1], JA Bunting[2], N Thébaud[3], D Hollingsworth[3], N Culpan[3], and J Vearncombe[3]

[1] Geological Survey of Western Australia, 100 Plain Street, East Perth, WA 6004
[2] JA Bunting and Associates Pty Ltd, 9 Dee Road, Applecross, WA 6153
[3] Mercator Gold PLC and Mercator Gold Australia Pty Ltd, PO Box 1256, Canning Bridge, WA 6153, Australia

Perth 2007

MINISTER FOR ENERGY; RESOURCES; INDUSTRY AND ENTERPRISE
Hon. Francis Logan MLA

DIRECTOR GENERAL, DEPARTMENT OF INDUSTRY AND RESOURCES
Jim Limerick

EXECUTIVE DIRECTOR, GEOLOGICAL SURVEY OF WESTERN AUSTRALIA
Tim Griffin

REFERENCE
The recommended reference for this publication is:
Wyche, S (compiler), 2007, A geological traverse across the northern Yilgarn Craton — a field guide: Geological Survey of Western Australia, Record 2007/20, 68p.

National Library of Australia Card Number and ISBN 978-1-74168-128-4 (PDF)

Grid references in this publication refer to the Geocentric Datum of Australia 1994 (GDA94). Locations mentioned in the text are referenced using Australia Map Grid Australia (AMG) coordinates, Zones 50 and 51. All locations are quoted to at least the nearest 100 m.

Cover image modified from Landsat data, courtesy of ACRES

Published 2007 by Geological Survey of Western Australia
This Record is published in digital format (PDF) and is available online at www.doir.wa.gov.au/GSWA/publications.
Laser-printed copies can be ordered from the Information Centre for the cost of printing and binding.

Further details of geological publications and maps produced by the Geological Survey of Western Australia are available from:
Information Centre
Department of Industry and Resources
100 Plain Street
EAST PERTH, WESTERN AUSTRALIA 6004
Telephone: +61 8 9222 3459 Facsimile: +61 8 9222 3444
www.doir.wa.gov.au/GSWA/publications

Contents

Figures

Tables

A geological traverse across the northern Yilgarn Craton — a field guide

compiled by

S Wyche

with contributions from

S Wyche[1], CV Spaggiari[1], CJ Forbes[1], JA Bunting[2], N Thébaud[3], D Hollingsworth[3], N Culpan[3], and J Vearncombe[3]

Preface

This field guide describes a traverse through the Archean granite–greenstone geology of the northern part of the Yilgarn Craton (Fig. 1). Along the traverse, the geology of the Youanmi Terrane, which occupies the central-western part of the craton, is contrasted with that in the adjacent Kalgoorlie Terrane of the Eastern Goldfields Superterrane to the east, and the Narryer Terrane to the northwest. Descriptions of geology and geological localities are derived from recent 1:100 000-scale mapping by the Geological Survey of Western Australia (GSWA) in the central and western Yilgarn Craton, along with recently published data generated through AMIRA International Limited and pmd*CRC projects, with contributions from mineral-industry geologists.

1 Geological Survey of Western Australia
2 JA Bunting and Associates Pty Ltd
3 Mercator Gold PLC

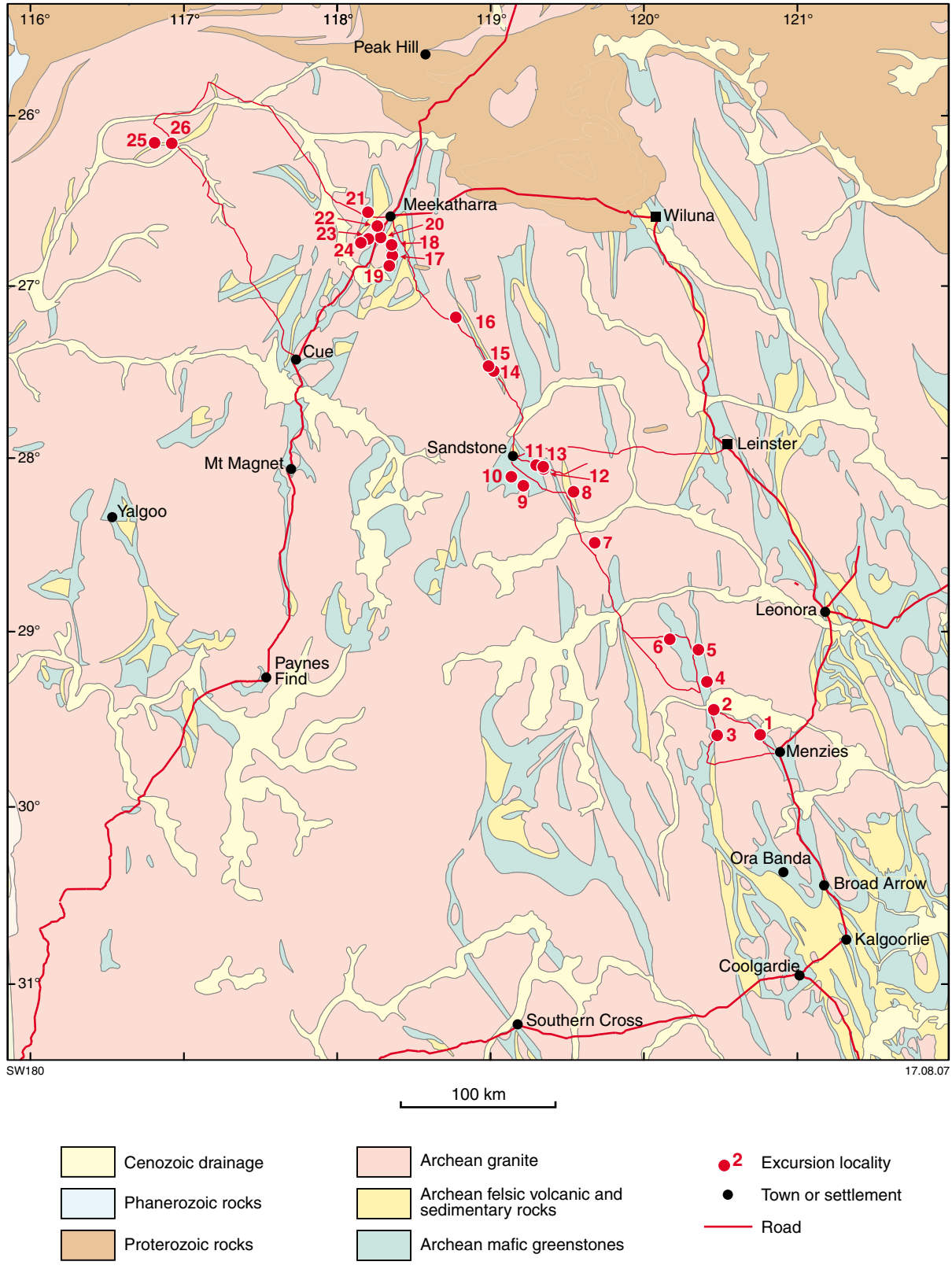

Figure 1. Simplified geology of the northern part of the Yilgarn Craton showing excursion localities

Part I: An overview of the geology along the Yilgarn traverse

Introduction

by S Wyche

The Yilgarn Craton (Fig. 2) is an Archean granite–greenstone terrain that hosts world-class deposits of gold and nickel, and significant deposits of many other commodities, including base metals, iron, uranium, rare-earth elements, tantalum, gemstones, and industrial minerals. It is bounded to the west by the Darling Fault system, to the north by the Capricorn Orogen, and to the south by the Albany–Fraser Orogen. The eastern boundary lies under the Officer Basin.

The Yilgarn Craton consists of metamorphosed felsic and mafic volcanic and instrusive rocks, metasedimentary rocks, and granites and granitic gneiss that formed principally between 3.05 and 2.62 Ga, with an older component earlier than 3.7 Ga in the northwest (e.g. Kinny et al., 1990; Pidgeon and Wilde, 1990; Nelson, 1997; Pidgeon and Hallberg, 2000; Cassidy et al., 2002; Barley et al., 2002, 2003). Granite intrusion occurred throughout the evolution of the Yilgarn Craton, but the nature and style of granite intrusion changed through time (Cassidy et al., 2002).

Gee et al. (1981) subdivided the Yilgarn Craton into four provinces: the Eastern Goldfields, Southern Cross, and Murchison Provinces and the Western Gneiss Terrain. However, the relationship between these provinces was enigmatic, with the boundaries not strictly based on observed geological features. Myers (1990a, 1995), Wilde et al. (1996), and Witt (1999) subdivided parts of the craton into superterranes and terranes based on greenstone ages and associations, and structural history. Swager et al. (1995) and Swager (1997) further subdivided the southeastern Yilgarn Craton into a series of terranes and domains.

According to the recently published scheme of Cassidy et al. (2006; Fig. 2), the Yilgarn Craton is subdivided into six terranes, the easternmost three of which constitute the Eastern Goldfields Superterrane. In the west, the Narryer Terrane and South West Terrane are dominated by granite and granitic gneiss, whereas the central Youanmi Terrane, and the Kalgoorlie Terrane, Kurnalpi Terrane, and Burtville Terrane of the Eastern Goldfields Superterrane, are composed of northerly trending greenstone belts separated by granite and granitic gneiss.

The Ida Fault (Fig. 2), which marks the boundary between the western Yilgarn Craton and the Eastern Goldfields Superterrane, has been shown by seismic profiling to be a major, east-dipping feature that extends to the base of the crust (Swager et al., 1997). Intruded in many places by late granite, in the north the fault appears to be truncated by a later, west-dipping structure, the Waroonga Fault system (Champion, 2004). Greenstone stratigraphic associations in the west Yilgarn differ from those in the Eastern Goldfields Superterrane in such respects as the relative abundance of komatiite and banded iron-formation, suggesting a substantially different depositional regime. Also, greenstones in the Youanmi Terrane are typically older than those in the Eastern Goldfields Superterrane. The major mafic-dominated successions in the west Yilgarn date back to 3.0 Ga (e.g. Pidgeon and Wilde, 1990; Geological Survey of Western Australia, 2007a), whereas the mafic and felsic successions of the Eastern Goldfields Superterrane were largely deposited after 2.8 Ga (e.g. Barley et al., 2003; Geological Survey of Western Australia, 2007a).

Geochronological constraints on deformation events suggest diachroneity of structural events across the Yilgarn Craton, but with the preserved structural grain reflecting a protracted period of east–west compression that coincided with peak metamorphism and the dominant period of granite intrusion (Binns et al., 1976). There is a distinct change in the type of granite magmatism at c. 2655 Ma, from voluminous, dominantly high-Ca granites to less voluminous, but widespread, low-Ca granites (Cassidy et al., 2002).

Eastern Goldfields Superterrane

by S Wyche

The Eastern Goldfields Superterrane (Cassidy et al., 2006) is a granite–greenstone terrain in the eastern part of the Yilgarn Craton. It is bounded to the west by the Youanmi Terrane, and separated from it by the Ida Fault (Swager, 1997). The northern boundary is marked by the Capricorn

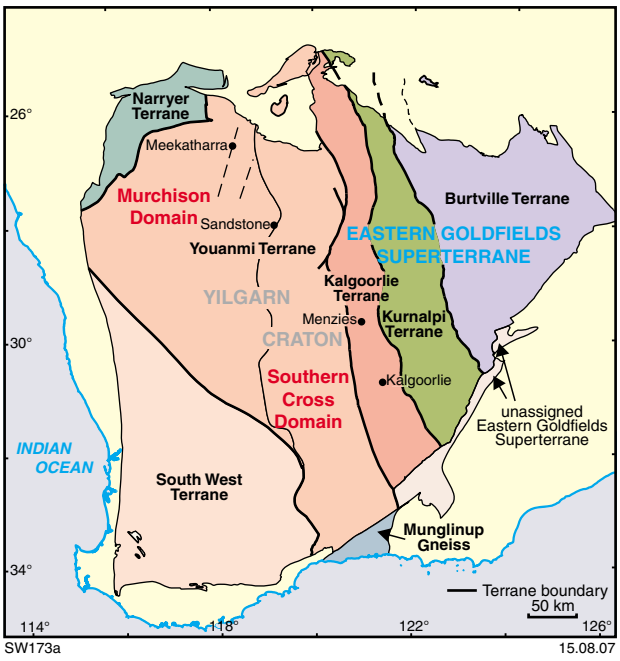

Figure 2. The Yilgarn Craton showing terrane subdivisions within the Eastern Goldfields Superterrane, and the domain subdivision of the Youanmi Terrane (modified from Cassidy et al., 2006)

Orogen, the southern boundary by the Albany–Fraser Orogen, and the eastern boundary lies under the Officer Basin. The Eastern Goldfields Superterrane is a highly mineralized region, with world-class gold and nickel deposits, and significant deposits of base metals, uranium, rare earth elements, and industrial minerals.

The Eastern Goldfields Superterrane contains at least three tectono-stratigraphic terranes — from southwest to northeast: the Kalgoorlie, Kurnalpi, and Burtville Terranes (Cassidy et al., 2006). These terranes are defined on the basis of distinct volcanic facies, geochemistry, and age of volcanism that ranges from older than 2810 to c. 2660 Ma. According to terrane accretion models, tectonic juxtaposition occurred after c. 2665 Ma (e.g. Barley et al., 2002, 2003). Each terrane is divided into structurally bounded domains that preserve dismembered parts of the succession that locally have distinct volcanic facies relationships (Swager et al., 1995, 1997; Barley et al., 2002). Widespread late-basin clastic sedimentary rocks that include conglomerates, sandstones, and mudstones (Krapež et al., 2000; Brown et al., 2001) were deposited after c. 2660 Ma.

The terranes and domains in the Eastern Goldfields Superterrane are bounded by interconnected systems of faults (e.g. Swager et al., 1995; Swager, 1997; Champion, 2004). From west to east, the terrane-bounding fault systems are the Ida, Ockerburry, and Hootanui Fault Systems (Fig. 2). Domain-bounding fault systems have been established within each terrane.

Numerous local studies and regional reviews of the deformation history in the Eastern Goldfields Superterrane suggest a broad consensus as to the sequence and timing of deformation events. Regional deformation studies in the Eastern Goldfields (e.g. Archibald et al., 1978; Swager et al., 1995; Swager, 1997; Weinberg et al., 2003) have long recognized four main phases of deformation — a poorly understood D_1 thrust stacking and recumbent folding event; east-northeast–west-southwest shortening that is characterized by upright folds (D_2) and regional-scale shear zones (D_3); and a D_4 regional shortening episode that produced conjugate brittle faults and fractures. The nature of the early (D_1) deformation has been interpreted variously as extensional (e.g. Passchier, 1994), compressional (e.g. Swager et al., 1995), or involving combinations of extension and compression (e.g. Williams and Currie, 1993). Post-D_1 and syn- to post-D_2 extensional events have also been proposed (e.g. Swager, 1997; Davis and Maidens, 2003). Undeformed granites that cut across major structures indicate that the major deformation had ceased by 2.63 Ga (Wyche, 2003). Peak metamorphism, locally at amphibolite facies, broadly coincided with widespread granite emplacement during D_2–D_3 (Binns et al., 1976; Mikucki and Roberts, 2004).

Stratigraphic associations have been documented in the terranes of the Eastern Goldfields Superterrane, but the only terrane for which a regional stratigraphy has been proposed is the Kalgoorlie Terrane (e.g. Swager et al., 1995). The stratigraphic associations of the Eastern Goldfields Superterrane have variously been ascribed to a mantle plume setting (e.g. Campbell and Hill, 1988; Bateman et al., 2001) and a convergent margin or arc–backarc environment (e.g. Barley et al., 1989; Krapež et al., 2000; Brown et al., 2001).

Kalgoorlie Terrane

The Kalgoorlie Terrane (Swager et al., 1995; Cassidy et al., 2006; Barley et al., 2002), the westernmost terrane of the Eastern Goldfields Superterrane, contains predominantly young (2.71 – 2.66 Ga) and minor old (>2.73 Ga) greenstones. It has been subdivided into a number of fault-bounded domains that have common stratigraphic elements. Older (>2.73 Ga) greenstone successions in the south (Norseman area), centre (near Leonora), and north are overlain by younger greenstones (Nelson, 1997; Barley et al., 2003). It is not known whether these older successions represent autochthonous basement to the younger greenstones. The eastern boundary is marked by a linked series of faults called the Ockerburry Fault System (Fig. 2; Champion, 2004).

Clearly defined lithostratigraphic sequences are restricted to domains in the southern part of the Kalgoorlie Terrane. Here, 2.71 – 2.66 Ga greenstone successions are divided into a 2.71 – 2.69 Ga tholeiitic and komatiitic mafic–ultramafic sequence and a 2.69 – 2.66 Ga felsic volcaniclastic sequence (Black Flag Group: Swager et al., 1995; Krapež et al., 2000; Barley et al., 2002, 2003). All greenstones are unconformably overlain by a post-2.66 Ga late-basin succession of clastic sedimentary rocks that are distributed across all terranes of the Eastern Goldfields Superterrane (Swager et al., 1995, Swager, 1997; Krapež et al., 2000; Barley et al., 2002).

The mafic–ultramafic sequence typically contains a lower basalt unit of komatiitic basalt and subordinate tholeiitic basalt that has local felsic volcanic and volcaniclastic intercalations (Swager et al., 1995). The lower basalt is overlain by an ultramafic unit dominated by komatiite, and an upper basalt unit, also with komatiitic basalt and subordinate tholeiitic basalt. Hill et al. (1995, 2001) consider the ultramafic unit of the Kalgoorlie Terrane succession to be a regionally extensive komatiite. The age of the mafic–ultramafic succession is constrained by sensitive high-resolution ion microprobe (SHRIMP) U–Pb zircon ages of c. 2708 Ma from volcanic rocks associated with komatiite near the Ballarat – Last Chance mine at Kanowna (Nelson, 1997) and at the Black Swan nickel mine (Barley et al., 2002), and an age of c. 2692 Ma on detrital zircons from the Kapai Slate, a clastic sedimentary formation within the upper basalt unit at Kambalda (Claoué-Long et al., 1988).

The felsic volcaniclastic sequence comprises felsic volcaniclastic and epiclastic rocks of trondhjemite–tonalite–granodiorite (TTG) type, with subordinate lavas, including tholeiitic basalt, that were deposited between 2.69 and 2.66 Ga (Krapež et al., 2000; Brown et al., 2001; Barley et al., 2002). According to Krapež et al. (2000) and Barley et al. (2003), several depositional and magmatic sequences within this succession can be grouped into unconformity-bounded lithostratigraphic packages that record deposition in a series of transtensional, deep-marine intra-arc basins.

Youanmi Terrane

by S Wyche

New regional mapping, SHRIMP geochronology, and new granite geochemistry and isotope data (Cassidy et al., 2002), suggest that in the central and western Yilgarn Craton, the Southern Cross and Murchison 'Provinces' of Gee et al. (1981), or 'Granite–Greenstone Terranes' of Tyler and Hocking (2001), do not represent allocthonous terranes that have come together during an accretionary event. Rather, they more likely formed part of the 3.0 – 2.7 Ga proto-Yilgarn Craton to which the elements of the Eastern Goldfields Superterrane accreted after c. 2665 Ma. As they are no longer considered to be terranes in the strict sense, they are now called domains within the Youanmi Terrane (Fig. 2; Cassidy et al., 2006). However, even within domains, some parts of the Youanmi Terrane clearly have ages and tectonic histories different from others. For example, the Ravensthorpe greenstone belt (Witt, 1999) contains 2.95 Ga calc-alkaline volcanics that host Cu–Zn–Au mineralization in an association that may have more in common with parts of the Murchison Domain than with other greenstone belts in the Southern Cross Domain. Thus there may be cryptic terranes within the Youanmi Terrane whose histories will be resolved only by more detailed mapping and the acquisition of new geochemical and geochronological data.

The Youanmi Terrane is bounded to the west by the Darling Fault system, to the north by the Capricorn Orogen, to the southeast by the Albany–Fraser Orogen, and to the southwest by the South West Terrane. The boundary with the Eastern Goldfields Superterrane is marked the Ida and Waroonga Faults. The boundary with the Narryer Terrane is taken to be the Yalgar Fault (Myers, 1993). The nature of this fault and the relationship between greenstones of the Narryer and Youanmi Terranes will be investigated during the current mapping program. The boundary with the South West Terrane is poorly defined, and will be investigated in future mapping programs.

The Youanmi Terrane is isotopically distinct from other terranes. A pre-3.0 Ga age for the initial formation of the Youanmi Terrane is based on Sm–Nd and Hf depleted-mantle model ages for granites and felsic volcanic rocks that indicate a 3.3 – 3.0 Ga felsic crustal component (Cassidy et al., 2002; Griffin et al., 2004). Detrital and xenocrystic zircon ages suggest 4.3 – 3.1 Ga sources for some rocks in the Murchison and Southern Cross Domains. They also suggest that greenstones of the Narryer Terrane that also contain pre-4.0 Ga detrital zircons may have had a common history with some of those in the Youanmi Terrane (Wyche et al., 2004; Wyche, in prep.).

The Murchison and Southern Cross Domains have comparable structural histories with early shallow to recumbent structures overprinted by upright folds, all overprinted by northwest to northeasterly trending shear zones (e.g. Watkins and Hickman, 1990; Spaggiari, 2006; Dalstra et al., 1999; Chen et al., 2004). Major shear zones and folds are readily visible on aeromagnetic images (Fig. 3). However, east–west folding that appears to have taken place early during the upright folding phase in the Murchison Domain has not been recognized in the Southern Cross Domain. It is also likely that the Murchison Domain shows evidence of Proterozoic deformation that is not so apparent in the Southern Cross Domain (Spaggiari, 2006, 2007a). Major movement on the regional-scale shear zones that have previously been suggested as granite–greenstone terrane boundaries post-dates all greenstone deposition and most granite intrusion. Chen et al. (2001, 2004) interpreted the regional-scale shear zones as having been produced by the impingement of large bodies of cooling granite into the greenstone belts during an extended period of east–west shortening.

Southern Cross Domain

The Southern Cross Domain contains at least two greenstone successions. The age of the older succession is poorly constrained but is probably greater than 2900 Ma. The older succession typically contains abundant banded iron-formation and chert, interbedded with mafic and subordinate ultramafic rocks, overlain by a mafic-dominated succession (Chen et al., 2003). Without more detailed geochronology, it is difficult to demonstrate correlations of individual units between greenstone belts and, in some instances, within greenstone belts. In the centre and north, greenstone belts along the eastern and western sides of the domain commonly preserve a quartzite or quartz-rich metasedimentary unit, with maximum depositional ages greater than 3.1 Ga, at the base of the exposed succession that is in either faulted or intrusive contact with much younger granite (Wyche et al., 2004). In the far south, the Ravensthorpe greenstone belt contains 2.95 Ga calc-alkaline volcanic rocks that host Cu–Zn–Au mineralization (Witt, 1998, 1999) in an association that has more in common with the succession in the Golden Grove region in the Murchison Domain than with other greenstone belts in the Southern Cross Domain.

The younger succession in the Southern Cross Domain is best known in the Marda–Diemals greenstone belt where it consists of the 2.73 Ga calc-alkaline Marda Complex and clastic sedimentary Diemals Formation (Hallberg et al., 1976; Chen et al., 2003). However, other greenstone belts also contain felsic volcanic rocks (Wang et al., 1998a). For example, 2.72 Ga dacite in the Gum Creek greenstone belt (Bodorkos et al., 2006) appears to be part of a widespread but very poorly exposed younger greenstone succession that also contains clastic sedimentary rocks, including abundant graphitic shale.

Murchison Domain

Greenstones in the Murchison Domain contain a similar mix but a broader range of rock types than that in the Southern Cross Domain. Previously established stratigraphic schemes (e.g. Watkins and Hickman, 1990) have a lower greenstone succession similar in character to that in the Southern Cross Domain with a complex upper greenstone succession. However, new precise SHRIMP geochronology has demonstrated that simple stratigraphic correlations are difficult across such a broad area (e.g. Pidgeon and Hallberg, 2000). Conventional U–Pb zircon geochronology indicates extensive 3.0 Ga felsic volcanism

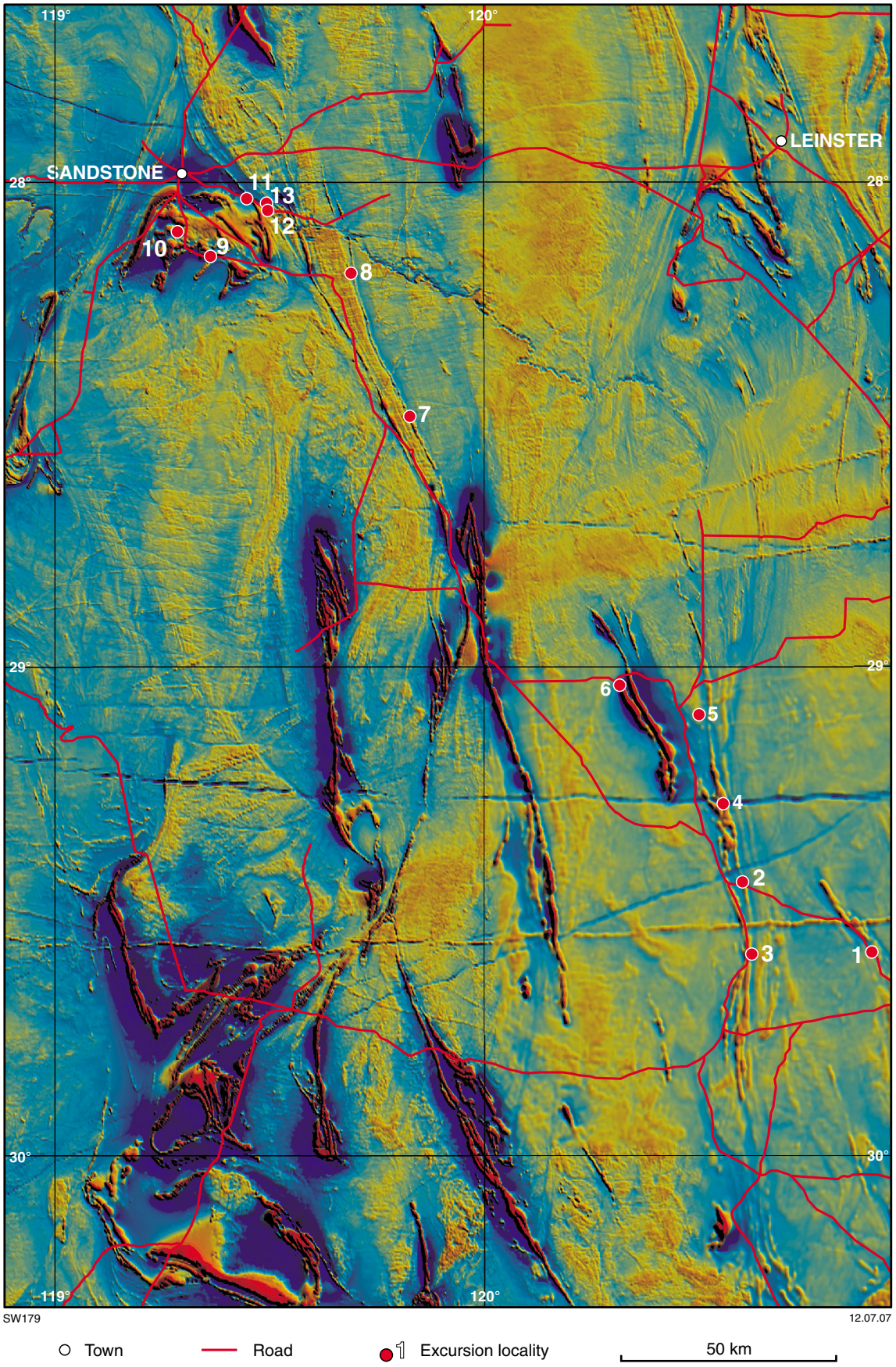

Figure 3. **Aeromagnetic image (TMI, reduced to pole) of the central Yilgarn Craton showing excursion localities in relation to the greenstone belts. Major faults and shear zones form regional-scale linear features**

in the Murchison Domain (Pidgeon and Wilde, 1990), with SHRIMP U–Pb zircon ages of 2.95 Ga obtained on felsic rocks at Golden Grove (Wang et al., 1998b) and in the Weld Range (Wingate and Bodorkos, 2007a). However, 2.8 Ga volcanic rocks have been identified at Golden Grove (Wang et al., 1998a), in the Mount Magnet area (Schiøtte and Campbell, 1996), near Windimurra (Nelson, 2001), and Youanmi (Nelson, 2002a), and in the Pollele Syncline near Meekatharra (Wingate and Bodorkos, 2007b). In the syncline, the 2.8 Ga age was obtained on a volcaniclastic sedimentary rock at the base of a series of komatiite flows (see Locality 17), clearly demonstrating the presence of some komatiite volcanism of this age. Widespread felsic rocks (andesite–rhyolite) range in age from 2.76 to 2.69 Ga (Schiøtte and Campbell, 1996; Pidgeon and Hallberg, 2000; Wingate and Bodorkos, 2007c). Clastic sedimentary rocks, including graphitic shales like those found locally in the Southern Cross Domain, are locally associated with the younger felsic volcanic rocks.

Layered mafic–ultramafic intrusions

Layered mafic–ultramafic intrusions in the central part of the Youanmi Terrane include the Windimurra (Ahmat and Ruddock, 1990; Mathison et al., 1991), Narndee (Ahmat and Ruddock, 1990), Barrambie (Ward, 1975; see Locality 14), Atley, and Youanmi intrusions that contain successions of cumulate mafic and ultramafic rocks. The age of these intrusions is poorly constrained but Sm–Nd isotope data from the Windimurra Complex suggest an age of 2.8 Ga (Ahmat and Ruddock, 1990). They may represent a mantle plume event to which the 2.8 Ga magmatism in the Murchison Domain is related. The layered intrusions contain significant deposits of vanadiferous magnetite (e.g. Windimurra, Barrambie) and have potential for nickel, copper, and PGEs.

Narryer Terrane

by CV Spaggiari

The Narryer Terrane is one of Earth's oldest crustal fragments and contains the oldest known rocks in Western Australia. The terrane is situated in the northwestern part of the Yilgarn Craton and comprises granitic rocks and granitic gneisses ranging in age from early through to late Archean (Kinny et al., 1988; Nutman et al., 1991; Pidgeon and Wilde, 1998). These are interlayered with minor occurrences of deformed and metamorphosed banded iron-formation, mafic and ultramafic intrusive rocks, and metasedimentary rocks (Williams and Myers, 1987; Myers, 1988a; Kinny et al., 1990). Only one greenstone belt — the Jack Hills greenstone belt — occurs within the terrane, along its southern margin. It comprises sequences of greenschist to amphibolite facies banded iron-formation, mafic and ultramafic rocks, and both Archean and Paleoproterozoic metasedimentary rocks (Spaggiari, 2007a). Amphibolite to granulite facies metasedimentary rocks at Mount Narryer, as in the Jack Hills greenstone belt, contain detrital zircons that are older than 4.0 Ga (Williams and Myers, 1987; Compston and Pidgeon, 1986; Wilde et al., 2001).

The oldest components of the Narryer Terrane are a dismembered layered igneous complex (anorthosite–gabbro–ultramafic intrusion) known as the Manfred Complex and felsic intrusive rocks of the Meeberrie Gneiss (Myers and Williams, 1985; Myers, 1988b). Leucogabbro and meta-anorthosite inclusions within syenogranitic gneiss (Dugel gneiss) that are part of the Manfred Complex have a magmatic SHRIMP U–Pb zircon age of 3730 ± 6 Ma (Kinny et al., 1988). Rocks of the Meeberrie Gneiss are generally migmatitic and the oldest component has a similar, maximum, SHRIMP U–Pb zircon age of 3730 ± 10 Ma (Kinny and Nutman, 1996). Both the Meeberrie Gneiss and the Manfred Complex were intruded by various felsic magmas (Dugel and Eurada gneisses) until a major magmatic event at 3.30 Ga, accompanied by deformation and amphibolite to granulite facies metamorphism (Kinny et al., 1988; Myers, 1988a; Nutman et al., 1991, 1993; Pidgeon and Wilde, 1998). Further felsic magmatism is believed to have occurred at 3.10 Ga (Nutman et al., 1991). These events occurred prior to the deposition of the supracrustal sequences predominantly exposed in the Jack Hills greenstone belt and the Mount Narryer region (Compston and Pidgeon, 1986; Maas and McCulloch, 1991).

The southern margin and boundary to the Youanmi Terrane is defined by the Balbalinga and Yalgar Faults; the latter is interpreted as a major dextral strike-slip fault (Myers, 1990b, 1993). The structural history of this fault is poorly understood, and the boundary is likely to be reworked and cryptic (Nutman et al., 1993). The early Archean gneisses of the Narryer Terrane have been interpreted as an allochthon that was thrust over approximately 3000 to 2920 Ma granitic crust of the Youanmi Terrane, prior to or during late Archean granitic magmatism that stitches the terranes (Nutman et al., 1993). Although there is evidence of deformation prior to the intrusion of these granites, the deformation that produced the main tectonic grain is believed to have occurred at amphibolite facies between c. 2750 and 2620 Ma, and affected both terranes (Myers, 1990b).

The Paleoproterozoic Capricorn Orogeny produced intracratonic, predominantly greenschist facies, and dextral transpressional reworking of both the northern and southern margins of the Narryer Terrane. These effects are evident in the Errabiddy Shear Zone (e.g. Occhipinti et al., 2004), the Jack Hills greenstone belt (Spaggiari, 2007a,b), and the Yarlarweelor Gneiss Complex in the northeastern part of the Narryer Terrane (e.g. Occhipinti et al., 2004).

Yilgarn granites

by S Wyche

Champion and Sheraton (1997) divided Archean granites and granitic gneisses of the Eastern Goldfields Superterrane into 'two major groups (high-Ca and low-Ca), and three minor groups (high-HFSE (high field strength elements), mafic, and syenitic). The high-Ca group (68–77% SiO_2) with high Al_2O_3, Na_2O and Sr, and low Y, shares many features with typical Archean tonalite–trondhjemite suites, but has higher K_2O, Rb, and Th contents. The low-Ca group (70–76% SiO_2) differs

from the high-Ca group in having lower Al_2O_3, CaO, and Na_2O, but higher K_2O, Rb, Th, Zr, Y, La and Ce contents. Granites of the high-HFSE, mafic and syenitic groups form a minor component (10–20%) of the Eastern Goldfields granites. The siliceous (74–77% SiO_2) high-HFSE granites . . . are characterized by high TiO_2, total FeO, MgO, Y, Zr and Ce, but only moderate Rb, Th and Pb contents. The A-type syenites (50–68% SiO_2) are distinguished by their high total alkalies and mainly occur along tectonic lineaments. The mafic group (55–70% SiO_2) is lithologically diverse and exhibits a wide range of K_2O, Rb, Th, La and Ce contents.'

Cassidy et al. (2002) extended the granite subdivisions of Champion and Sheraton (1997) to the west across the northern part of the Youanmi Terrane and collected a large body of geochronological data that indicate that peak granite magmatism took place at different times in the Yilgarn Craton. In the Murchison and Southern Cross Domains of the Youanmi Terrane, several peaks of magmatism are evident between c. 3010 and c. 2630 Ma. However, the c. 2800 Ma peaks appear to be less well represented in the Southern Cross Domain than in the Murchison Domain. These peaks are broadly coincident with periods of felsic volcanism. The majority of Eastern Goldfields Superterrane granites are younger than c. 2720 Ma. Both the Youanmi Terrane and the Eastern Goldfields Superterrane show a marked change from dominantly high-Ca to dominantly low-Ca magmatism at 2655–2650 Ma. Inherited zircon ages in the Youanmi Terrane and Eastern Goldfields Superterrane mainly follow known ages for older granites and greenstones.

Economic geology

by S Wyche

The Yilgarn Craton is a major mineral-producing province with substantial endowments of gold, silver, iron, nickel, copper, lead, zinc, vanadium, uranium, and rare earth elements. The distribution of various commodities across the craton is uneven. Although the genesis of many of the deposit types is not completely understood, there are clear controls on the style and distribution of mineralization based on structural and tectonic setting. Individual mineral deposits to be visited during the course of the excursion will be discussed in the relevant locality description.

Gold

The structural and metamorphic settings, host rocks, alteration, and relative timing of mineralization in gold deposits of the Eastern Goldfields Superterrane have been widely documented (e.g. Hagemann et al., 2001; Blewett et al., in prep.). Gold deposits in the western Yilgarn are less well documented with only a few deposits in the Southern Cross Domain (e.g. Bloem et al., 1994; Beeson et al., 1993) and the Murchison Domain (e.g. Mueller et al. 1996; Yeats et al., 1996; Locality 20) having been described in any detail. Watkins and Hickman (1990) described the major characteristics of many gold deposits in the Murchison Domain.

The deposits in the western Yilgarn Craton have much in common with those in the Eastern Goldfields Superterrane in that they are epigenetic, broadly contemporaneous (post-2.67 Ga), have strong structural controls on their distribution, and are hosted by a wide range of rock types. However, there is a marked decrease in the volume of gold production, and the number of historical gold workings, from east to west across the Ida Fault. This suggests a major change in the source of gold mineralization, or some significant structural control, but the reason for this change has not been closely examined.

Nickel

For a general discussion of the nickel deposits of the Yilgarn Craton, see Marston (1984) and Barnes (2006). For discussion of komatiites and nickel mineralization along the traverse, see Localities 4 and 9.

VHMS deposits

Although a number of VHMS-style deposits have been identified in the Yilgarn Craton (Marston, 1979), only the 2.7 Ga deposits at Jaguar and Teutonic Bore (Hallberg and Thompson, 1985; Ellis, 2006), and the 2.95 Ga deposits at Golden Grove (Sharpe and Gemmell, 2002), have any significant production history.

Iron

A number of significant iron deposits have been identified in the Yilgarn Craton (Cooper and Flint, 2007). In the north Yilgarn, the only mine that is currently in production is the Jack Hills deposit of Murchison Metals Ltd, where ore is mined and carried by truck to the port at Geraldton. The company has plans to develop a railway for larger scale shipping. Probable Ore Reserves at the Jack Hills Project are estimated at 8.5 million tonnes at an average grade of 63% Fe. Current resources are estimated at 67 million tonnes at 62% Fe (Murchison Metals Ltd, 2007). The other significant deposit in the region is that at Weld Range, where Midwest Corporation Ltd are exploring a number of goethite–hematite orebodies, at least one of which contains a resource of 132.1 million tonnes at 55.6% Fe (Midwest Corporation Ltd, 2007).

Part II: Excursion localities

All locality descriptions by S Wyche unless otherwise indicated

Locality 1: Kalgoorlie Terrane stratigraphy at Ghost Rocks

adapted from Swager (1990)

Drive 17 km along the Menzies–Sandstone Road from the Goldfields Highway at Menzies to a track intersection on the north side of the road at MGA 297715E 6724958N. The traverse begins 0.5 km to the northeast along the track.*

A short southwest to northeast traverse, along and beside the track across the southwestern limb of a syncline (Fig. 4), crosses the following units:

1. From the main road, there are small outcrops of basaltic schist (Missouri Basalt of Swager et al., 1995). Along the track, this passes into metagabbro and cumulate-textured metapyroxenite.

2. A narrow layer of olivine cumulate (MGA 298330E 6724968N) which is serpentinized and silicified (at a prominent mesa to the northwest). This is the Walter Williams Formation of Gole and Hill (1990) and Hill et al. (1995) — see Locality 4. A strongly cleaved grey shale/slate unit within the ultramafic unit (MGA 298532E 6724977N) was probably an interflow sediment.

3. Across a small gulley there is common outcrop and float of coarsely spinifex-textured komatiite (MGA 298399E 6724948N). Although foliated in places, the platy olivine-spinifex texture is well preserved. This is the Siberia Komatiite of Swager et al. (1995). Two shallow pits in the komatiite on top of the rise (MGA 298469E 6724949N; 298456E 6724937N) have exposed small patches of copper mineralization.

4. Metagabbro above the komatiite (MGA 298503E 6724944N).

5. Above the contact with the overlying metabasalt (MGA 298609E 6724962N), strongly cleaved metabasalt becomes more massive and locally very coarsely feldspar-phyric (MGA 298670E 6724962N).

Locality 2: Pillow basalts at Snake Hill (Lake Ballard)

Return to the Menzies–Sandstone Road and travel northwest for 34.3 km to the turnoff (MGA 267793E 6738854N) to the Inside Australia sculpture installation on Lake Ballard. Continue into the designated parking area, and walk across the lake surface to Snake Hill.

* All Localities from 1 to 6 are in MGA Zone 51. All subsequent localities are in MGA Zone 50.

The 'Inside Australia' installation by British sculptor Antony Gormley (www.antonygormley.com), best known for his 'Angel of the North' sculpture near Newcastle in the UK, was commissioned for the 2003 Perth International Arts Festival. The figures are based on body scans of the residents of Menzies.

Pillow-lava structures in a weakly to strongly deformed, steeply east-dipping unit of komatiitic basalt on Snake Hill indicate east younging (Fig. 5). This outcrop lies within a broad zone of deformation associated with the Ida Fault. Because of the intense deformation in this area due to movement on the Ida Fault, it is not possible to place this unit into a stratigraphic context but it clearly belongs to the Kalgoorlie Terrane stratigraphic succession. The best outcrops of pillow structures are found on the eastern side of the hill, about two-thirds of the way up (MGA 267771E 6740248N). They can be reached by a footpath that begins at the base of the hill on the south side.

Locality 3: Gneiss and granite (Ida Fault) at 18 Mile Well

From the Lake Ballard turnoff, drive 2.5 km northwest to the turnoff (MGA 265311E 6739124N) to Riverina Homestead. The 18 Mile Well locality is about 16 km south (MGA 269915E 6724075N), on the eastern side of the road.

This locality is representative of gneiss and foliated granite that extends for more than 100 km along the eastern side of the East Ida greenstone belt. The East Ida greenstone belt represents all of the greenstones in this belt that are considered to lie east of the Ida Fault, and thus to lie within the Kalgoorlie Terrane. Greenstones in the West Ida greenstone belt are considered to be part of the Youanmi Terrane (Geological Survey of Western Australia, 2007b).

The gneiss and foliated granite on the eastern side of the Ida Fault grade into gneissic granite with decreasing strain to the east, away from the granite–greenstone contact and major fault zones. The best exposures of granitic gneiss and gneissic granite outcrop within about 5 km of the granite–greenstone contact, particularly in the northern part of the greenstone belt. The eastern and southern extents of these deformed rocks are evident on aeromagnetic images (Fig. 3), which also suggest that they have undergone complex polyphase folding.

The granitic gneiss (Williams et al., 1993; Wyche, 1999; Wyche, 2003) is a fine- to coarse-grained, quartz–feldspar–biotite rock characterized by compositional banding defined by variations in grainsize and relative abundance of biotite. The gneiss is mainly granodioritic or monzogranitic in composition, and rocks are typically fine grained due to cataclastic grainsize reduction of the protolith. The rocks typically contain various proportions of quartz, K-feldspar, plagioclase, and biotite. Accessory minerals may include opaque oxides, zircon, apatite,

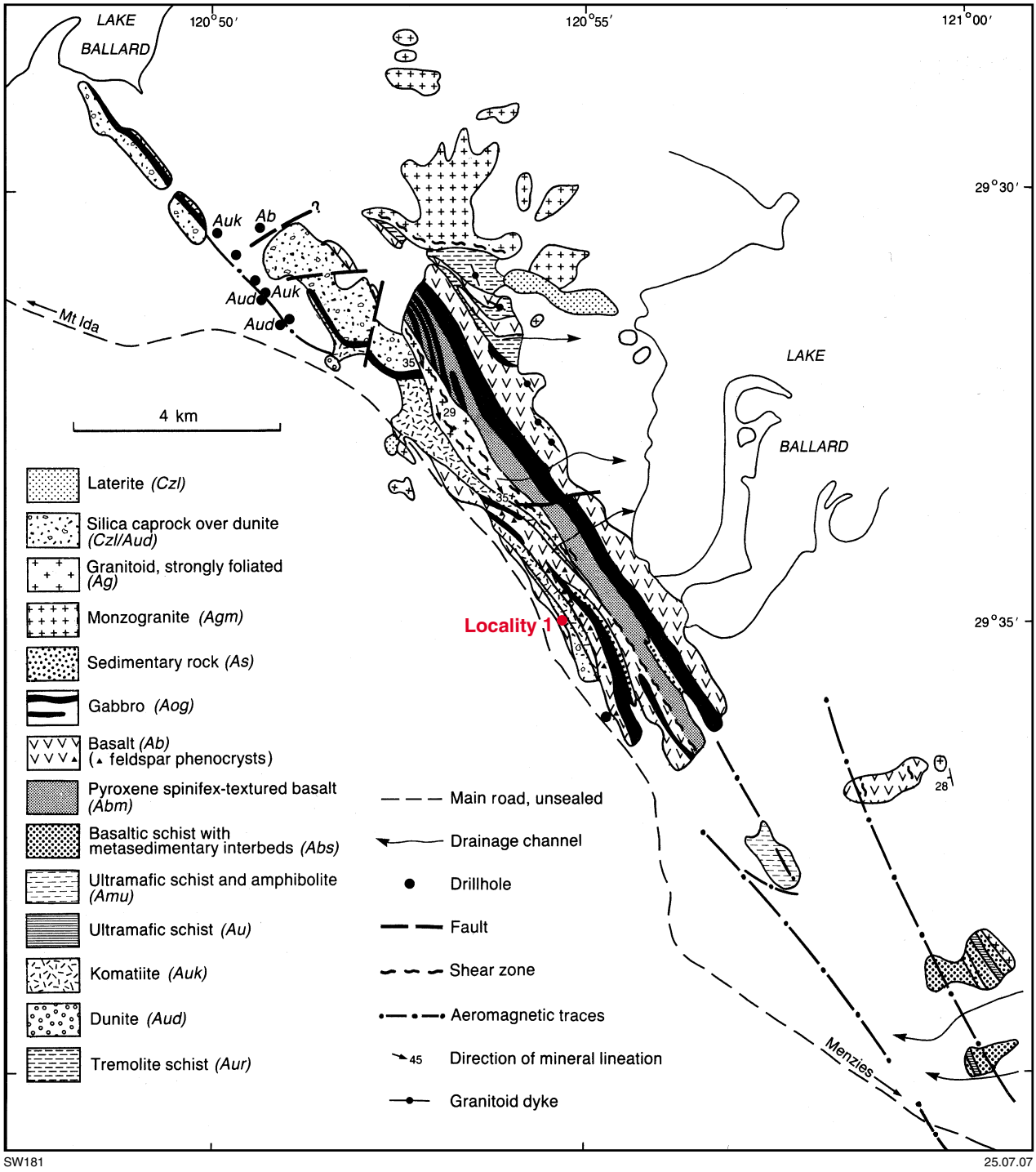

Figure 4. Interpreted geology of the Ghost Rocks area (modified from Swager, 1994)

garnet, and titanite. Secondary minerals may include sericite, muscovite, epidote, titanite, and chlorite. The gneiss contains concordant slivers of amphibolite and mafic schist up to 2 m thick. Banding is on a scale of millimetres to tens of centimetres, and there is a common shallow-plunging mineral lineation. Some bands contain feldspar porphyroclasts up to 5 cm across, but pressure shadows around these grains do not give clear shear sense (Fig. 6). Some of the numerous quartz and pegmatite veins that cut the gneiss at various angles are tightly folded. The lack of any clear shear sense suggests a very strong compressional component to the last stages of deformation. These rocks may be comparable in age to similar gneiss at the northern end of the East Ida greenstone belt that has U–Pb SHRIMP ages of c. 2676 and c. 2678 Ma (Cassidy et al., 2002).

Fresh outcrop that gives a three-dimensional view of the rock can be seen at a blast site about 160 m east of the road (MGA 270176E 6723993N).

SW184 08.08.07

Figure 5. Pillow structures in metabasalt on Snake Hill (MGA 267771E 6740248N)

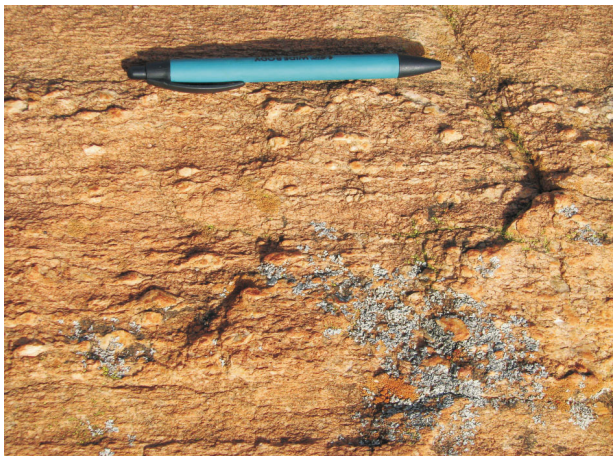

SW185 08.08.07

Figure 6. Porphyroclasts in the gneiss at 18 Mile Well do not provide unequivocal evidence of shear sense

Locality 4: The Walter Williams Formation in the Kurrajong Anticline (East Ida greenstone belt)

Return to the Menzies–Sandstone Road and drive 13 km northwest to the turnoff to Mount Ida and Leonora (MGA 259232E 6750139N). Proceed north along the Mount Ida Road for about 9 km (MGA 257499E 6758895N), and turn northeast onto a track. After about 400 m, cross a creek and head southeast for about 700 m to a track junction with an east–west track (MGA 258385E 6758813N). Follow this track about 1 km east to a junction (MGA 259529E 6758978N) and take the right fork onto a fenceline. Follow this track for about 3.5 km to an intersection (MGA 262475E 6757985N), go to the left and proceed to a low hill on the south side of the track to begin the traverse (MGA 262907E 6758027N).

The Walter Williams Formation

modified from Hill et al. (2001)

The supracrustal rocks that extend from Siberia to Menzies, and farther north through to Kurrajong, are broadly correlative with rocks of the Kalgoorlie–Kambalda region. There is one striking feature of the komatiitic rocks — a laterally extensive unit of coarse-grained olivine adcumulate. This is the most extensive body of olivine adcumulate known in the Yilgarn Craton. It forms part of the Walter Williams Formation, which can be traced continuously from southwest of Siberia to the shores of Lake Ballard northwest of Menzies, and to the Kurrajong Anticline in the East Ida greenstone belt (Fig. 7).

The Walter Williams Formation is a layered body, traceable over an area of about 35 × 130 km, consisting of a lower zone of olivine cumulates and an upper zone of gabbroic rocks (Gole and Hill, 1990; Hill et al., 1995). The proportion of olivine cumulates to gabbro varies along strike as does the igneous porosity within the lower olivine-cumulate zone.

The formation is interpreted as part of a very large komatiite flow field. The southern part formed as a vast sheet lobe, resulting in the development of an extensive thick pile of olivine cumulates. In the north, the flow underwent ponding, fractionation in situ, and repeated influxes of new batches of lava (Gole and Hill, 1989, 1990).

Stratigraphic profiles through the Walter Williams Formation (Fig. 8) show the gross layering and lateral lithological variations. South of Ghost Rocks, the lower ultramafic zone of the Walter Williams Formation is dominated by a thick olivine-adcumulate layer, which grades laterally to olivine mesocumulates and orthocumulates to the north between Ghost Rocks and Lake Ballard, and at Kurrajong. North from Yunndaga, the upper zone of the Walter Williams Formation is a layered gabbro, which thickens from approximately 30–40 m at Yunndaga to 100 m at Ghost Rocks and 180 m at Kurrajong.

Estimates of the true thickness of the unit are greatly hampered by the lack of dip information, and the relative thicknesses shown in Figure 8 are conjectural. At Vetters Hill the estimated thickness is about 200 m, just south of Menzies it is only 50 m, and at Ghost Rocks it is again 100–200 m. The unit certainly appears to thin from an area about 10 km south of Menzies northward to Lake Ballard, although this may in part be due to deformation, as some of the rocks in this area are highly strained. In this excursion, only the northern segment between Menzies and the Kurrajong area will be visited.

The best exposure of the Walter Williams Formation in the north is in the fault-bounded Kurrajong Anticline, in the East Ida greenstone belt about 35 km northwest of Ghost Rocks (Figs 7, 9).

The stratigraphy of the Kurrajong Anticline comprises, from bottom to top: pillowed tholeiitic basalt, a thin black shale, the Walter Williams Formation, a sedimentary horizon, a thin basalt, spinifex-textured komatiite flows,

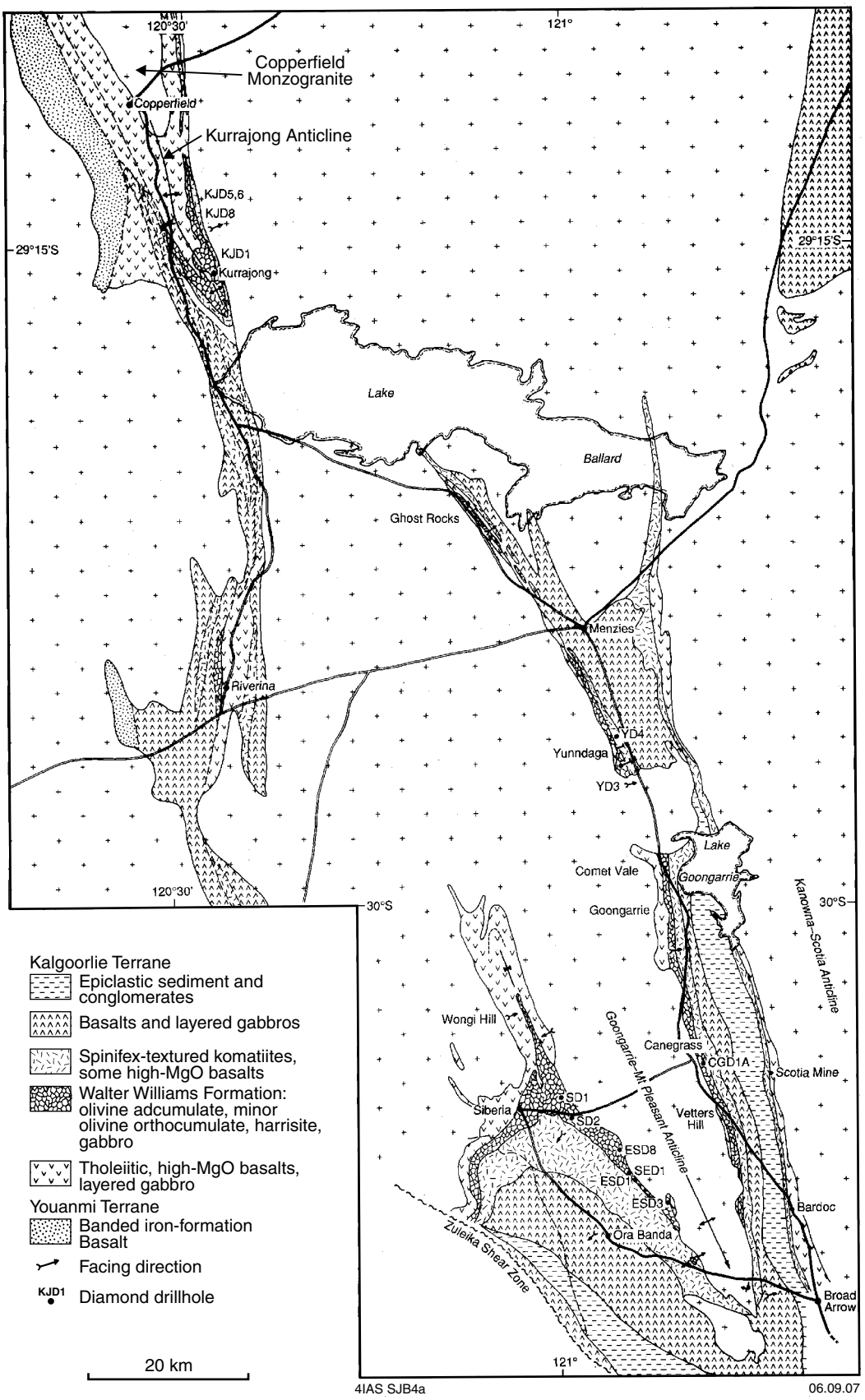

Figure 7. Geological map of the Walter Williams Formation, showing the distribution of the olivine adcumulate unit. Data from CSIRO mapping, incorporating data from GSWA mapping by Swager et al. (1995), and mapping by J Hallberg, N Harrison, and N Herriman (modified from Hill et al., 2001)

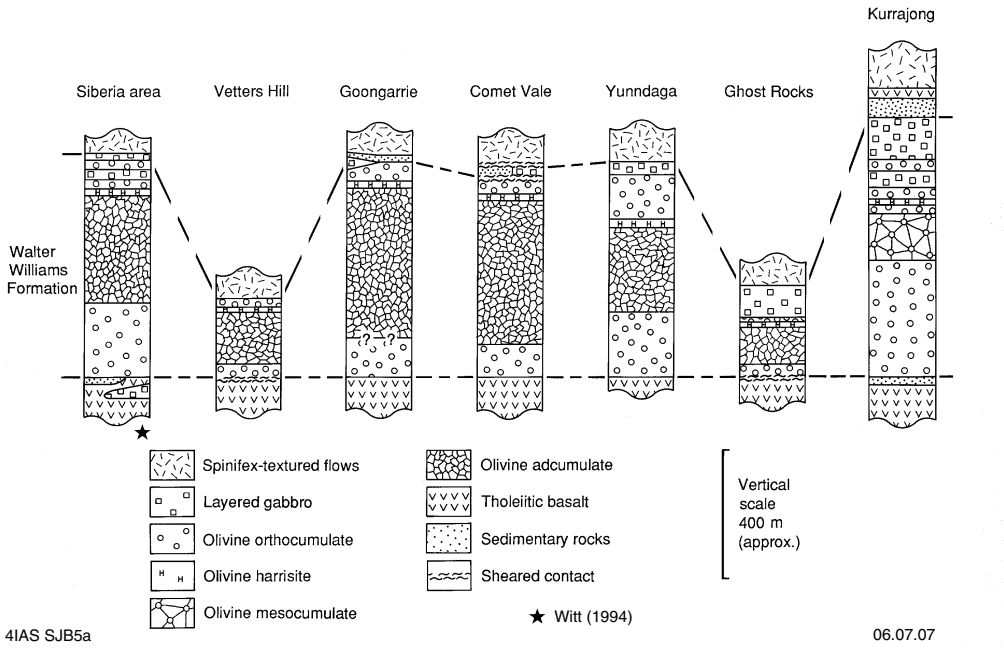

Figure 8. Stratigraphic profiles through the Walter Williams Formation. See Figure 7 for locations (modified from Hill et al., 2001)

and an upper gabbroic unit. The sedimentary rocks overlying the Walter Williams Formation consist of medium- to fine-grained arkosic to sandy units with minor chert. The sequence is most complete and best exposed near the exploration drillhole KJD1 (Fig. 9).

The northern part of the anticline is completely buried by loose pisolitic laterite, whereas in the south the laterite has mostly been stripped, except over the more olivine-rich ultramafic lithologies where siliceous capping is still present. The siliceous capping preserves the igneous textures of the underlying rocks. The area was explored by CRA for nickel in the late 1960s and early 1970s and nickel sulfides were discovered in the northern part of the east limb of the anticline around KJD5 and KJD6 (Fig. 7). CRA drilled a total of 12 diamond drillholes within the anticline. One of these, KJD1 (Fig. 9), was drilled in an area where the gabbro member, as well as the upper part of the ultramafic succession, is very well exposed. Data from this drillhole and from two nearby surface traverses are plotted in Figure 10.

The stratigraphy is similar to that between Ghost Rocks and Siberia (Fig. 7), although the thickness of the spinifex flow unit, equivalent to the Siberia Komatiitic Volcanics, is much reduced within the Kurrajong Anticline. The Walter Williams Formation is about 800 m thick in the KJD1 area on the eastern limb of the fold, but thins along the western limb. Although part of the change in apparent thickness may be due to a change in dip and attenuation, the preservation of delicate igneous textures in rocks along the western limb suggests that the reduction in thickness is partly an original feature. The ultramafic zone of the Walter Williams Formation consists mostly of olivine orthocumulate with olivine mesocumulate in the central part. In the central part there are at least four thin Mg-augite–olivine adcumulate layers, which are 0.5–3 m thick and consist of Mg-augite (or an altered assemblage) and altered olivine in a polygonal aggregate.

Traverse 1: Walter Williams Formation near exploration drillhole KJD1

modified from Hill et al. (2001)

Start traverse in the ultramafic zone (MGA 262907E 6758027N).

In the upper section of the ultramafic zone in the KJD 1 area (Fig. 9) a 5 mm-thick chromite layer (MGA 262936E 6758016N) is developed within an olivine–Mg-augite–chromite orthocumulate with about 30 modal percent chromite. Chromite shows a characteristic ‘chicken wire’ texture around original olivines (Fig. 11).

Traverse 1 proceeds from KJD1 to the chromite layer then turns south along the ridge to the harrisite outcrop (MGA 263046E 6757907N). This is a very coarse grained olivine harrisite with pyroxene oikocrysts, similar to that seen at Comet Vale (Fig. 7). This unit is very laterally persistent and can be traced for at least several kilometres along strike. The traverse then proceeds east up the section to a layer of olivine–clinopyroxene cumulate with plagioclase oikocrysts (MGA 263105E 6757881N). This section is an excellent illustration of the way new cumulus phases appear in the section first as oikocrysts then as idiomorphic grains.

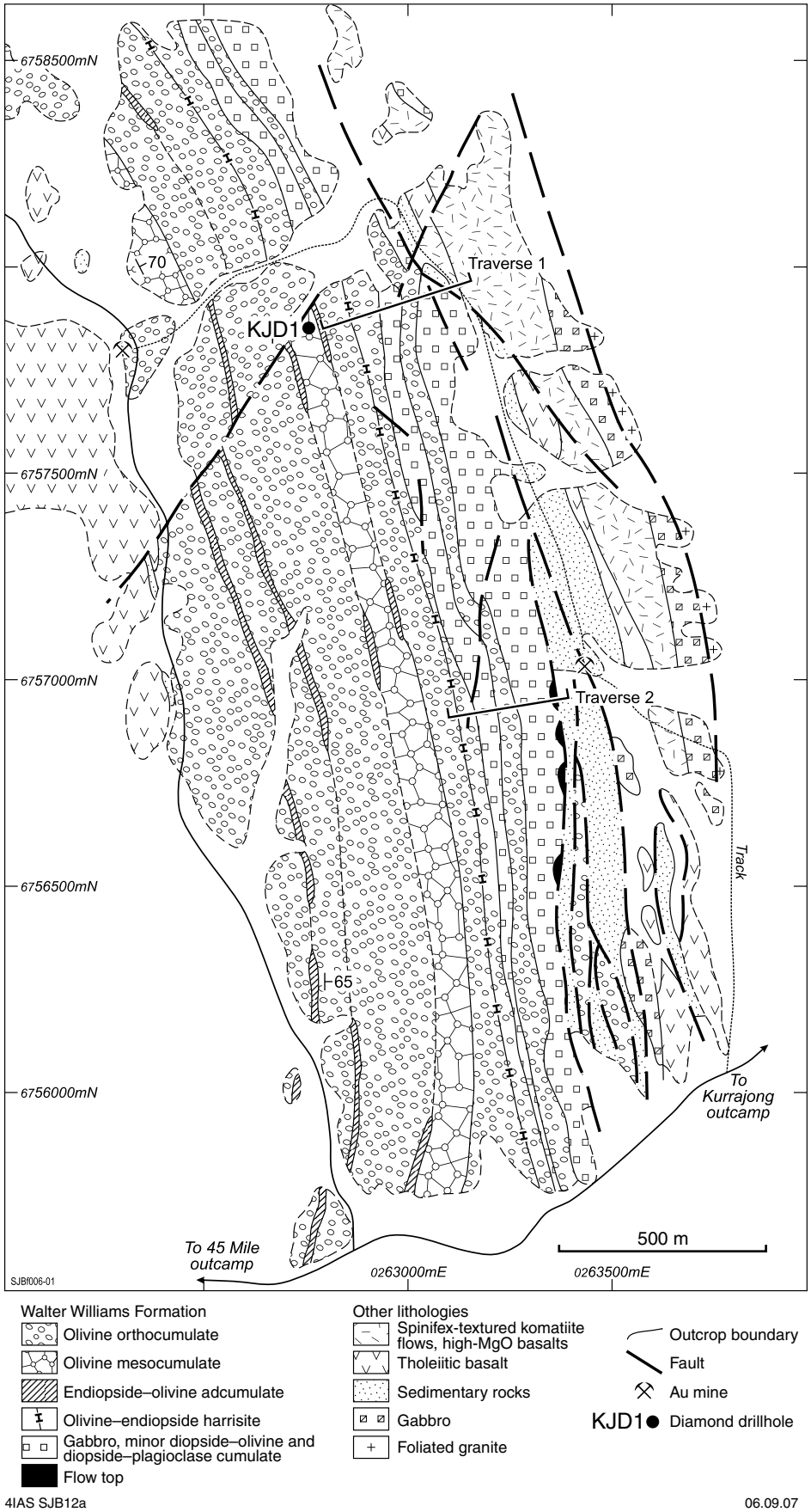

Figure 9. Geological map of the Locality 4 area within the Kurrajong Anticline (modified from Hill et al., 2001)

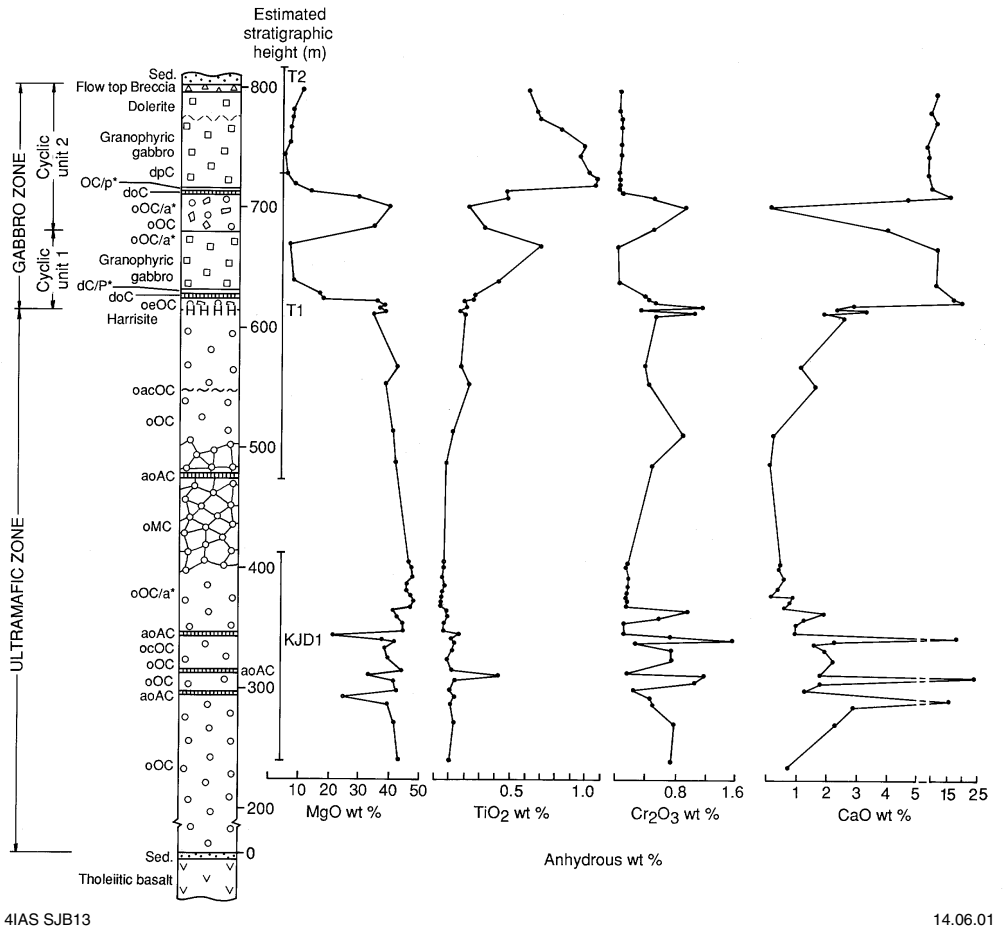

Figure 10. Composite profile showing variations in lithology and whole-rock geochemistry along Traverse 1 – KJD1, and the upper part of Traverse 2, KJD1 area, Kurrajong. See Figure 12 for location. Abbreviations: aoAC = augite olivine adcumulate; dC/p* = diopside cumulate with plagioclase oikocrysts; doC = diopside olivine cumulate; dpC = diopside plagioclase cumulate; oacOC = olivine augite chromite orthocumulate; oeOC = olivine enstatite orthocumulate; oMC= olivine mesocumulate; oOC = olivine orthocumulate; oOC/a* = olivine orthocumulate with augite oikocrysts; ocOC = olivine chromite orthocumulate; OC/p* = orthocumulate with plagioclase oikocrysts; Sed = sediment (after Hill et al., 2001)

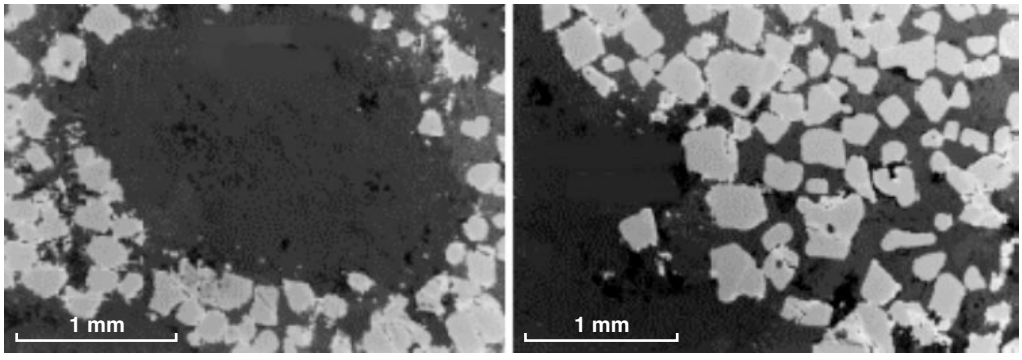

Figure 11. Photomicrograph of chromite-rich layer, with 'chicken-wire' texture, from Traverse 1, KJD1 area (after Hill et al., 2001)

Traverse 2: Top of Walter Williams Formation

adapted from Hill et al. (2001)

For Traverse 2, continue east along the track just north of KJD1. The track turns to the south-southeast, parallel to the strike of the ultramafic rocks, and leads to an abandoned mine site (MGA 263427E 6757253N).

Traverse 2 begins at the flow-top breccia of the Kurrajong section of the Walter Williams Formation, which is exposed patchily (around MGA 263491E 6757229N). Fine-grained, quartz-rich, volcaniclastic sandstone rests directly above the 'string-beef' pyroxene-spinifex rocks that can be found as float, and possibly in outcrop, just west of the shaft (MGA 263469E 6757165N). The nature of this contact is unclear but it has been interpreted as a fault (Fig. 9). However, the lack of strong deformation at the contact suggests that the volcaniclastic sandstone may have been deposited on the pyroxene-spinifex-textured basalt. If so, the recently obtained SHRIMP U–Pb zircon age of 2703 ± 6 Ma (Bodorkos, S, 2007, written communication) for the sandstone confirms previously determined ages for the komatiite unit of the Kalgoorlie Terrane stratigraphy. The traverse then continues to the west down the section through gabbros, layered olivine–pyroxene cumulates, and olivine orthocumulates.

Geochemical profile, KJD1 area (Hill et al., 2001)

The geochemical profile through the Walter Williams Formation (Fig. 10) clearly shows the lithological layering just described. The section within KJD1 contains cyclic layering in the central part of the ultramafic zone. Upward increases in CaO and decreases in MgO reflect changes in the modal proportions of olivine and pyroxene below each of the three Mg-augite–olivine cumulate layers intersected. Above the third layer, similar geochemical variations are present, but here the cycles stopped before a clinopyroxene layer could form. The rocks formed in each successive cycle in this sequence contain more MgO and less CaO, reflecting an increase in the packing density of olivine. It may also reflect, in part, a change to more forsterite-rich olivine compositions.

In the gabbro zone, the two fractionation cycles are clearly defined by the geochemical profile (Fig. 10). Through most of the upper diopside–plagioclase cumulate and granophyric gabbro unit, MgO increases and TiO_2 decreases upward (as does FeO and P_2O_5), suggesting that the rocks in the upper section crystallized downward from the flow-top breccia. This is also indicated by the upward fining of grain sizes. The lower gabbro unit contains less TiO_2 and P_2O_5 than the upper gabbro, but these components increase upward, suggesting that the lower gabbro was cut off before they could accumulate to the levels seen in the upper gabbro. Clinopyroxenes in the Walter Williams Formation are chromium-rich Mg-augites and diopsides. They contain up to 1.4 wt% Cr_2O_3 and 3.55 wt% Al_2O_3 and have low concentrations of TiO_2. Those from the peridotites are commonly less calcium-rich than those from clinopyroxenite layers. However, pyroxene is only sporadically preserved throughout the formation, so it is not possible to determine whether there are any systematic changes in composition with locality or stratigraphic height.

Locality 5: Copperfield Monzogranite

modified from Rattenbury (1993)

Return to the Mount Ida Road, and proceed north for about 18.5 km to a turnoff to the east (MGA 254249E 6776770N). Follow this track around the south side of a low hill for about 3.2 km (MGA 257100E 6777895N).

The Copperfield Monzogranite outcrops in the core of the Kurrajong Anticline (Fig. 7), within the West Ida greenstone belt. The granite slightly transgresses the greenstone belt stratigraphy which suggests an intrusive relationship. The contact, however, is strongly deformed. The granite has a very well developed, pervasive stretching lineation, particularly around the pluton margins. The granite also has a weakly developed foliation which is subparallel to the boundary with the mafic–ultramafic volcanic rocks around the Kurrajong Anticline. The contact between the mafic metavolcanic rocks and the lineated Copperfield Monzogranite is strongly sheared but the fabric intensity diminishes southwards and eastwards into the mafic–ultramafic metavolcanic rocks indicating that penetrative ductile deformation is localized in the lower part of the stratigraphy. The metavolcanic rocks are pervasively lineated east of the Copperfield Monzogranite, and have been crenulated by the D_2 upright fold axial planar cleavage.

The granite lineation is formed by relatively large, unstrained quartz grains, up to 2 mm long, separated by 1–3 mm plagioclase grains and 0.3–0.8 mm microcline. The plagioclase is typically unstrained with muscovite inclusions. The microcline occurs as subgrains with small mismatches in twin boundary orientations across grain boundaries. Dark green-brown biotite is the predominant mafic mineral present, with minor magnetite and apatite. Dynamic recrystallization of microcline is indicative of high temperatures during significant strain. The weak foliation within the granite and the foliation within the greenstone belt suggests that the deformation predated the upright folding, despite the occurrence of the stretching lineation sub-parallel to the Kurrajong Anticline fold axis. Several attempts to date this granite have been unsuccessful owing to a lack of zircons suitable for SHRIMP dating.

The region has been a significant gold producer with historic production from numerous deposits in greenstones at the margins of the Copperfield Monzogranite. Historical production data and estimated resources of deposits in the region can be obtained via the GeoVIEW.WA interactive map on the Department of Industry and Resources (DoIR) website (www.doir.wa.gov.au/aboutus/geoview_launch.asp). The Baldock deposit, a current underground mining development near the historical Timoni deposit at Copperfield is being mined by International Goldfields Ltd. The deposit has measured resources of 0.055 Mt at 32.8 g/t, indicated resources of 0.006 Mt at 33.8 g/t, and inferred resources of 0.083 Mt at 17.5 g/t (based on a report to the Australian Stock Exchange by International Goldfields Ltd, 31 March 2005).

The westernmost limit of the Ida Fault zone lies to the west of the workings around Copperfield. Historical gold production data suggest a significant decrease in the amount of gold hosted by greenstones west of the Ida Fault in this area but the reason for this is not well understood.

Locality 6: Banded iron-formation at Mount Bevon (West Ida greenstone belt)

Return to the main road, drive north for 2.9 km, past the Timoni minesite, to the Perrinvale turnoff (MGA 252827E 6779297N). Follow the Moore Wills Road for 5.2 km to the Perrinvale turnoff (MGA 251167E 6784173N). Turn west onto the Perrinvale road and drive for 13.7 km to the turnoff to Mount Bevon (MGA 238757E 6785157N). Turn south and drive 0.8 km up the hill to the Telecom mast (MGA 238924E 6784338N).

The major trace of the Ida Fault is interpreted as passing through the greenstones between Localities 5 and 6. All the banded iron-formation in this greenstone belt lies west of the Ida Fault, which is taken to be the boundary between the Eastern Goldfields Superterrane and the Youanmi Terrane.

Mount Bevon forms part of a long series of ridges of banded-iron formation that are typically found low in the stratigraphic successions of the Southern Cross Domain of the Youanmi Terrane. The banded iron-formation typically consists of fine laminae (0.5 – >5 mm) of recrystallized quartz and quartz–hematite–magnetite). Grunerite (iron-rich amphibole) may be present in areas of higher (amphibolite facies) metamorphic grade. Beds within banded iron-formation commonly show evidence of tectonism and some ridges preserve refolded intrafolial folds that most likely developed during the earliest deformation of these rocks.

These ridges are being actively explored for iron ore resources. For example, the Mount Mason deposit, about 10 km south-southeast of Mount Bevon, has an inferred resource of hematite ore of 1.8 Mt at 60.3% iron (based on a report to the Australian Stock Exchange by Jupiter Mines Ltd, 7 September 2006).

Locality 7: Ancient detrital zircons near Kohler Bore (Maynard Hills greenstone belt)

From the Mount Bevon turnoff, drive about 25 km west to join the Menzies–Sandstone Road (MGA 214311E 6784100N). Turn north and drive for about 70 km to a turnoff to the east (MGA 770149E 6844692N) near Bulga Downs Homestead. For GPS users, note that the boundary between MGA Zones 51 and 50 occurs along this road. Drive 7 km east along this formed track to the top of the ridge (MGA 776886E 6845330N).*

* All Localities from 1 to 6 are in MGA Zone 51. All subsequent localities are in MGA Zone 50.

Quartzite and quartz-rich clastic metasedimentary rocks have been reported from a number of greenstone belts in the eastern Youanmi Terrane (e.g. Gee, 1982; Chin and Smith, 1983; Riganti, 2003; Wyche, 2003). Quartz sandstone and quartz–mica schist are preserved at the base of the exposed greenstone succession over a wide area in the north, with the most extensive development of these rocks in the Maynard Hills and Illaara greenstone belts (Fig. 12).

Primary textural and sedimentological features in the quartzites of the Illaara and Maynard Hills greenstone belts are poorly preserved owing to the effects of deformation and recrystallization. The quartz-rich, clastic metasedimentary rocks in the Illaara greenstone belt lie along the eastern side of the belt and represent the lowest preserved part of the succession. This unit has a maximum thickness of about 900 m, and consists of prominent, ridge-forming, fine- to coarse-grained, strongly recrystallized quartzite, and recessive intervals that range from micaceous quartzite to quartz–mica schist.

The Maynard Hills greenstone belt lies within the regional-scale Edale Shear Zone (see Locality 8). Stratigraphic relationships of quartz-rich metasedimentary rocks in the Maynard Hills greenstone belt are less apparent than those in the Illaara greenstone belt owing to strong deformation and recrystallization, but the rock associations in this belt suggest a similar stratigraphic setting (Riganti, 2003; Wyche et al., 2004).

Near Locality 7, rocks are extensively deformed with preservation of tight folds (MGA 777017E 6845058N) and evidence of multiple deformation events that includes overprinting fabrics (MGA 777050E 6845126N). A strong bedding-parallel cleavage commonly obscures primary sedimentary structures, but they are probably thin to medium bedded and derived from mature quartz arenites. Original grainsize is difficult to determine owing to extensive recrystallization, but some beds contain subrounded quartz pebbles. Muscovite is the dominant mica in the mica schist (Fig. 13), but bright green fuchsite is found locally in both the quartzite and quartz–mica schist. Very fine grained tourmaline gives some beds a dark colouration. The association of quartzite with quartz–mica schists that were probably derived from submature to immature quartz arenites and the local preservation of cross bedding suggest that these rocks were deposited in a fluvial to shallow-marine environment (Wyche, 2003; Wyche et al., 2004).

Froude et al. (1983a) identified detrital zircons in the Maynard Hills greenstone belt ranging in age between c. 3300 and c. 3700 Ma but their analytical results were never published. Recently, eight quartzite samples have been analyzed from the Illaara and Maynard Hills greenstone belts, confirming the results of Froude et al. (1983a), but also identifying a number of >4000 Ma zircons (Geological Survey of Western Australia, 2007a). A sample from the Gum Creek greenstone belt, which lies north of Sandstone, has indicated that the old detrital-zircon-bearing metasedimentary units are more widespread than has been previously documented (Wingate and Bodorkos, 2007d).

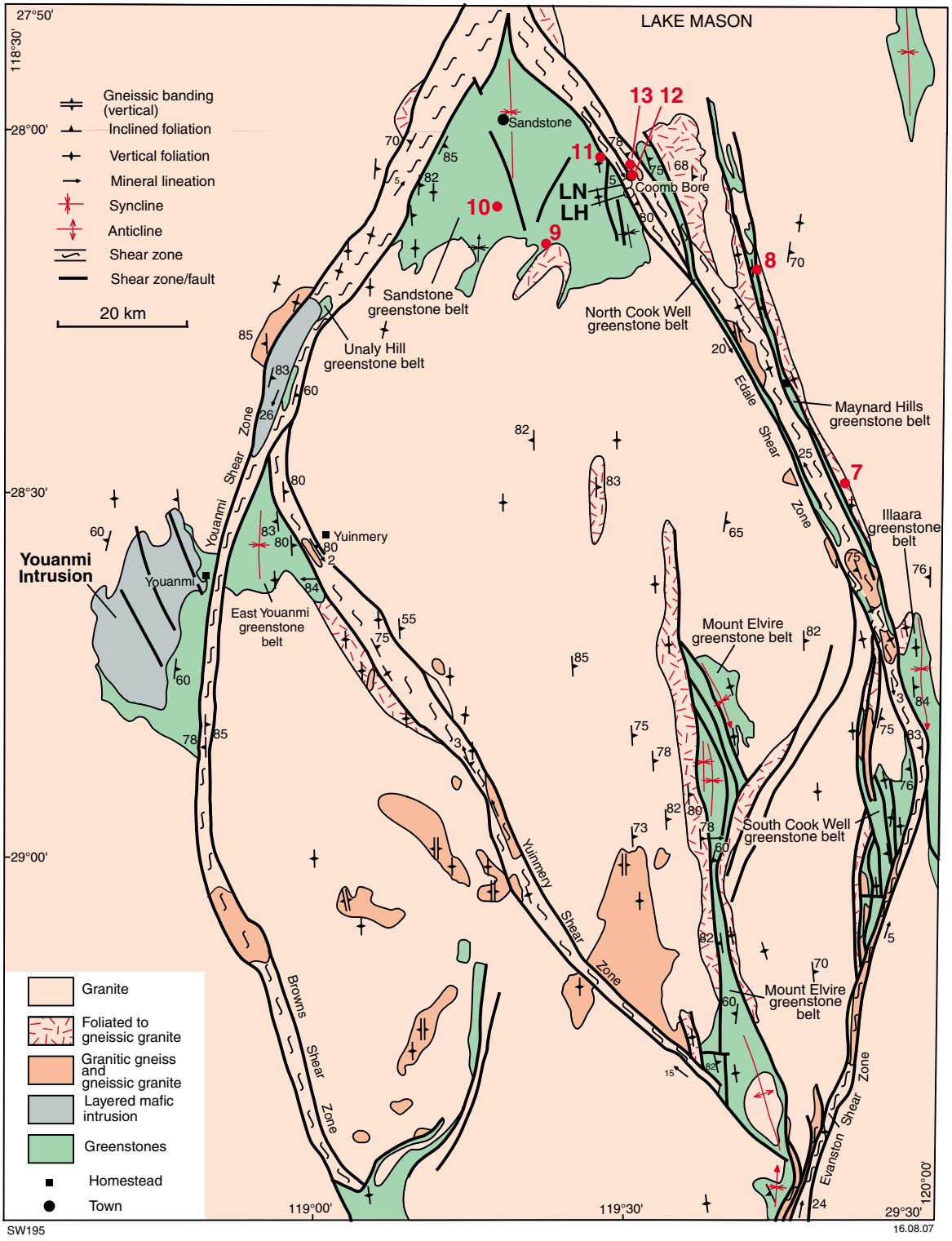

Figure 12. Interpreted granite–greenstone geology of the central-northern part of the Southern Cross Domain showing the distribution of major D_3 shear zones. B, Bulchina gold mine; LH, Lord Henry goldmine; LN, Lord Nelson gold mine (modified from Chen, 2005)

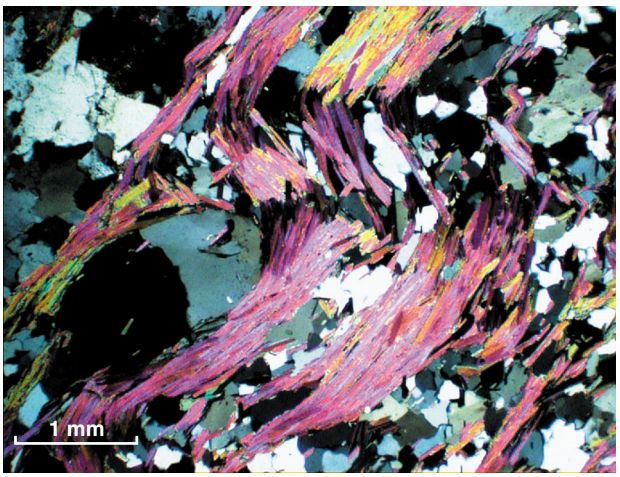

Figure 13. Photomicrograph of muscovite-bearing quartzite from the Maynard Hills greenstone belt, showing folding and kinking of muscovite laths around a polygonized quartz clast in a matrix of granoblastic quartz; GSWA 164921, crossed polars (modified from Riganti, 2003)

A sample of quartzite taken from an outcrop about 250 m south of the track (MGA 777070E 6845090N) yielded detrital zircons that mainly ranged in age between c. 3300 and c. 3700 Ma, but also contained a c. 4350 Ma zircon (Fig. 14; Nelson, 2005a). This age is of the same order as the age of the oldest zircons identified in the Jack Hills greenstone belt in the Narryer Terrane (Wyche et al., 2004; Wyche, in prep.), the oldest zircons that have been discovered on Earth (Compston and Pidgeon, 1986; Wilde et al., 2001; Cavosie et al., 2004). Other >4000 Ma zircons have also been obtained from a sample from the Illaara greenstone belt (Nelson, 2005b). The youngest detrital zircon identified, from a sample taken about 100 m south of the very old zircon sample site (MGA 777080E 6845000N), indicates a maximum depositional age for these rocks of c. 3131 Ma (Nelson, 2002b).

Wyche et al. (2004) argued that the widespread occurrence of >3000 Ma detrital zircons in quartzites in the eastern Youanmi Terrane, the South West Terrane, and the Narryer Terrane suggested a common provenance. The only rocks in the Yilgarn Craton that date back to include part of the age range of these detrital zircons are some gneisses of the Narryer Terrane.

Locality 8: Amphibolite in the Edale Shear Zone at Rocky Creek (Maynard Hills greenstone belt)

After returning to the Menzies–Sandstone Road, drive north for about 34.5 km to a turnoff to the east, north of Rocky Creek (MGA 760180E 6877150N). Take the north fork and drive for about 4.3 km (MGA 764213E 6878147N). Walk up the hill on the north side of the track to an outcrop of amphibolite (MGA 764177E 6878316N).

The Edale Shear Zone is one of the shear zones that form the distinctive, regional-scale, rhomb-shaped pattern in the central Yilgarn Craton (Fig. 12). They formed during an extended period of east–west shortening, and are interpreted as having been produced by the impingement of large bodies of cooling granite into the greenstone belts after the main period of upright folding. Foliations in the shear zones are steep and commonly dip steeply towards the greenstones near granite–greenstone contacts, and dip away from the contacts in granite distal from contacts. Although they may have had a significant pre-history, the major movement that accounts for the current disposition of the shear zones took place during D_3 progressive, inhomogeneous shortening, and was probably finished by c. 2650 Ma (Chen et al., 2001; 2004).

The Edale Shear Zone (Riganti, 2003) extends south-southeast for more than 100 km from north of Sandstone (where it merges with the Youanmi Shear Zone) to the northern end of the Illaara greenstone belt. In the south, the shear zone ranges from 6 to 10 km in width, and encompasses the corridors of greenstones represented by the Maynard Hills and North Cook Well greenstone belts, the intervening granitic rocks, and an outer zone of deformed monzogranite up to 2 km wide (Fig. 12). The intensity of deformation in this outer zone decreases rapidly away from the greenstone belts, with the transition from strongly foliated to undeformed monzogranite commonly over a distance of a few hundred metres to one kilometre. Within the shear zone, deformation intensity typically increases from the centre towards the greenstones, with a gradual transition from strongly foliated monzogranite to gneissic granite to gneiss at the contact with the greenstones. Textures in the gneiss vary from granoblastic to blastomylonitic near the contact. Within the Maynard Hills and North Cook Well greenstone belts, intense shearing has resulted in a complex interleaving of mafic igneous, sedimentary, and granitic rocks, down to metre and, locally, centimetre scale. The strong layer-parallel foliation is vertical to subvertical across the shear zone, with steep east-northeasterly and west-southwesterly dips on the western and eastern flanks of the ridges that mark the Maynard Hills greenstone belt.

Kinematic indicators are consistent with a sinistral strike-slip movement sense for the Edale Shear Zone, and include asymmetric feldspar porphyroclasts in gneiss and foliated granite; S–C fabrics; imbricated boudins in layer-parallel quartz bands within banded iron-formation; S-shaped, small-scale folds with north-northwesterly trending axial planes preserved in a range of rock types.

Metamorphic grade within the Edale Shear Zone ranges from the greenschist facies into the amphibolite facies (Riganti, 2003). Most areas have undergone some retrograde metamorphism. At Locality 8 (MGA 764177E 6878316N), a short traverse illustrates some of the amphibolite-facies metasedimentary rocks. At the beginning of the traverse, fine- to medium-grained grained amphibolite shows thin light and dark layers that probably reflect bedding in the sedimentary protolith. The rock is strongly deformed with locally preserved, coarse, flattened garnets up to 1 cm across. Downslope, the rock is more clearly a metasediment with layers of quartzite and

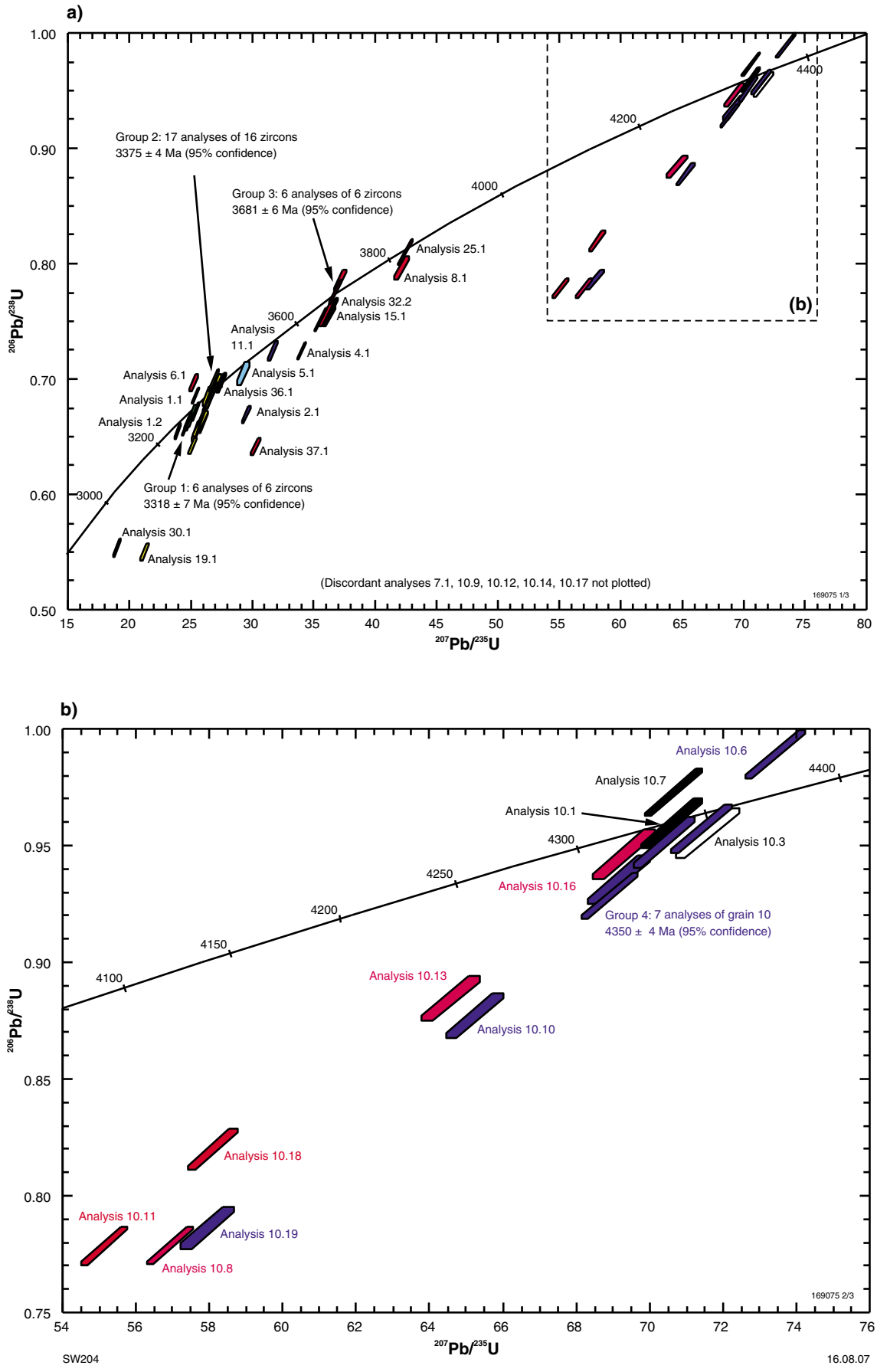

Figure 14. a) U–Pb analytical data for zircon from sample 169075: quartzite, Kohler Bore; b) Inset from Figure 14a (after Nelson, 2005a)

quartz–mica schist interbedded with amphibolite (MGA 764231E 6878290N).

Sandstone greenstone belt

The Sandstone greenstone belt (Chen, 2005) occupies a triangular area between the northeasterly trending Youanmi Shear Zone and the northwesterly trending Edale Shear Zone, with the northern apex of the triangle at the junction of the shear zones, and the southern margin disrupted by granite intrusions (Fig. 15). The triangle is approximately 40 km along its southern margin, and 35 km from south to north. Greenstones are locally well exposed in the western, eastern, and southeastern parts, and exposure is poor in the centre and south, with extensive areas of laterite, colluvium, and sheetwash.

Stewart et al. (1983) interpreted greenstones in the Sandstone area as a regional-scale, north-plunging anticline that largely defined the stratigraphy of the Sandstone greenstone belt. The lower part of their stratigraphic column was composed of ultramafic rocks and komatiitic basalt; the middle part consisted mainly of tholeiitic basalt, banded iron-formation, and chert, with minor gabbro and ultramafic rocks; and the upper part was dominated by shale, with minor gabbro and limestone. However, based on new geological mapping, observations of rock distribution based on exploration drillholes, and new aeromagnetic data, Chen (2005) has reinterpreted the northerly plunging anticline of Stewart et al. (1983) as the northerly trending Sandstone Syncline (Fig. 15). In the new interpretation, an early, tight syncline has been refolded to form a complex, greenstone-belt-scale synclinorium which has been extensively intruded by granite along its southern margin.

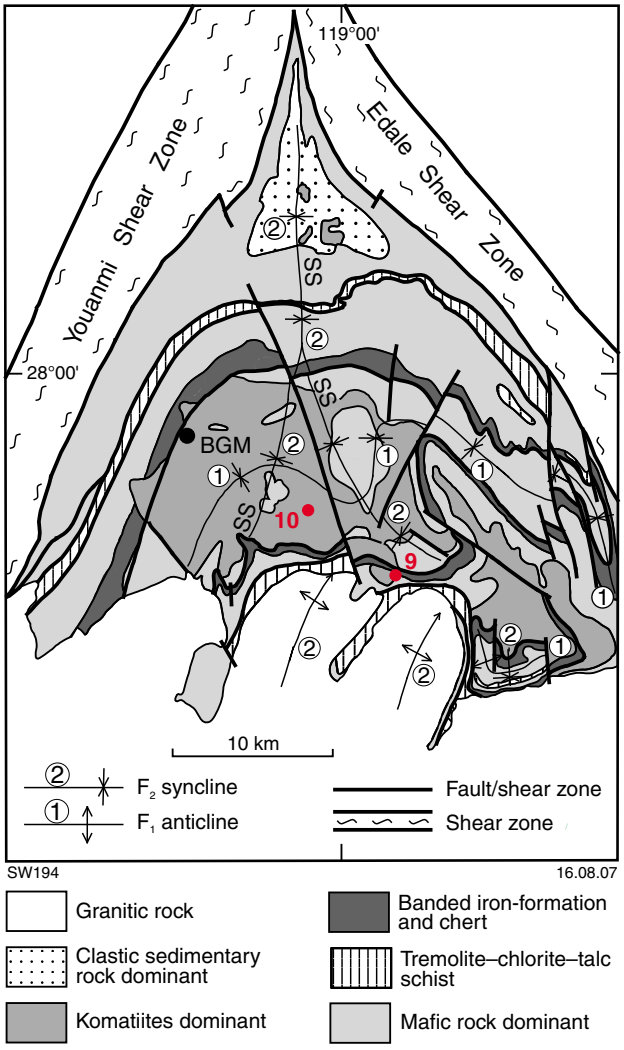

Figure 15. Interpreted geological map of the Sandstone greenstone belt. BGM, Bulchina gold mine; SS, Sandstone Syncline (after Chen et al., 2005)

Structural complexity, poor exposure, and lack of geochronological data make it difficult to establish an overall stratigraphy for the Sandstone greenstone belt (Chen, 2005). A structurally lower, mafic-dominated succession is preserved mainly on the limbs of the regional-scale Sandstone Syncline (see Locality 10). This part of the succession contains at least two intervals with abundant banded iron-formation with local subordinate clastic metasedimentary and Mg-rich meta-igneous rocks including komatiitic basalt, and tremolite–chlorite(–talc) schist (Fig. 15).

Rare outcrop, extensive mineral exploration drillholes, areas of silica caprock, and local outcrop of serpentinized peridotite (see Locality 9) in the central-southern part of the Sandstone greenstone belt indicate the presence of widespread ultramafic rocks (dominantly komatiite) that appear to occupy a structurally high position in the stratigraphy (Chen, 2005). The stratigraphic relationship of this structurally higher, ultramafic-dominated succession with the structurally lower, mafic-dominated succession described above is uncertain due to the poor exposure. They may be unconformable, separated by a fault, or the ultramafic-dominated succession may be the intensely folded and detached top part of the mafic-dominated succession in this area. Whatever the relationship, this apparent abundance of ultramafic rocks is unusual for the Southern Cross Domain of the Youanmi Terrane (Chen et al., 2005). However, it is of interest to note that recent geochronology has demonstrated the existence of at least two widely separated periods of komatiite volcanism in the Meekatharra–Wydgee greenstone belt in the Murchison Domain of the Youanmi Terrane (see Locality 17).

The only geochronological constraint from within the Sandstone greenstone belt is a SHRIMP age for a porphyritic microgranite that intrudes ultramafic rocks in the Bulchina openpit (Figs 12, 15). This rock has a U–Pb zircon age of 2731 ± 14 Ma (Nelson, 2004a), and a SHRIMP U–Pb monazite age of 2731 ± 3 Ma (Nelson, 2005c).

The Sandstone greenstone belt has produced about 30 t of gold with more than 7 t produced from Troy Resources' Bulchina mine, which closed in 2004 (Fig. 15). At Bulchina, gold mineralization related to north-northeasterly trending, steeply dipping quartz veins was hosted by mafic and clastic sedimentary rocks in the western part of the openpit, and porphyritic

micrograniteand ultramafic rocks in the eastern part (Chen, 2005). Two other small deposits, the Lord Henry and Lord Nelson deposits, lie in the western part of the Edale Shear Zone in the southeastern part of the Sandstone greenstone belt (Fig. 12). At the Lord Henry deposit, mineralization is hosted in stacked, shallow north-dipping lodes within sericite–quartz–carbonate–pyrite-altered granodiorite. At Lord Nelson, there is both supergene and primary gold mineralization. The primary mineralization is found in sheared basaltic and granodioritic rocks close to or along a contact with a steeply dipping footwall ultramafic unit. The north-northwesterly trending and west-dipping mineralization is hosted in quartz–carbonate–pyrite veins that occur in quartz–biotite–pyrite-altered brittle–ductile shear zones (Troy Resources NL, 2007).

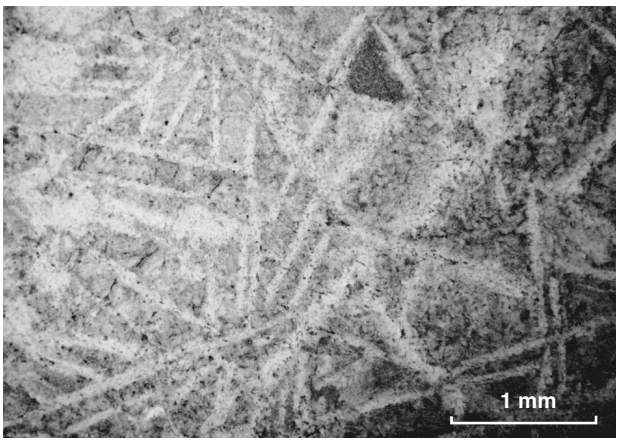

SW208 27.08.07

Figure 16. Metakomatiite with a relict, random olivine-spinifex texture pseudomorphed by serpentine — plane-polarized light; GSWA 165378 (after Chen, 2005)

Locality 9: Peridotite in the Sandstone greenstone belt

adapted from Chen et al. (2005)

After returning to the Menzies–Sandstone Road, continue west-northwest for about 15 km to the turnoff (MGA 745620E 6880417N) to the west to Dandaranga Homestead, about 100 m past the turnoff to Troy Resources' Lord Henry and Lord Nelson deposits. Travel west along this road for about 13.8 km to an open area with some low outcrop on the south side of the road (MGA 732050E 6882904N).

Although the upper ultramafic unit in the southern Sandstone greenstone belt is very poorly exposed with komatiite typically seen only in drillholes, it is locally exposed in small outcrops and in the Bulchina openpit, where relict platy and random olivine-spinifex textures are common, with pseudomorphed olivine plates up to 5 cm long.

Petrographic examination of komatiites from drillholes indicates that primary olivine is rarely preserved; serpentine, talc and tremolite are the most abundant secondary minerals, with phlogopite and calcite common in some samples; accessory minerals include magnetite, titanite, anatase and ilmenite. Komatiites are commonly metamorphosed to greenschist facies and are typically altered, with serpentinization and talc–carbonate alteration the most common, and chloritization and albitization locally observed. Despite metamorphism, alteration and locally intense deformation, relict olivine-cumulate and olivine-spinifex textures are commonly preserved. In olivine orthocumulates, olivine is typically pseudomorphed by serpentine, and less commonly by talc; the interstices comprise fine-grained tremolite and talc. In olivine mesocumulates, olivine has been largely replaced by serpentine, talc, and phlogopite, in a tremolite- or talc-rich groundmass. In spinifex-textured komatiites, olivine-spinifex texture (Fig. 16) is preserved by serpentine in a groundmass of serpentine and tremolite.

Twenty-eight samples from the komatiite-dominated succession have been analysed for major element oxides and some trace elements (Chen, 2005; Chen et al., 2005). Based on Al_2O_3/TiO_2, komatiites can be divided into aluminium-depleted komatiite (ADK — Barberton type: Al_2O_3/TiO_2 5–15) and aluminium-undepleted komatiite (AUDK — Munro type: Al_2O_3/TiO_2 15–25) (Nesbitt et al., 1979; Sproule et al., 2002). Samples from the komatiite-dominated succession of the Sandstone greenstone belt fall into two broad groupings in terms of Al_2O_3/TiO_2 (Fig. 17a), with a break at about 15 (i.e. on the ADK–AUDK boundary). The presence of both ADK and AUDK is further supported by $(Al_2O_3/TiO_2)_{MN}-(Gd/Yb)_{MN}$ (Fig. 17b). Both Al and Yb are more strongly partitioned into garnet relative to either Ti or Gd, meaning that samples with lower $(Al_2O_3/TiO_2)_{MN}$ and higher $(Gd/Yb)_{MN}$ are from a source in which garnet has been retained, or represent a melt from which garnet has crystallized. If the variation in Al_2O_3/TiO_2 reflected alteration, then the relationship with $(Gd/Yb)_{CN}$ would not be expected.

In the nickel-mineralized Forrestania greenstone belt in the southern part of the Youanmi Terrane, south of Southern Cross, komatiites from the lower part of the stratigraphy are ADK, whereas AUDK are found at higher stratigraphic levels. Perring et al. (1996) argued that this could be attributed to less retention of garnet in the source over time, as well as progressively shallower depths of melting. More speculatively, if this process involved a mantle plume (commonly invoked for komatiites), initial melting of the asthenosphere by the rising plume head could account for basalts in the mafic-dominated succession, and their paucity in the komatiite-dominated succession representing the plume tail (Campbell et al., 1989).

Although many of the analysed komatiites in the Sandstone greenstone have features favourable for the development of nickel mineralization (e.g. >20% MgO and >1000 ppm Ni; association with sedimentary rocks), no significant nickel mineralization has been identified in the northern part of the Southern Cross Domain, or anywhere within the Murchison Domain.

At Locality 9 (MGA 732040E 6882795N), there is a rare exposure of the serpentinized ultramafic unit. Here, the rock is a serpentinized peridotite in which original olivine grains up to 1 mm have been completely replaced by serpentine, talc, and magnetite. The rock is undeformed and the original olivine orthocumulate texture is locally preserved. An XRF analysis of a rock from this locality indicated an SiO_2 content of 40.86%; an MgO content of 30.61%; a Cr content of 3435 ppm; and an Ni content of 2188 ppm (Sample 183331 in the Geological Survey of Western Australia WACHEM database).

A costean on the northern side of a northeasterly trending, south-dipping ridge of banded iron-formation about 100 m south of Locality 9 exposes talc–chlorite(–carbonate) schist. There is outcrop of tremolite–chlorite schist just north of the track, and scattered float of metabasalt with relict pyroxene-spinifex texture with tremolite–actinolite pseudomorphing primary clinopyroxene needles up to 3 cm long in the vicinity of the track.

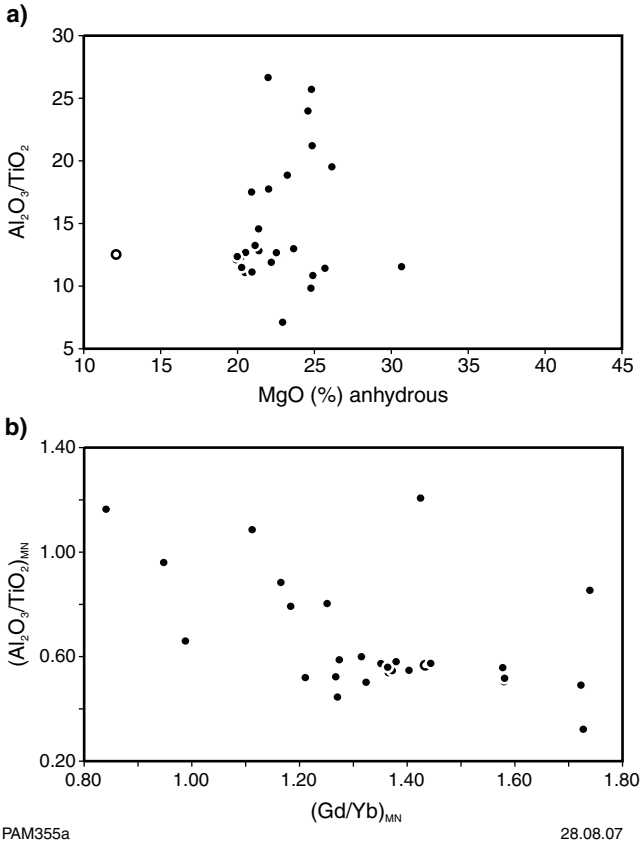

Figure 17. a) (Al_2O_3/TiO_2) vs MgO (% anhydrous) for komatiite (solid circles) and komatiitic basalt (open circle) from the Sandstone greenstone belt; b) Mantle-normalized (Al_2O_3/TiO_2) vs (Gd/Yb) for komatiite and komatiitic basalt from the Sandstone greenstone belt: symbols as in (a). Mantle normalization values are pyrolite values from McDonough and Sun (1995)

Locality 10: Folding in banded iron-formation on Mount Klemptz (Sandstone greenstone belt)

From Locality 9, continue west for 5.8 km to the abandoned Dandaranga Homestead, turn north and follow the road to Sandstone for 3.5 km to Troy Resources' haul road. At the time of writing, this haul road was still in use and public access was not allowed without the permission of Troy Resources NL. Locality 9 lies along an old fenceline that splays off the haul road, about 1.2 km west of the road to Dandaranga Homestead.

At Mount Klemptz (MGA 724555E 6888737N), complexly refolded banded iron-formation forms a large ovoid feature near the middle of the synclinorium of Chen (2005) — see **Sandstone greenstone belt** above and Figure 15.

The large ovoid feature at Mount Klemptz is part of a large-scale interference fold within the Sandstone Syncline. The abundant, tight, commonly shallowly plunging folds at Mount Klemptz probably formed during the F_1 deformation (Fig. 15) that produced the tight, greenstone-belt scale syncline that has been refolded in the Sandstone Syncline.

Locality 11: Proterozoic sill beside the old Agnew–Sandstone Road

modified from Wingate and Bodorkos (2007e)

Returning to the main road, drive north for 9.2 km to rejoin the Menzies–Sandstone Road (MGA 724660E 6897640N). Proceed to Sandstone, turn east onto the bypass and drive along the Agnew–Sandstone Road to the old Agnew–Sandstone Road (via Black Hill) junction (MGA 728034E 6902117N; 2.1 km east of the National Hotel). Follow this road for about 15 km (MGA 740595E 6895964N). Locality 11 is on the north side of the road.

At this locality, mafic and ultramafic rocks of the southeastern Sandstone greenstone belt are intruded by a medium- to coarse-grained gabbro sill that is about 5 m thick and dips about 5° to the north. The shallow-dipping sill forms a prominent west-northwest-trending feature on aeromagnetic images (Fig. 3) and appears to extend for more than 400 km in the central Yilgarn Craton. Similar magnetic anomalies extend for about 400 km farther to the south and may be expressions of the same sill.

Thirty analyses were obtained from 30 baddeleyite crystals, and 13 analyses were obtained from 13 zircons. Results are shown in Figure 18. The mean $^{207}Pb/^{206}Pb$ date of 1070 ± 18 Ma for a group of 29 analyses of baddeleyite is interpreted as the age of magmatic crystallization of the gabbro sill. This age is consistent with a single zircon with high U, Th, and Th/U values that are typical of primary zircons in differentiated mafic intrusions, that has a $^{207}Pb/^{206}Pb$ date of 1054 ± 8 Ma (1σ). The crystallization age determined for this sample indicates that the sill belongs to the c. 1075 Ma Warakurna Large Igneous Province (Wingate et al., 2004), which extends from the western Bangemall Superbasin to the

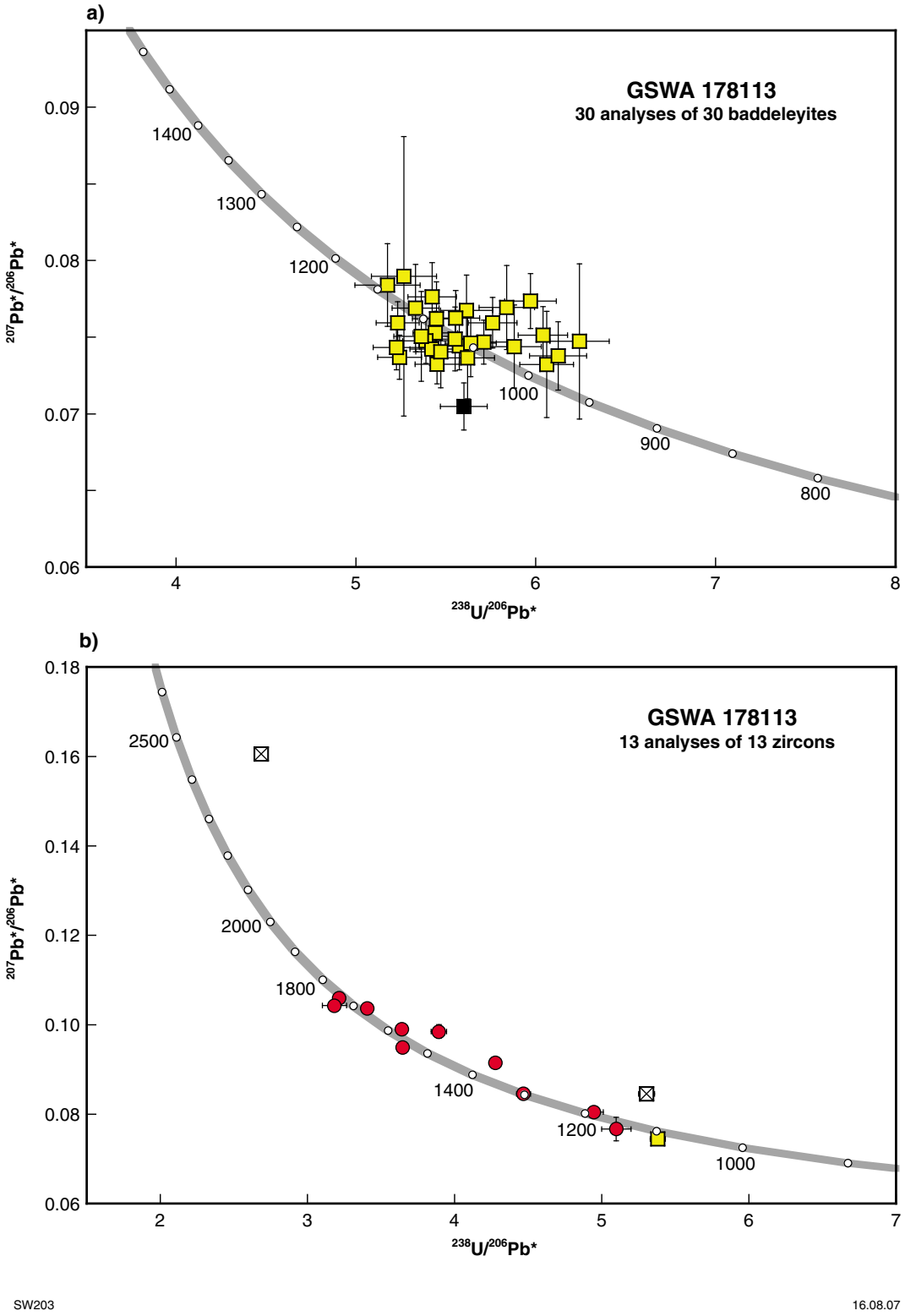

Figure 18. a) U–Pb analytical data for baddeleyite from sample 178113: gabbro sill, Kurrajong Bore. Black square indicates minor Pb loss. Dispersion in $^{238}U/^{206}Pb^*$ is due, at least in part, to crystal orientation effects (Wingate and Compston, 2000); b) U–Pb analytical data for zircons from sample 178113: gabbro sill, Kurrajong Bore. Yellow square indicates probable magmatic zircon; red circles indicate xenocrystic zircons; crossed squares indicate ungrouped data (discordance >10%)

eastern Musgrave Province in central Australia, and shows that the Warakurna Province extends well into the central Yilgarn Craton.

Locality 12: Mylonite at Coomb Bore

Continue southeast for about 5.8 km to the turnoff (MGA 745480E 6893474N) to Coomb Bore, which is on the south side of the road. Park near the bore and walk across to the south side of the creek.

In this area, the main section of the Edale Shear Zone is 7 km wide and includes strongly deformed granitic rocks west of Black Hill Homestead and the northernmost extension of the North Cook Well greenstone belt (Fig. 12). Foliation and a locally developed coplanar gneissic banding trend northwesterly (300°–350°, typically 320°–330°), and are vertical or dip steeply to the northeast (Riganti, 2003). The most intense deformation is found in the vicinity of Coomb Bore. Here, a strong lineament corresponds to the Edale Fault of Stewart et al. (1983) and is characterized in outcrop by the presence of mylonitized gneiss and greenstone.

Very strong deformation of greenstones at Locality 12 (MGA 745320E 6893240N) has produced a mylonite of very fine siliceous and chloritic layers. The felsic material is finely laminated but forms units between about 5 cm and 1 m thick that may represent original bedding (Fig. 19a). These units are locally boudinaged. There is a strong, subhorizontal stretching lineation. Late, north-northwesterly trending brittle structures are locally filled by quartz veins. The northern end of the outcrop contains a lens of strongly deformed metagabbro. Farther north, in the creek (MGA 745306E 6893291N), the siliceous material contains possible subhorizontal, 10 cm-scale sheath folds (Fig. 19b), and there is a fine, easterly trending crenulation in the chloritic schist.

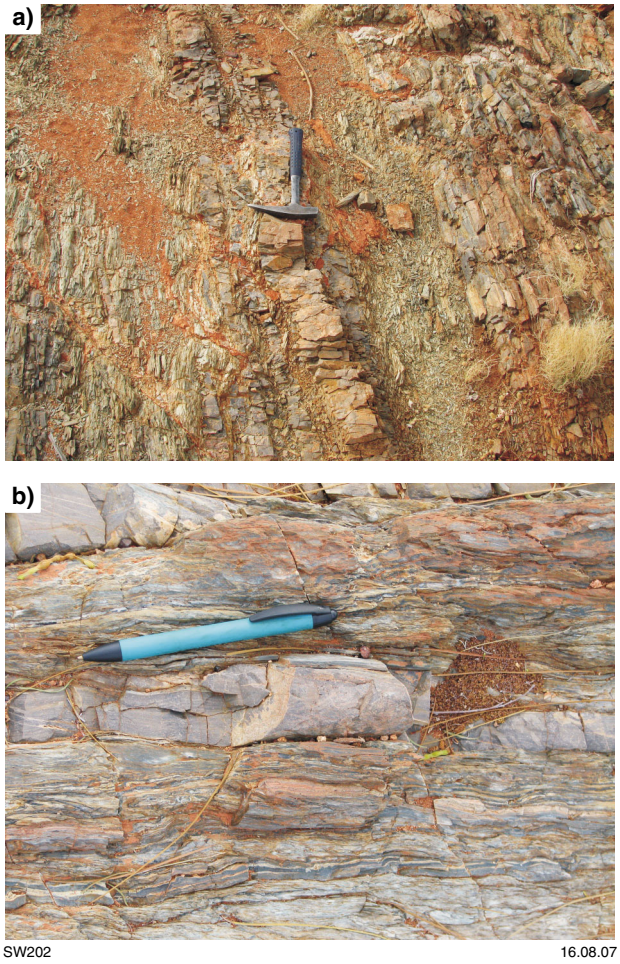

Figure 19. a) Mylonite near Coomb Bore (MGA Zone 50, 745320E 6893240N); b) Shallow- to horizontal-plunging, possible sheath fold in mylonite near Coomb Bore (MGA 745306E 6893291N)

Locality 13: Granophyre in the Coomb Bore Granite

modified from Riganti (2003)

Return to the old Agnew–Sandstone (via Black Hill Homestead) Road, and continue southeast for about 1 km, turn north off the road and drive cross-country across an open area with scattered outcrops of granite for about 2 km to the eastern side of an extensive granite outcrop (MGA 745070E 6894850N).

The Coomb Bore Granite is a small, foliated intrusion that forms an elongate, northwesterly trending pluton, about 1 by 3 km, that is entirely enclosed by strongly foliated monzogranite of the Edale Shear Zone. Whereas the surrounding deformed granite forms pavements and low-lying outcrops that are commonly deeply weathered, the Coomb Bore Granite is less weathered and forms prominent bouldery hills within a flat area of colluvial and alluvial deposits. Monzogranite is the dominant rock type in the Coomb Bore intrusion, but granodiorite and syenogranite phases are present, with an overall increase in the proportion of K-feldspar from southeast to northwest. The intrusive phases are typically medium grained, equigranular to porphyritic, and vary from dark pinkish grey to pale red, with the changes related more to clay alteration and iron staining (limonite or hematite after magnetite) of K-feldspar and plagioclase than to increased K-feldspar abundance alone. All exposures are characterized by a weak to moderate foliation, mainly defined by biotite and strings of quartz, that trends northwesterly and is either vertical or dips steeply to the east-northeast. Textural and mineralogical characteristics suggest that the Coomb Bore Granite intrusion was metamorphosed under at least amphibolite facies conditions, with low-temperature alteration followed by oxidation during weathering. As observed in other strongly foliated granitic rocks within the Edale Shear Zone, c-axes of quartz grains are mainly oriented at a low angle to the foliation. Centimetre-scale compositional layering is present in a few exposures and is defined by changes in the proportion and size of feldspar crystals. Poorly developed S–C fabrics in the more strongly foliated southeastern

part of the intrusion suggest a sinistral sense of shear. Two samples from a granodioritic phase of the Coomb Bore Granite yielded SHRIMP U–Pb zircon crystallization ages of c. 2690 Ma (Nelson, 2002c, 2004b).

At Locality 13, a small body of granophyre within the Coomb Bore Granite contains numerous milky quartz blebs up to 10 cm in size, and angular fragments and blocks up to 70 × 40 cm in size composed of syenogranite, pegmatite, monzogranite, and vein-quartz. In thin section, the granophyre contains K-feldspar (45 vol.%), plagioclase (25 vol.%), quartz (25 vol.%), hornblende (4–5 vol.%), and opaque oxide (<1 vol.%), with trace amounts of accessory magnetite, ilmenite, pumpellyite, prehnite, chlorite, smectite, clay, hematite, and zircon. Inclusions of plastically deformed granite, and large, fritted plagioclase grains and lenses of quartz, probably inherited from the original granite, are set in a granophyric matrix formed by remelting.

The granophyre at Locality 13 yielded zircons with a SHRIMP U–Pb zircon crystallization age of 2689 ± 6 Ma (Nelson, 2005d), within error of ages obtained on the Coomb Bore Granite (Nelson, 2002c, 2004b). Based on aeromagnetic images, the granophyre at Locality 13 is very close to the southeastern extension of the c. 1070 Ma Proterozoic sill exposed north of the road at Locality 11, and is interpreted to be a differentiate of the sill that has intruded and partially melted the Coomb Bore Granite. The c. 2690 Ma age obtained on the granophyre is due to inheritance of zircons from the Coomb Bore Granite. Similar areas of granophye and granite, also containing large fragments of granite, and also near the interpreted trace of the Proterozoic sill, outcrop about 40 km to the southeast (Riganti, 2003).

Locality 14: Barrambie Intrusion

Return to Sandstone. Travelling north from Sandstone, turn northwest onto the Meekatharra–Sandstone Road after 27 km. Continue towards Meekatharra for about 38 km to a turnoff to the east (MGA 712820E 6957950N). Follow the track for 1.6 km to a Y-junction (MGA 714200E 6957310N), turn onto the right fork and continue for another 400 m (MGA 714380E 6956910N).

The Barrambie Intrusion is one of a number of mafic–ultramafic layered intrusions in the middle of the Yilgarn Craton that are probably related, if not coeval. They include the Windimurra, Atley, Narndee, and Youanmi intrusions (Fig. 20), all of which outcrop to the south and west of the Barrambie Intrusion. Similar rocks are also found at Gabanintha, about 80 km to the northwest. All of these intrusions have been subjected to Archean deformation and metamorphism but the only published age is a poorly constrained Sm–Nd age of c. 2800 Ma (Ahmat and Ruddock, 1990). This may represent a mantle plume event to which the widespread 2.8 Ga magmatism in the Murchison Domain is related.

The Barrambie Intrusion (Ward, 1975) contains anorthosite, magnetite anorthosite, gabbro, magnetite gabbro, and magnetitite. The anorthosite is composed of cumulate labradorite with minor quartz, apatite, and opaque oxides. In the gabbro, clinopyroxene has been partly replaced by actinolitic amphibole. Chlorite and epidote are common secondary minerals in all these rocks.

Magnetitites are rocks with greater than 80% magnetite, commonly altered to martite, goethite, ilmenite, and leucoxene. Grain size may be up to 5 mm. The ilmenite originally occurred as exsolution lamellae or graphic intergrowths with magnetite, or as discrete, possibly primary, grains. Vanadium occurs in solid solution with magnetite and ilmenite, which are the main ore minerals (Ward, 1975).

Ward (1975) described an indicated vanadium resource for the Barrambie Intrusion of 27 Mt at 0.7% V_2O_5, with 15% TiO_2, and 26% Fe. The deposit has never been mined but Reed Resources Ltd is currently drilling the prospect with a view to detailing the resources. According to Reed Resources Ltd (2007), "The first JORC-compliant resource calculation over just 4 km of the 11 km strike of the Eastern Zone estimates indicated and inferred resources of nearly 48 Mt at 0.496% V_2O_5".

The Barrambie Intrusion appears to intrude strongly altered and deformed greenstones that include metamorphosed banded iron-formation and quartz–chlorite(–sericite) schist that may be derived from sedimentary or felsic volcanic rocks (Tingey, 1985; Chen et al., 2006; see Locality 15).

A short traverse up the rise at Locality 14 crosses plagioclase-rich metagabbro (MGA 714360E 6956860N) with cumulus plagioclase crystals up to 1 cm and less abundant, coarse, insterstitial pyroxene (now replaced by actinolite). Local outcrops of pegmatitic metagabbro contain large (up to 12 cm) crystals of altered clinopyroxene. There are also lenses and pods of meta-anorthosite. Farther up the rise there are more outcrops of mafic meta-pegmatite and metagabbro. The first layer of magnetitite is underlain in the slope by metapyroxenite (MGA 714215E 6956760N). The magnetitite layers are typically 2–3 m thick and are cumulates with crystals (1–2 mm in size) of vanadium-bearing titaniferous magnetite (altered to martite). Across the rise, layers of magnetitite are separated by metagabbro and there are local patches of magnetite-bearing meta-anorthosite. Small enclaves of finer mafic rock may be greenstone that has been caught up in the intrusion, or dolerite intrusions. Because of the limited exposure, way-up in the Barrambie Intrusion is unknown. Magnetitite layers on top of the rise are vertical to steeply east dipping.

Locality 15: Quartz–chlorite(–sericite) schist beside the Meekatharra–Sandstone Road

Return to the Meekatharra–Sandstone Road, and continue northwest for about 2.8 km to a low range of hills on the north side of the road (MGA 711164E 6960242N).

The strongly altered rocks at Locality 15 is typical of the greenstones in the Barrambie greenstone belt

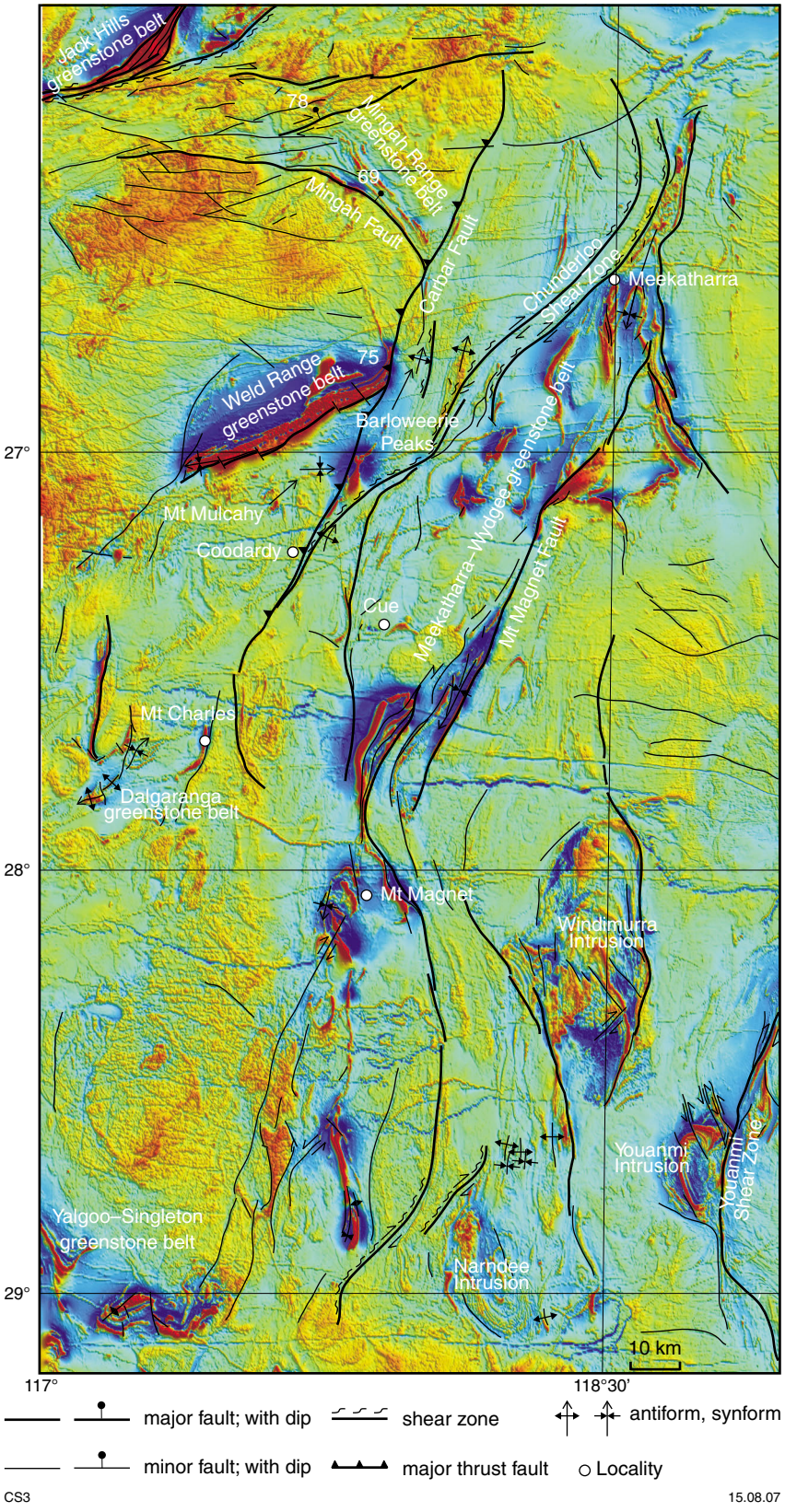

Figure 20. Simplified interpreted structural map of the northern Murchison Domain, showing localities and major structures, overlain on a reduced to pole, total magnetic intensity image. Structures shown are derived from the interpreted bedrock geology map in Geological Survey of Western Australia (2006), Hallberg (2000), GSWA's 1:250 000-scale geological series map sheets, and the Watkins and Hickman (1990) 1:500 000 geological map (after Spaggiari, 2006)

that occur with metamorphosed ultramafic rock, metabasalt, metamorphosed banded iron-formation, and metamorphosed clastic sedimentary rocks. The protolith most likely pre-dates the emplacement of the Barrambie Intrusion (Tingey, 1985; Chen et al., 2006) but the cause and timing of the alteration is unknown. Similar strongly altered rocks have been described near the base metal prospects at Freddie Well and Pincher Well which lie adjacent to the Youanmi Intrusion southwest of Sandstone (Figs 12, 20; Marston, 1979; Stewart et al., 1983). The protolith to these fine-grained quartz–chlorite(–sericite) schists is unclear but textural variation across the outcrop may reflect original bedding. Outcrops with angular clasts up to 3 cm suggest fragmental textures indicating a possible felsic volcanic or volcaniclastic component. At a larger scale, recessive units across the outcrop indicate a compositional variation, possibly related to original bedding, of the order of 100 m. Patches of sericite in some samples may represent retrograde alteration of andalusite.

Locality 16: Yarrabubba Impact Structure

by JA Bunting

Continue northwest along the Meekatharra–Sandstone Road for about 42 km to the prominent Barlangi Rock on the north side of the road (MGA 681774E 6991834N).

Recognizing a major eroded impact site is important not only because it can help explain otherwise puzzling lithological or structural features, but also because of implications for mineralization. Until recently, the only documented impact structures on the Yilgarn Craton were the small Dalgaranga crater (about 75 km west of Mount Magnet), and the Shoemaker structure (predominantly within the Proterozoic Earaheedy Basin). However, the impact record elsewhere suggests that major impact sites should exist on the Yilgarn Craton. The recently documented Yarrabubba structure (Macdonald et al., 2003) is one such site that gives regional clues to finding others in deeply eroded Archean terrains (Bunting and Macdonald, 2004).

At Yarrabubba, evidence for impact includes shatter cones, planar deformation features in quartz, pseudotachylites and impact breccias — all within the muscovite-bearing Yarrabubba Granite. The centre of the structure is the Barlangi Granophyre, a skeletal-textured felsic rock that is interpreted to have intruded as a multi-lobed sheet of subcrater impact melt derived from the Yarrabubba Granite (Fig. 21). The original size of the structure is not known, but some impact effects have been seen in outcrop at least 10 km north (the limit of outcrop) and 9 km south of Barlangi Rock. There is also a 25 × 15 km zone of flat aeromagnetic signature that may represent demagnetization of the regional granite as a result of the impact (Fig. 22).

Unlike most major impact structures, Yarrabubba has no obvious circular geological feature, because it appears

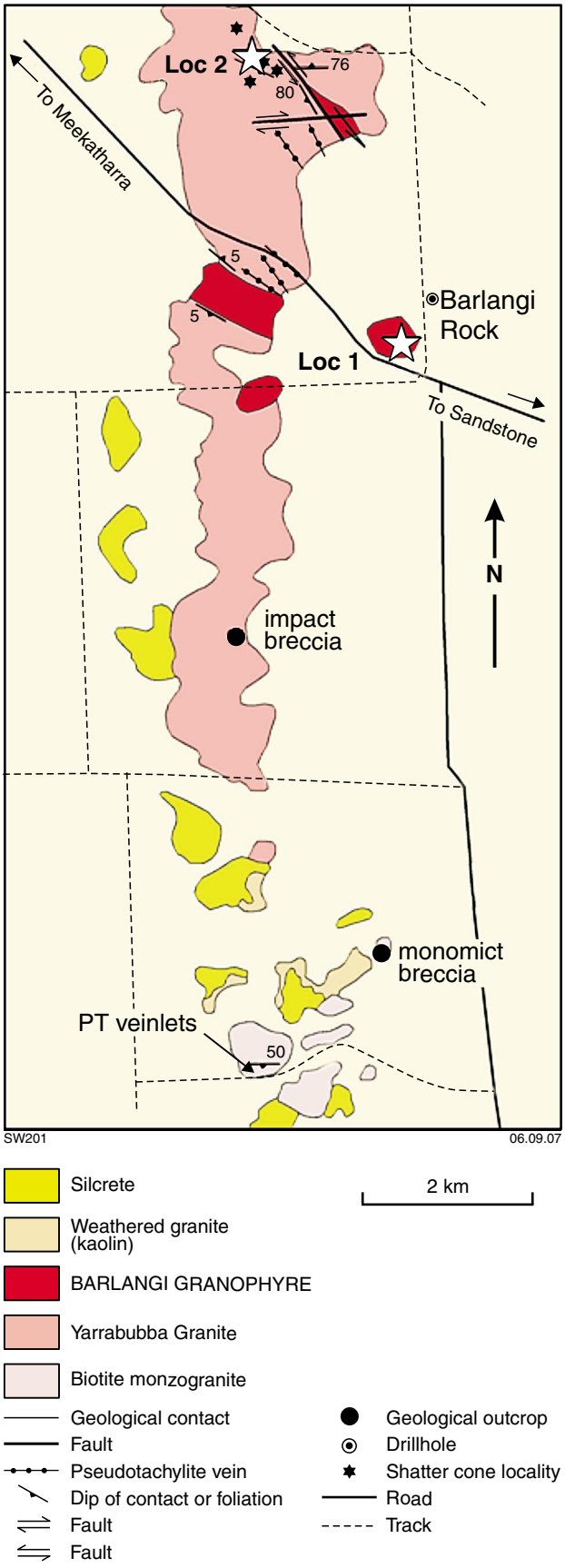

Figure 21. Yarrabubba simplified geology

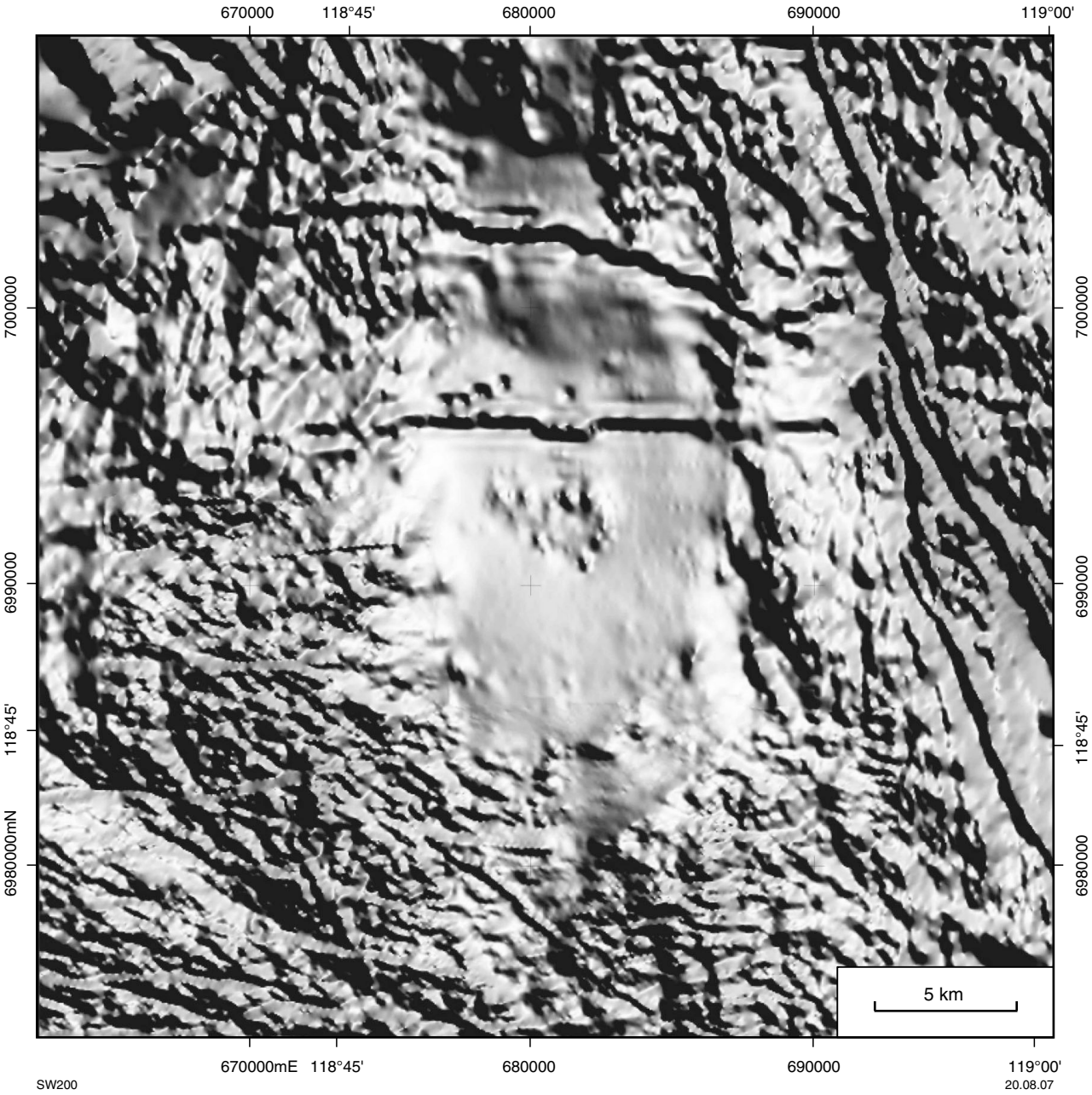

Figure 22. Yarrabubba aeromagnetic TMI image

to have been eroded to a level well below the crater floor. Discovery resulted from recognition by the GSWA of shock metamorphism in a single thin section of granite collected in 1979 during regional mapping, and mentioned briefly in the SANDSTONE 1:250 000 Sheet Explanatory Notes (Tingey, 1985). This was not followed up until the study by Macdonald et al. (2003) when the shatter cones, pseudotachylites, and minor breccias were discovered.

Three features at Yarrabubba are discernible on existing regional-scale datasets: (1) the muscovite-bearing Yarrabubba Granite — possibly evidence for alkali metasomatism; (2) the Barlangi Granophyre, distinguished by its unusual skeletal textures — interpreted as a sub-crater melt; and (3) the flat magnetic signature — interpreted as demagnetization immediately after impact.

The age of the impact is not known with any certainty. Zircons from the Yarrabubba Granite and Barlangi Granophyre give typical Archean ages around 2.6–2.7 Ga (Cassidy et al., 2002). Macdonald et al. (2003) concluded on regional grounds that the age was probably early Proterozoic. Pirajno (2005) reported an Ar–Ar age of 1134 ± 26 Ma from sericitized pseudotachylite, but this could be an alteration age and is therefore a minimum age. Macdonald et al. (2003) recognized K-metasomatism and reddening of feldspar in the granite. Pirajno (2005) ascribed these to hydrothermal alteration, along with veins of bladed calcite with fluorite, biotite (and chlorite), and prehnite.

Locality 16–1: Barlangi Rock

Barlangi Rock is the best of several outcrops of the Barlangi Granophyre. The granophyre is a pink, fine-grained rock, with scattered coarser grains of quartz and feldspar, and xenoliths of coarse-grained granite that range from a few centimetres to 0.4 m across (best seen a few metres north of the summit cairn). Unlike the Yarrabubba Granite, the granophyre contains no quartz veins, mafic dykes, or pseudotachylites. Fracturing (crude columnar jointing?) and gently southwest-dipping terraces are developed on Barlangi Rock, but not in the surrounding granites. The granophyre forms a multi-lobed sheet-like body that is interpreted as a subcrater intrusion of impact-generated melt. Evidence for this includes REE and trace element patterns that are identical to the Yarrabubba Granite and show no evidence for fractionation (Fig. 23).

In thin section, the coarser grains in the granophyre appear to be xenocrysts. The quartz xenocrysts are rounded, in part resorbed, and consist of a fine mosaic of granulated quartz (Fig. 24a). Similar granulated textures appear in quartz in the granite xenoliths and in the granite near the granophyre contact, but not in the main Yarrabubba Granite. Quartz needles in the Barlangi Granophyre form skeletal textures, indicating rapid quenching (Fig. 24a). These needles often radiate from quartz xenocrysts or around siliceous spherules, similar to nucleation textures described in the Vredefort (South Africa) impact melt. Shock features have not been observed in the granulated quartz, the granophyre, or the xenoliths; such is the case with most of the granular quartz of the Vredefort impact melt.

Locality 16–2a: Shatter cones and hairline pseudotachylites in Yarrabubba Granite

Return to road, turn left (southwest), drive 200 m and turn left on track. Drive north along the west side of a fence for 3.7 km (MGA 682045E 6995428N). Turn left onto a track and drive west for 1.5 km (MGA 680620E 6995563N). Turn left and drive cross-country for 250 m to Locality 2a at the base of the granite outcrop (MGA 680488E 6995339N). Please don't use hammer or remove shatter cones from this locality.

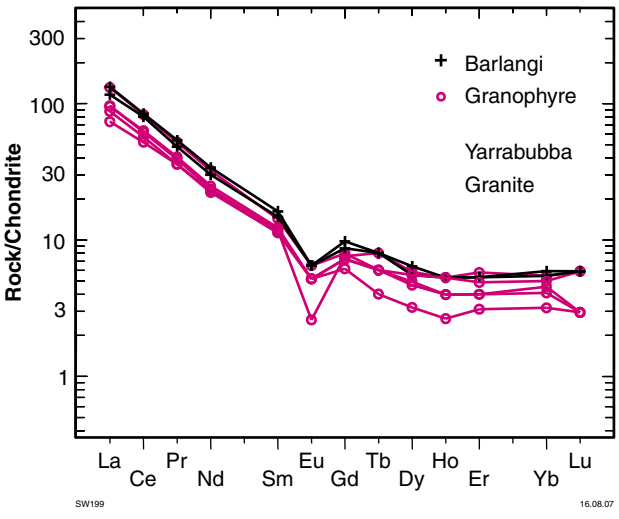

Figure 23. Element plots of five samples of Yarrabubba Granite and two samples of Barlangi Granophyre (data from Cassidy et al., 2002). C1 – rare earth elements; C2 – trace elements

This is the place where shatter cones (Fig. 24b) were first discovered at Yarrabubba in 2002. The original GSWA thin section, from which planar deformation features were first described by WG Libby, was from a sample of granite collected by SJ Williams about 1.5 km east of here in 1979.

The Yarrabubba Granite is a pale pink, medium- to coarse-grained monzogranite, consisting of quartz, albitic plagioclase and microcline, with subordinate muscovite and biotite. Here and near Barlangi Rock, quartz grains in the Yarrabubba Granite display multiple sets of planar deformation features (Fig. 24c). Plagioclase twin lamellae and cleavages in mica are commonly disrupted or bent. Biotite is commonly altered to a mixture of chlorite and iron oxides, and it also appears that muscovite was formed from hydrothermal alteration of biotite. Although brecciation in the Yarrabubba Granite is rare, in some outcrops the granite is so highly fractured that it could be classified as monomict breccia.

In general, shatter cones point upwards and have very divergent striation, indicating that the current exposure is far below the original source of the shock wave. Cones range from up to a metre in size to small reversed cones that are only about 10 cm in height. Also present are shatter fractures, the diagnostic feature of which is the presence of diverging striated features, known as 'horse-tailing'. Many of the shatter features at Yarrabubba are best described as shatter surfaces, which represent a transitional state between shatter coning and shatter cleavage. Also note sets of curved, discontinuous cleavage.

Also at this locality are millimetre-thick, black pseudotachylite veins that display 'cobweb' patterns. The veins consist of glassy recrystallized granite which in places, especially in thicker parts where veins join, is a microbreccia (Fig. 24d). Note evidence of movement along the veins where pegmatite veins are displaced by a few centimetres. Elsewhere at Yarrabubba, similar black pseudotachylites up to 20 cm thick have been noted.

Locality 16–2b: Xenolithic 'pseudotachylite' dyke

Walk about 230 m east-southeast to Locality 2b (MGA 680684E 6995227N).

Within the Yarrabubba structure are numerous dyke-like bodies that range in thickness from a few tens of centimetres to more than a metre. These bodies are generally of a flinty green aphanitic felsic rock that is intensely altered (?devitrified) to sericite and quartz (Fig. 24e), with rare inclusions of granulated quartz and feldspar. The texture is perhaps best described as ultramylonitic. Fault movement is indicated by displacement of pegmatite veins with partially melted pegmatitic clasts strung out within the melt. Here,

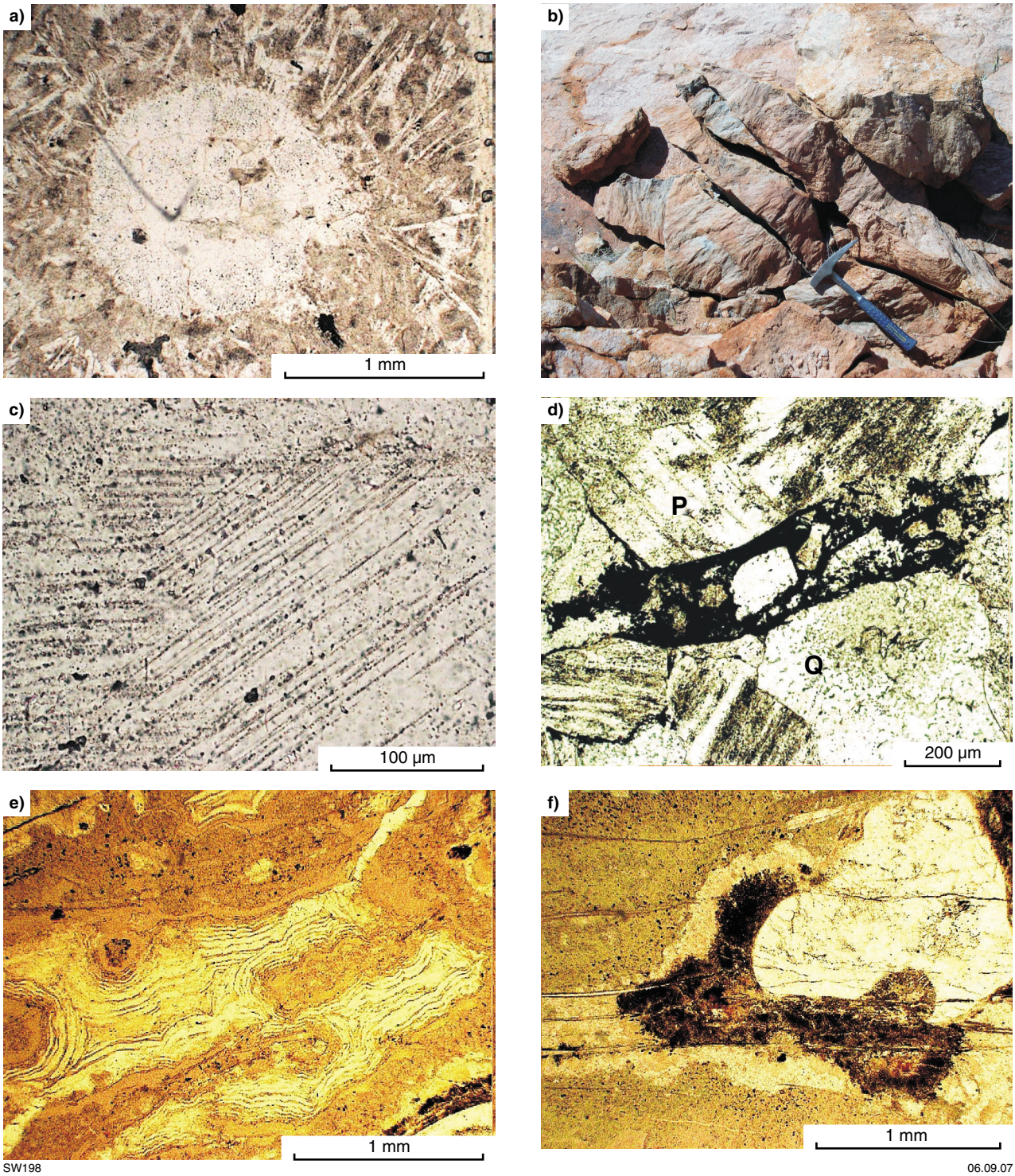

Figure 24. a) Barlangi Granophyre, Locality 1, showing spheroid (?xenocryst) of granulated quartz in groundmass of skeletal-textured quartz and feldspar; b) Shatter cones in Yarrabubba Granite, Locality 2a; c) PDFs in quartz, Yarrabubba Granite; GSWA sample 60399 X25, collected by S Williams, 1979; d) Pseudotachylite vein (black) in Yarrabubba Granite; P – plagioclase, Q – quartz; e) and f) 'Pseudotachylite' dyke, locality 2b; (e) – devitrified glass with flow texture; f) – resorbed and granulated quartz (white) and iron-stained feldspar (dark) with pink feldspar overgrowth, in devitrified glass, with later fractures

the thickest (up to 3 m) of these dykes has a central portion containing small (1–2 cm) streaked-out granitic xenoliths with potassium-feldspar overgrowths (Fig. 24f). Fracture cleavage (partly after flow layering?) and steeply-plunging rodding are also present. These dyke-like bodies are probably fault melts, related to the Barlangi granophyre, which can be loosely termed pseudotachylites.

The Pollele Syncline (Meekatharra–Wydgee greenstone belt) and the Abbotts greenstone belt

The Meekatharra–Wydgee and Abbotts greenstone belts (Fig. 25; Geological Survey of Western Australia, 2007c) contain a range of volcanic, volcaniclastic, and metasedimentary rocks that are typical greenstones of the Murchison Domain.

The Pollele Syncline lies at the northern end of the Meekatharra–Wydgee greenstone belt. Watkins and Hickman (1990) assigned the structurally lower part of the Pollele Syncline to their lower succession, the Luke Creek Group. They assigned the structurally upper part, containing a range of ultramafic, mafic and felsic volcanic rocks, to the Porlell Subgroup of the Mount Farmer Group. Recent SHRIMP U–Pb zircon geochronology, in which rocks have been dated at c. 2799 Ma (Locality 17; Wingate and Bodorkos, 2007b) and c. 2755 Ma (Locality 19; Wingate and Bodorkos, 2007c) in the centre of the syncline, suggests that there may be several unconformable successions in the syncline.

The Abbotts greenstone belt is different in character from the Meekatharra–Wydgee greenstone belt in that it contains numerous differentiated mafic–ultramafic sills. Watkins and Hickman (1990) assigned the Abbotts greenstone belt to their lower greenstone succession, the Luke Creek Group. Pidgeon and Hallberg (2000) suggested that the major, mafic part of the Abbotts Range greenstone succession belonged to their widespread, mafic-dominated Assemblage 3. However, as there is no geochronology from this belt, regional correlations remain speculative.

Locality 17: Felsic volcaniclastic and ultramafic sequence on the western limb of the Pollele Syncline, Meekatharra–Wydgee greenstone belt

by CJ Forbes

From Barlangi Rock, continue for about 40 km towards Meekatharra, past the prominent Mount Yagahong, an outlier of flatlying to shallow-dipping Proterozoic sandstone and conglomerate on the north side of the road. Southwest of Mount Yagahong, go past a major intersection (MGA 664210E 7022530N) to a broad bend (MGA 661750E 7023840N). Turn left onto the road to Pollele Homestead, and follow it for about 5.6 km to a north-trending fenceline (MGA 656420E 7022140N). Turn right (north) onto this fenceline and follow it for about 7.1 km to a gate on the north side of the rabbit-proof fence (MGA 656536E 7029280N). Turn left through the gate and follow the track for about 7.7 km (past Lordy Bore at about 4 km) to a track intersection (MGA 650265E 7032591N). Turn north onto the track and cross the creek. Just north of the creek, turn left at an intersection (MGA 650216E 7032688N) and cross a smaller creek. Drive cross-country for about 300 m to the base of a low rise (MGA 649946E 7032467N).

Locality 17 is on the western limb of the Polelle Syncline, close to the interpreted hinge trace. The metamorphosed volcaniclastic sediments in this area dip shallowly to the west beneath a sequence of metamorphosed peridotite–komatiite–pyroxene-spinifex-textured basalt that extends about 3 km to the north.

The volcaniclastic sediments are exposed on the eastern side of the small rise, and trend north-northwesterly. They include silicified, fine-grained, dark grey rock with subordinate coarser grained sandstone. In the sandstone, a very fine grained matrix of quartz and feldspar with minor biotite contains feldspar and lithic fragments that grade from 0.5 mm to <0.25 mm in size. Right-way-up (westwards) younging is given by graded bedding and bedding truncations (Fig. 26a). This rock has a SHRIMP U–Pb zircon age of 2799 ± 2 Ma (Wingate and Bodorkos, 2007b).

Up the rise to the west, the sediments are overlain by medium- to coarse-grained peridotite. Peridotite bodies occur as thin lenses, up to 30 m wide, within a succession of komatiite and komatiitic basalt and extend for up to 500 m in strike length, with a northerly trend that is subparallel to the volcaniclastic sediments. In this area there are at least two distinct peridotite lenses. The contact is undeformed and slightly uneven but appears to be conformable. The peridotite contains olivine and pyroxene, commonly altered to serpentine, and cumulate textures are locally preserved. The peridotite has a high magnetic susceptibility, and typically shows evidence of chloritization and retrogression.

Rubbly outcrop of komatiite west of the peridotite preserves coarse (up to 3 cm), randomly oriented, platy olivine-spinifex texture. The komatiite layers are generally less than 10 m thick. West of the komatiite, massive, coarse-grained, pyroxene-spinifex-textured basalt (Fig. 26b) contains needles of tremolite (after pyroxene) that are up to 10 cm long and 1 cm thick.

The differentiation trend across this shallow west-dipping succession indicates west younging, consistent with the graded bedding in the volcaniclastic sediments. The c. 2799 Ma age of the volcaniclastic sediments, and the fact that these rocks dip shallowly to the west on the western side of a syncline, suggest that this succession may be unconformable on the mafic–ultramafic–metasedimentary succession that makes up most of the Pollele Syncline. There is no geochronology on the main

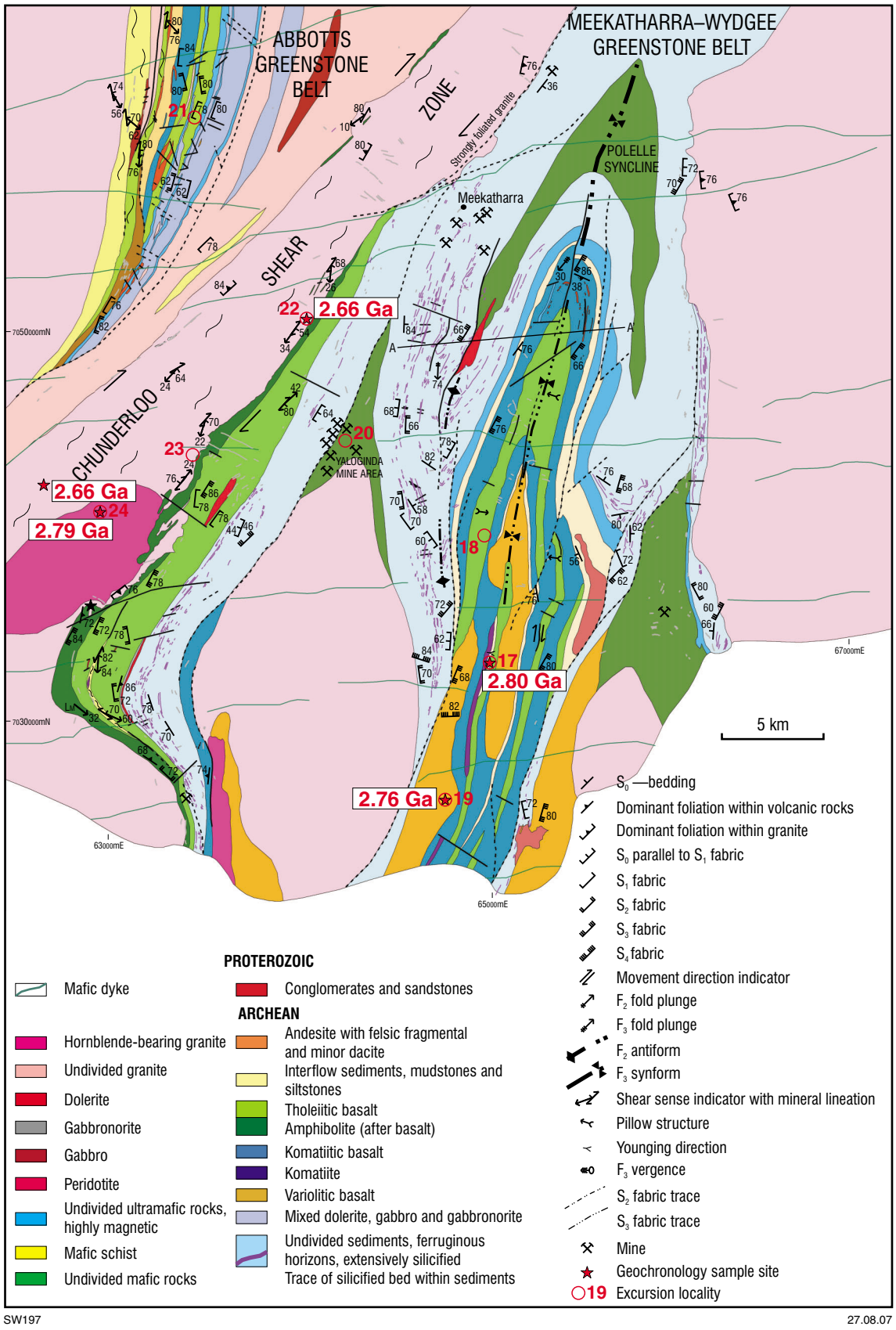

Figure 25. Interpreted bedrock geology near Meekatharra

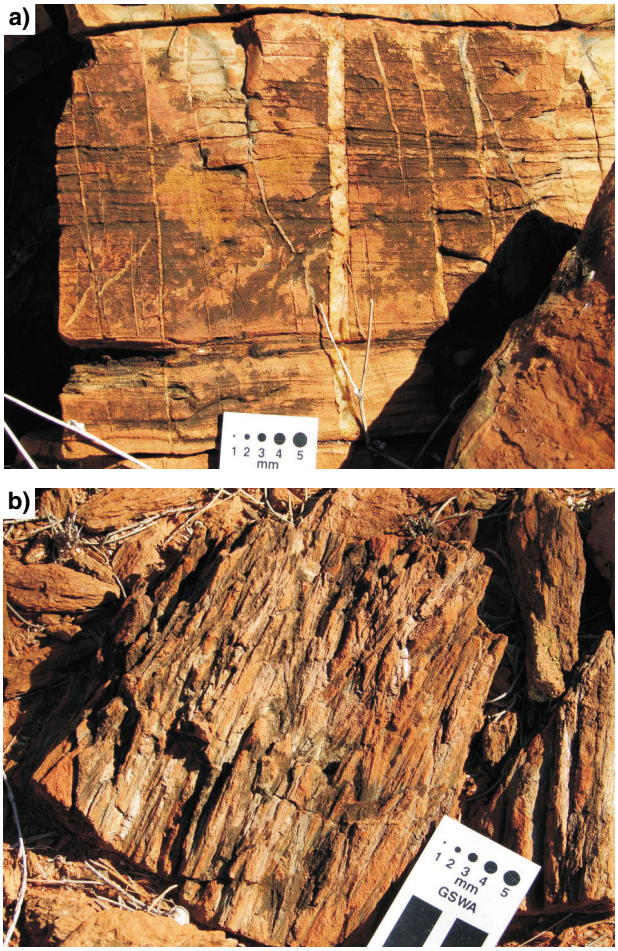

Figure 26. Volcanogenic rocks at Locality 17: a) Bedded felsic volcaniclastic rock with graded bedding and bedding truncations; b) Coarse-grained pyroxene-spinifex-textured basalt

(lower) part of the succession in the Pollele Syncline but it may be similar in age to the 2.95 Ga succession (Wingate and Bodorkos, 2007a) in the Weld Range to the southeast that also contains banded iron-formation.

Locality 18: Pillow basalts on the western limb of the Polelle Syncline, Meekatharra–Wydgee greenstone belt

by CJ Forbes

From Locality 17, go back across the small creek to the first intersection (MGA 650216E 7032688N), turn left and travel 7.9 km. The locality is at the northern end of the low range of hills (MGA 649655E 7039444N).

This locality is on the western limb of the Polelle Syncline. Well-preserved pillow structures in tholeiitic basalt show younging to the east, demonstrating that this large-scale synformal structure is a syncline. Andesitic volcanic and volcaniclastic rocks to the east lie in the core of the syncline (see Locality 19).

Locality 19: Andesite in the Meekatharra–Wydgee greenstone belt (Pollele Syncline)

by CJ Forbes

Return to the intersection south of the main creek near Locality 17 (MGA 650265E 7032591N). Turn right (west) at the track junction, cross a small creek, and go 1.9 km to a gate in the rabbit-proof fence. Go through the gate, continue south for 5.0 km to an intersection (MGA 647873E 7026852N), and turn left. Go past Woolgra Bore and follow the track heading southeast for about 400 m. Head off road in a southwesterly direction and go to the base of the hill and the locality (MGA 647935E 7025895N).

There are good exposures of andesitic volcanic and volcaniclastic rocks, close to the top of the exposed greenstone sequence, in the Meekatharra–Wydgee greenstone belt. Here, they are located on the western limb of the Polelle Syncline.

The andesite at Locality 19 has a very fine grained, pale green matrix with euhedral to subhedral phenocrysts of clinopyroxene and feldspar (up to 8 mm) that constitute up to 10% of the rock. The andesite has a SHRIMP U–Pb zircon age of 2755 ± 5 Ma (Wingate and Bodorkos, 2007c). This age is significantly younger than the c. 2799 Ma age determined on volcaniclastic rocks at the base of the komatiite succession at Locality 17, suggesting the presence of at least two ?unconformity-bound successions in the Polelle Syncline.

In the vicinity, outcrops of poorly sorted felsic fragmental rock contain angular, randomly oriented blocks of andesitic material up to 40 cm. The composition of the andesite blocks appears similar to the massive andesite at this locality. The fragmental rock is also host to more mafic, dark grey-green clasts that are better rounded than the andesitic clasts, but are still subangular. The clasts of the fragmental rock are set in a very fine grained, grey-green, siliceous matrix. Coarse, twenty-centimetre-scale bedding appears to fine to the east. There is common minor epidote alteration.

Meekatharra Goldfield

From Locality 19, go back past Woolgra Bore and travel 7.1 km to Rabbit Bore on the rabbit-proof fence (MGA 645336E 7031754N). Pass through the fence and drive 1.3 km north to a track junction (MGA 645175E 7033036N). Take the left fork and continue north, past Geoff Bore on the left, for 3.9 km to a major northwesterly trending track with a power line (MGA 645686E 7036834N). Turn left (northwest) onto this track and follow it for 7.2 km to the Great Northern Highway (MGA 650265E 7032591N). Turn right and drive about 2 km north to the entrance to the Mercator Bluebird minesite.

Summary by N Thébaud and J Vearncombe

Mercator Gold PLC (MCR)

Mercator Gold PLC listed on the London Stock Exchange (AIM) in October 2004. In January 2006, Mercator announced its intention to acquire, at a cost of A$18 million dollars, 100% control of the St Barbara Ltd's Meekatharra assets. The acquisition included ownership of the historically productive gold areas at Paddys Flat, Yaloginda, Nannine, and Reedy.

At Yaloginda, as part of the St Barbara purchase, Mercator Gold Australia acquired the Yaloginda Mill, with a rated capacity of 3 000 000 tpa of oxide material or 1 250 000 tpa of primary fresh ore.

Mercator's management is transforming the Company from junior explorer to mid-tier producer, and working towards profitable and sustainable production as soon as practicable.

Exploration work has been focused on defining viable gold resources capable of sustaining production. Specifically, exploration has concentrated on:

- Rapid exploration targeting and resource drilling in areas with demonstrated potential for mineable resources, focusing initially on Bluebird, Surprise and Prohibition–Vivian–Consols.
- Using up-to-date geological models and data analysis tools, including SpaDiS™, to identify both greenfield and brownfield exploration targets where large gold deposits may occur, and to rapidly drill test these targets.
- Maximizing the benefit of the valuable, yet imperfect, database with continuing data validation, collection of new geology data, and new active drilling.
- The consistent use of detailed structural geology to predict the location, continuity directions and shapes of ore zones.
- Keeping abreast of scientific discoveries and using the latest deposit models.

Mercator is creating value from the massive inherited but less than perfect database (Table 1). Data have been collated from more than twenty companies with digital and hard copy sources.

The commercial value of this database is not capable of quantification with any certainty but the Directors estimate that at today's values it would cost A$150 millions to acquire anew. These data were collected over a period of rapidly changing technologies from the 1970s pre-computer era, through the initial periods of digital data entry, to the modern period of data-integrating technologies. The data are variable in quality, and Mercator recognizes both the strengths and weaknesses of the data.

Recent resource evaluations take Mercator closer to mining with advanced mine optimization and scheduling studies at Prohibition, Vivian–Consols, Maid Marion, and Bluebird. These are expected to add to the company's Probable Reserves.

Table 1. Data components of Mercator Australia's Meekatharra region database

Technique	*Extent*
Diamond drilling	442 holes for 91 819 m
RC drilling	21 289 holes for 1 625 704 m
RAB drilling	44 160 holes for 1 389 752 m
AC drilling	3 419 holes for 167 876 m
Geophysics	15 different surveys

Since admission to AIM in October 2004, Mercator has identified and announced gold resources at Meekatharra of about one million ounces. These are in addition to the resources purchased from St Barbara Ltd in January 2006. Mercator's resource inventory is summarized in Table 2.

Regional geology

The Yaloginda and Paddys Flat mining areas are situated within the Meekatharra greenstone belt, which lies in the Northern part of the Murchison Goldfield (Fig. 27). Made up almost entirely of narrow Archean greenstone belts surrounded by granite and gneissic complexes, the Meekatharra greenstone belt is cross-cut by numerous Mesoproterozoic mafic dykes (Watkins and Hickman, 1990; Wingate et al., 2004). Geochronological studies suggest that most felsic intrusive and granitic rocks were emplaced between c. 3006 and c. 2626 Ma (SHRIMP and U–Pb model ages on zircons (Pidgeon and Hallberg, 2000; Cassidy et al., 2002)). The main supracrustal rocks comprise a sequence of submarine to subaerial mafic to ultramafic volcanic rocks, with interflow sedimentary rocks. Felsic intrusive rocks are also present within the belt, with dacitic to rhyolitic porphyry dykes and small granitic bodies common throughout the Meekatharra area. Overall, the supracrustal rocks are regionally metamorphosed in the middle greenschist facies, with metamorphic grades increasing in the vicinity of the granites (Alexander et al., 1991).

The Meekatharra greenstone belt consists of a northeasterly trending structural corridor located on the northwestern limb of an upright isoclinal fold, the Polelle Syncline (Spaggiari, 2006). The Meekatharra greenstone belt is interpreted as a major zone of shear-related deformation (Spaggiari, 2006) bounded to the west by the dextral Chunderloo Shear Zone, and to the east by the Mount Magnet – Meekatharra shear zone. The Yaloginda area sits in the northern strain shadow of the Archean Norie Pluton (2760 ± 8 Ma; Wiedenbeck and Watkins, 1993). The precise role of intrusion of the Norie Pluton into the Meekatharra greenstone belt with respect to the development of mineralization is not clear.

Mercator aim to achieve profitable and sustainable gold production. The Surprise and Prohibition deposits were foci of early exploration because of pre-existing legacy data that indicated potential mineable resources.

Table 2. Resource inventory for Mercator Australia's Meekatharra operations

	Indicated			*Inferred*			*Total*		
	Tonnes	*Grade*	*Ounces*	*Tonnes*	*Grade*	*Ounces*	*Tonnes*	*Grade*	*Ounces*
Yaloginda									
Bluebird	5 450 000	2.0	351 000	1 660 000	2.6	137 000	7 110 000	2.1	488 000
Bluebird South	1 433 000	1.1	52 000	1 346 000	1.6	67 500	2 779 000	1.3	119 500
Surprise[a]	3 603 000	0.9	109 000	1 303 000	0.6	25 000	4 906 000	0.9	134 000
Subtotal	*10 486 000*	*1.5*	*512 000*	*4 309 000*	*1.7*	*229 500*	*14 795 000*	*1.6*	*741 500*
Paddys Flat									
Prohibition	2 510 000	4.0	320 000	160 000	3.9	21 000	2 670 000	4.0	341 000
Vivian–Consols	405 600	9.3	120 800	276 100	7.4	65 700	681 700	8.5	186 400
Mickey	12 375 000	1.0	396 000	7 119 000	0.9	213 000	19 494 000	1.0	609 000
Doolan									
Ingliston	1 329 000	1.1	45 500	100 000	1.1	3 500	1 429 000	1.1	49 000
Golden Bar	379 000	1.4	17 000	50 000	1.1	2 000	429 000	1.4	19 000
Maid Marion	706 000	1.3	30 400	174 000	1.2	6 600	880 000	1.3	37 000
Subtotal	*17 704 600*	*1.6*	*929 700*	*7 879 100*	*1.2*	*311 800*	*25 583 700*	*1.5*	*1 241 400*
Reedy									
South Emu	618 000	3.4	68 000	100 000	3.0	10 000	718 000	3.4	78 000
Rand	891 000	1.9	55 000	1 458 000	2.7	125 000	2 349 000	2.4	180 000
Jack Ryan	534 000	2.1	36 000	846 000	1.7	47 000	1 380 000	1.9	83 000
Subtotal	*2 043 000*	*2.4*	*159 000*	*2 404 000*	*2.4*	*182 000*	*4 447 000*	*2.4*	*341 000*
Total	**30 233 600**	**1.6**	**1 600 700**	**14 592 100**	**1.5**	**723 300**	**44 825 700**	**1.6**	**2 323 900**

NOTES: Grade is in g/t. Ounces are Troy ounces. Small numeric differences may occur due to number rounding
(a) The Surprise resource is inclusive of the Company's Probable Reserves at Surprise of 992 000 tonnes @ 2.36 g/t for 75 000 ounces. This represents a conversion of resource ounces to reserves of 68%

Locality 20a: Surprise gold mine

N Thébaud, J Vearncombe, and N Culpan

The Surprise gold mine is approximately 800 km north of Perth and 15 km south of Meekatharra.

Introduction

The Surprise gold mine is located at Yaloginda (formerly Bluebird mining camp) adjacent to the Great Northern Highway. The Yaloginda area has produced over 1.4 Moz of gold from over a dozen deposits such as Bluebird, South Junction, Great Northern Highway (including Bluebird East), Surprise, Romsey, Mystery, Gibraltar, Maranui.

Gold deposits in the Yaloginda area are hosted in deformed and metamorphosed ultramafic rocks and felsic porphyry intrusives. Early models of mineralization at Yaloginda considered gold to be hosted by a regional ductile–brittle shear corridor referred to as the Gabanintha shear (Winnal et al., 1998). Previous studies reported a strong structural control on mineralization at Yaloginda, and highlighted many different structural settings of gold mineralization across several pits.

The Yaloginda/Bluebird mining area received most attention in the 1980s by Endeavour Resources, Metana and St Barbara Mines Ltd, and is now one of the several areas of focus for Mercator in the Meekatharra greenstone belt.

The Surprise pit was mined by St Barbara Mines Ltd between September 1997 and January 1998, and produced approximately 13 000 oz of gold. The exploration program by Mercator Gold Australia since 2004 has defined a new resource at Surprise of 134 000 oz and reserve of 992 000 t @ 2.36 g/t for 75 000 oz gold.

Deposit geology

Lithology

Two main rock types are observed in the Surprise pit (Fig. 28). These are high-Mg (komatiitic) basalts generally sheared to talc–chlorite–carbonate schist and porphyritic microgranite.

High-Mg basalts are metamorphosed to the greenschist facies, variably deformed and present as chlorite–amphibole(–talc–calcite) schist. Lower strain domains observed in the pit preserve relict pillow structures and spinifex texture.

Gold mineralization is hosted within porphyritic microgranite, generally referred to as 'porphyry', that is bounded by the high-Mg basalts. The porphyry contains 3–5% of 1–2 mm, round quartz phenocrysts and around 1% disseminated euhedral pyrite. This high-level intrusive

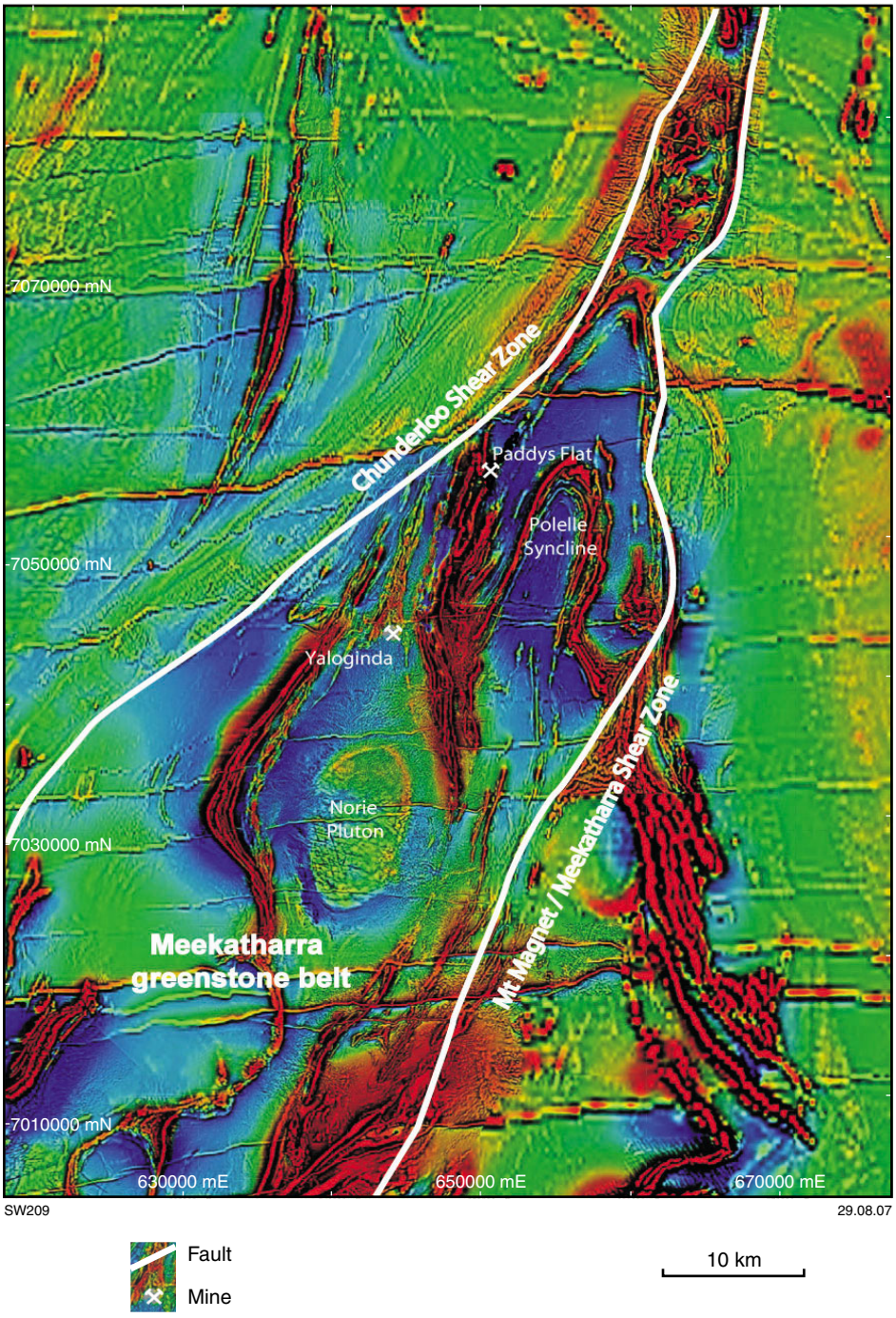

Figure 27. Regional aeromagnetic second vertical derivative image of the Meekatharra greenstone belt (GDA 94 Zone 50)

body varies in width between 5 and 50 m (true width), dips steeply (>80°) towards the west, and strikes between 000° and 020°. The porphyry extends over 700 m along strike, and aeromagnetic data over the Yaloginda area show a well-defined magnetic low that coincides with the known extent of the porphyry as determined by drilling.

Structure

Twenty metres away from the porphyry, the schistosity in the high-Mg basalt is subvertical and trends 160°, oblique to the trend of the porphyry. High-strain zones are localized along the porphyry margins, and earlier 160°-trending structures within 20 m of the porphyry have been rotated parallel to the porphyry (at 010°) with dextral shear sense (Fig. 29). Internally, the porphyry has very localized domains of steeply dipping schistosity at its margins and near its centre in the south.

Three overprinting foliations have been recognized around low-strain zones in the mafic schists, adjacent to the porphyry. The oldest foliation is subvertical and strikes

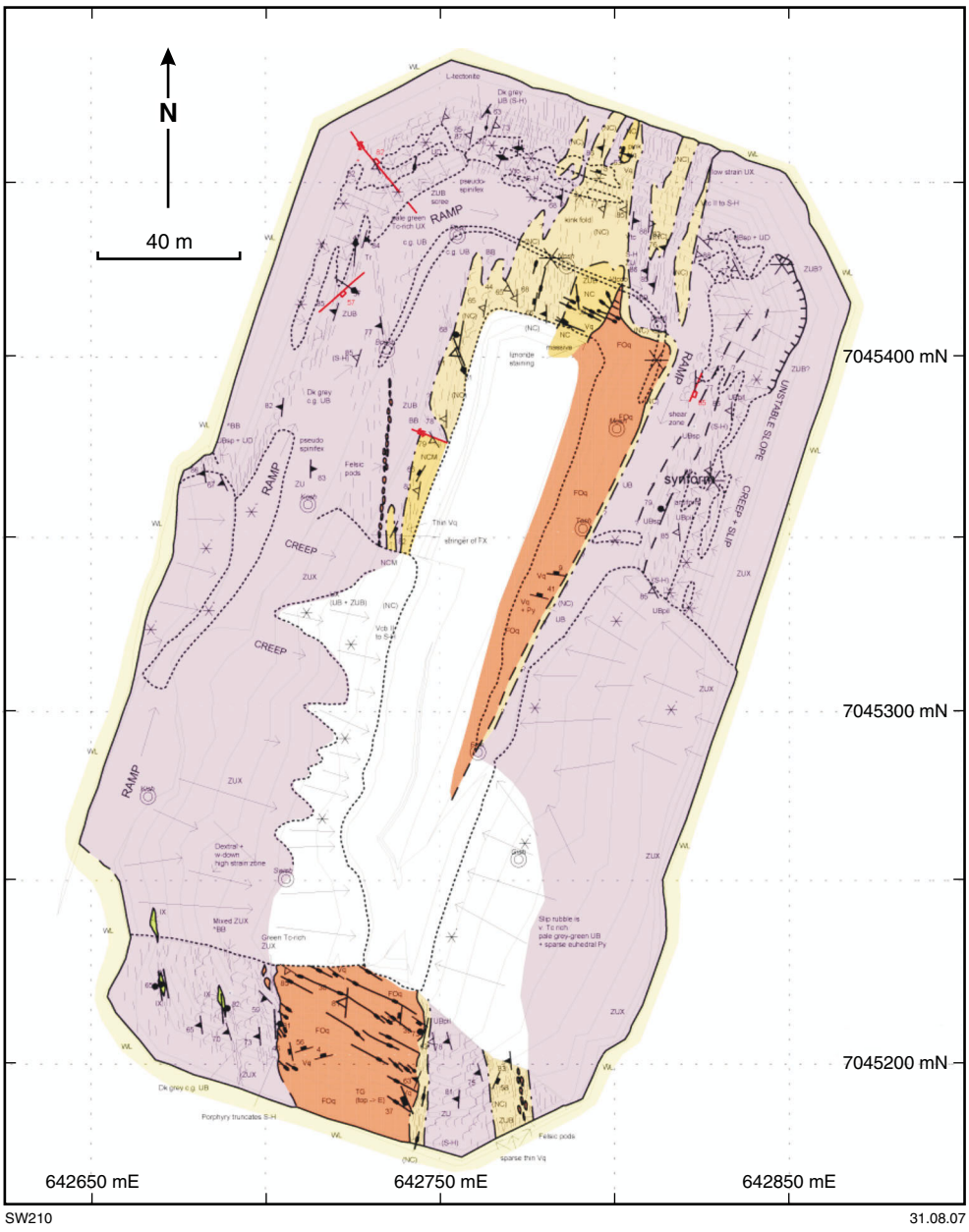

Figure 28. Geological map of the Surprise pit (Timms, 2006)

Figure 29. 3D Surpac-generated image of the mineralized Surprise porphyry

northwesterly. This foliation is overprinted by a subvertical northeasterly trending foliation which is truncated by a subvertical northerly striking cleavage.

Alteration and mineralization

Mineralization at Surprise is associated with a subhorizontal quartz vein package in the porphyry and on the western porphyry–high-Mg basalt contact. On this western contact, the high-Mg basalt is extensively carbonated, silicified, and contains numerous quartz–carbonate veins. Low-grade mineralization envelops trends to the north-northeast following the porphyry orientation (Fig. 29). Within that low-grade envelope, the high-grade zone trends to the northeast and dips steeply to the northwest.

Alteration associated with gold mineralization within the porphyry is sericite–quartz–pyrite(–gold). Veins in porphyry are mostly flat with a wide variation to 30° dip in any direction. A second set of steep quartz veins that strike east and dip south is recognized in an outcrop at the base of the pit. Pyrite is disseminated throughout the porphyry (typically <1%), but tends to increase in abundance in areas of quartz veining. Quartz veins vary from 1 mm to over 2 m wide, and are typically fractured and iron stained after sulfides. Quartz varies from milky white to translucent grey. Larger quartz veins commonly preserve earlier milky quartz, brecciated and annealed by later translucent quartz. Wallrock and chloritic bands are commonly entrained within the veins. Free gold has been observed within quartz and entrained silicate wallrocks in quartz veins. While there appears to be no rigorous link between the gold grade and the amount of quartz veining, intervals that are gold mineralized are invariably veined with quartz.

Quartz veins in host high-Mg basalt are mostly steep, parallel to schistosity and/or porphyry margins, and restricted to alteration zones. The sheared contact zone between the porphyry and the high-Mg basalts is locally Au mineralized, with typically only the immediately adjacent 1–2 m affected. However, wider zones of alteration and mineralization in the basalt have been encountered, particularly at the western contact with the porphyry in the northern end of the pit. Alteration of the basalt away from the contact with the porphyry is a pervasive, regional carbonate (calcite) alteration. At the contact with the porphyry, the alteration (gold mineralization) assemblage is Fe carbonate (ankerite)–quartz(–sericite/fuchsite–pyrite).

Other alteration noted at Surprise is pervasive silicification of portions of the porphyry, and chloritic alteration — either as narrow, subhorizontal veinlets, or finely disseminated. Neither the silicification nor chloritic alteration appear to have any relevance to the location of gold mineralization.

Resource and production

The ore reserve for the optimal open pit, based upon a gold price of A$750 per ounce, is 992 000 t at 2.36 g/t for 75 300 oz gold. The open pit will produce gold at

a cash cost of A$342/oz (US$260/oz). The Surprise pit optimization and final pit design have been based on current openpit mining practices; mining dilution of 10% and ore recovery of 95%; and metallurgical test work confirming recoveries of 93 to 95% from ore with a Bond Mill Work Index of 12 to 15 kwh/tonne. The optimal open pit at A$750 per ounce is 992 000 t @ 2.36 g/t for 75 293 oz gold. The pit has a strip ratio of 5.6:1 and a net cash cost per ounce of A$342. The Surprise pit is located within 100 m of a major public highway. As a cutback is required to take this pit deeper, the highway must be diverted to meet safety codes. Tenders and approvals from statutory authorities have been received to execute this work.

Production from the Surprise pit, taking into account the high nugget effect within the Surprise orebody, the cut and uncut grade models, and the mining dilution and recovery factors, is expected to produce between 60 000 and 68 000 oz of gold. This production should take place over a six to seven month period.

Acknowledgement

N Timms is thanked for his landmark geological report on the Surprise deposit, and S Vearncombe and D Hollingsworth for their critical insights.

Locality 20b: Prohibition gold mine

N Thébaud, D Hollingsworth, and J Vearncombe

The Prohibition gold mine is about 800 km north of Perth and 1 km southeast of Meekatharra.

Introduction

The Prohibition gold mine, located within the Paddys Flat mining area, lies immediately southeast of the Meekatharra township (Fig. 30).

The Paddys Flat mining area is located on a northeasterly trending, steeply dipping shear zone. Forming a 200 m-wide deformation zone, the Paddys Flat mining area has been variably deformed and altered, with much of the primary lithological texture destroyed. The host rocks are now represented by talc schists, talc–chlorite and chlorite schists, and carbonate–(quartz–fuchsite–sulfide) rocks forming alteration haloes around intrusive K-feldspar porphyries and discontinuous iron-rich chert bodies.

Mineralization in the Paddys Flat mining area is structurally controlled, with four distinctive styles (Fig. 31). The first style is associated with intensely altered intermediate to felsic volcanic rocks located on the western side of the shear zone (Butler and Commodore). The second style is associated with quartz veins within the felsic porphyries and disseminated throughout the quartz–carbonate–fuchsite–sulfide-altered ultramafic rocks in the middle of the shear (Consols, Vivian, Ingliston, Albert). The third style is sitting within a strongly altered ultramafic assemblage on the eastern edge of the shear (Phar Lap, Mickey Doolan, McQuarie, Halcyon, Democrat). The fourth mineralization style occurs in the iron-rich cherts located on the western margin of the Paddys Flat shear zone (Prohibition).

There is little control on the age of the main deformation and mineralization events throughout the Murchison Goldfield. However, the development of the Meekatharra and Chunderloo shear zones is likely to be syn- to post-emplacement of the granitic bodies dated at around 2650 Ma (Spaggiari, 2006).

Gold was first found at Paddys Flat in 1896. Historic production from underground mines was around 900 000 oz. Fenian, the largest historic underground mine, produced 1.55 Mt of ore at an average grade of 16.8 g/t (630 000 oz).

Modern mining (mainly open pit) of the Paddys Flat central district was conducted between 1979 and 1995, and resulted in the production of 16.63 Mt @ 2.1 g/t for 1 005 000 oz from numerous pits (Fig. 30). Owned in succession by Forsyth NL, Patshore Pty Ltd, Plutonic Resources Ltd, Dominion Mining Ltd, Barrick Gold Corporation and St Barbara Mines Ltd, the Paddys Flat tenements were acquired by Mercator in January 2006.

Mineralization within the ‘Prohibition BIF’ has been exploited by both underground and open-pit mining for over 100 years. Recorded historical underground production reached 30 676 oz, with open-pit mining conducted by Dominion between 1989 and 1995 producing 91 720 oz. The Prohibition deposit is now managed by Mercator and a recent extensive exploration program led to the redefinition of the geological style of the deposit and its resource. Recent calculation suggests a total resource of 2 670 000 @ 4.0 g/t for 341 000 oz of gold.

Deposit geology

Lithology

The Prohibition deposit is located in a sequence of easterly dipping interflow tuffaceous and locally iron-rich cherty sedimentary rocks known as the ‘Prohibition BIF’. The sedimentary rocks lie within a sequence of mafic rocks immediately west of the Paddys Flat shear zone. The textural and mineralogical features of these units are discussed below.

Metabasalt

Chlorite schist in the Prohibition deposit is interpreted to represent an original sequence of basaltic flows. Channel-like features with textures different from those of the surrounding basalt can be seen in low-strain areas. The channel-like structures contain large chloritic and/or chalcedonic amygdales in a coarse matrix. The contact between the channel-like structures and the surrounding basalt is sharp and distinct. The structures have been interpreted as degassing tubes through which volatiles escaped from the cooling lava.

Figure 30. Paddys Flat mining area location map

A strong metamorphic overprint is evident in the form of chlorite and carbonate alteration. The chlorite is strongly aligned and defines the dominant fabric in the rock.

Volcaniclastic sediments

Interflow volcaniclastic sedimentary rocks range in thickness from less than 1 m up to approximately 40 m (i.e. the sedimentary rock containing the banded chert known as the 'Prohibition BIF'). Much of the sedimentary rock is composed of fine volcanic ash and pumice fragments with rare lapilli. Fragments of volcanic detritus are up to 4 cm in diameter. However, there is also abundant fine-grained, silty, and well-laminated sedimentary rock. Consistent younging towards the east is based on the presence of graded laminations and erosional truncation of bedding laminations.

The interflow sedimentary rocks are dominated by fine-grained chlorite and carbonate. In the absence of

bedding, the extensive chloritization of the sediments and alignment of chlorite along the foliation can make it difficult to distinguish the sedimentary rock from the mafic-derived chlorite schist. The chloritization has also affected coarse volcanic fragments and lapilli. In most samples, the internal texture/structure of the clasts has been partially or completely destroyed.

Banded chert

The 'Prohibition BIF' is a sequence of iron-rich banded chert of uncertain origin. This lithotype is composed of interbedded, ferruginous, cherty sedimentary rocks with chlorite-rich (possibly representing chloritized ash flows) and chert/jaspilite bands of varying thickness.

The banded chert contains numerous magnetic dark bands consisting of medium- to fine-grained, xenoblastic magnetite aggregates forming overgrowths on fine, disseminated hematitic layers. Xenoblasts of magnetite commonly occur with euhedral, iron-rich carbonate (ankerite or siderite). Both the carbonate and magnetite are clearly secondary as they overgrow the original banding and define the foliation.

Chlorite-rich bands that form the second main constituent of this lithotype are composed of interlocking mosaics of granoblastic chlorite surrounding microcrystalline quartz aggregates.

Structure

The Prohibition deposit is located on the western limb of the Polelle Syncline, a regional upright fold in the middle of the greenstone belt. A series of northeasterly trending dextral shears that pass to the east, and possibly the west, of the Prohibition deposit are related to, or post-date, development of the Polelle Syncline.

The stratigraphy within the Prohibition deposit has been folded prior to development of the brittle Prohibition fault set. A moderately to steeply plunging, west-verging asymmetric (Z) fold is clearly visible on the western side of the Prohibition pit (Fig. 31). An axial-planar foliation associated with this fold event is well developed throughout the volcaniclastic sedimentary and mafic volcanic rocks within the pit, and dips steeply to the east.

While the fabric is preserved only within the mafic volcanic part of the sequence, the contact between the mafic volcanics and volcaniclastic sediments is clearly folded. Abundant small-scale folding is evident within both the banded chert and the surrounding volcaniclastic sedimentary rocks. Small-scale folds within the banded chert commonly show variation in axis orientation and plunge consistent with a high degree of non-cylindrical behaviour.

Numerous westerly dipping faults (the Prohibition fault set) have been recognized within, or interpreted beneath, the Prohibition pit (Fig. 32). Of these faults, the Prohibition fault has the greatest displacement (40 m), with subsidiary faults displaying offset of less than 10 m. The faults are evident in the 'BIF' as zones of brecciation, veining, and sulfidation, up to 10 m wide. Within the less competent sedimentary rocks and chlorite schist, the faults are a series of anastomosing brittle–ductile faults. In the northern wall of the pit, secondary linking faults are present where the primary faults are separated by less than 30 m.

Mineralization

Mineralization in the Prohibition deposit is intimately associated with the intersection between the banded chert and the westerly dipping Prohibition fault set where fracturing is widely developed (Fig. 33).

Alteration associated with mineralization consists of quartz–chlorite–albite–sulfides +/- carbonate-brecciated zones. In gold-rich zones, the dominant alteration assemblage is moderately sulfidic, indicating a strong correlation between sulfur and gold (Fig. 34). The dominant sulfide phase is pyrite, but significant amounts of arsenopyrite (or lollingite) have been documented, representing up to 30% of the sulfide content. At a finer scale, the ore zones commonly display an intergrowth of pyrite and arsenopyrite within and adjacent to breccia veins, with gold grains of between 5 and 200 mm evident along fractures within, or at the margin of, pyrite.

The alteration texture suggests that the alteration process was selective with the replacement of iron-rich bands by pyrite and arsenopyrite. This replacement is typically adjacent to vein structures and forms centimetre-scale replacement haloes. The sulfides have a zoned distribution, with arsenopyrite being the dominant proximal species and pyrite becoming dominant farther away from the veins. A similar pattern occurs at a larger scale (faults).

Rare gold-bearing quartz veins have been encountered within the mafic schist outside the banded chert.

Acknowledgement

S Vearncombe is thanked for her critical insights; and E Maidens for her valuable work on the definition of the Prohibition resource. A van Roij is thanked for structural measurements of drillcore from Prohibition that helped to define the overall geometry of the orebody.

Locality 21: Layered mafic–ultramafic sequence in the Abbotts greenstone belt

by CJ Forbes

From Meekatharra, head west on the Gascoyne Junction–Carnarvon Road for 15.2 km. Turn right onto the track at the yellow diamond-shaped corner sign (MGA 633625E 7058160N). Follow this track for about 3.2 km (MGA 635670E 7062077N). Turn left off the track and travel cross-country in a westerly direction to the base of the prominent ridge (MGA 634443N 7060920N).

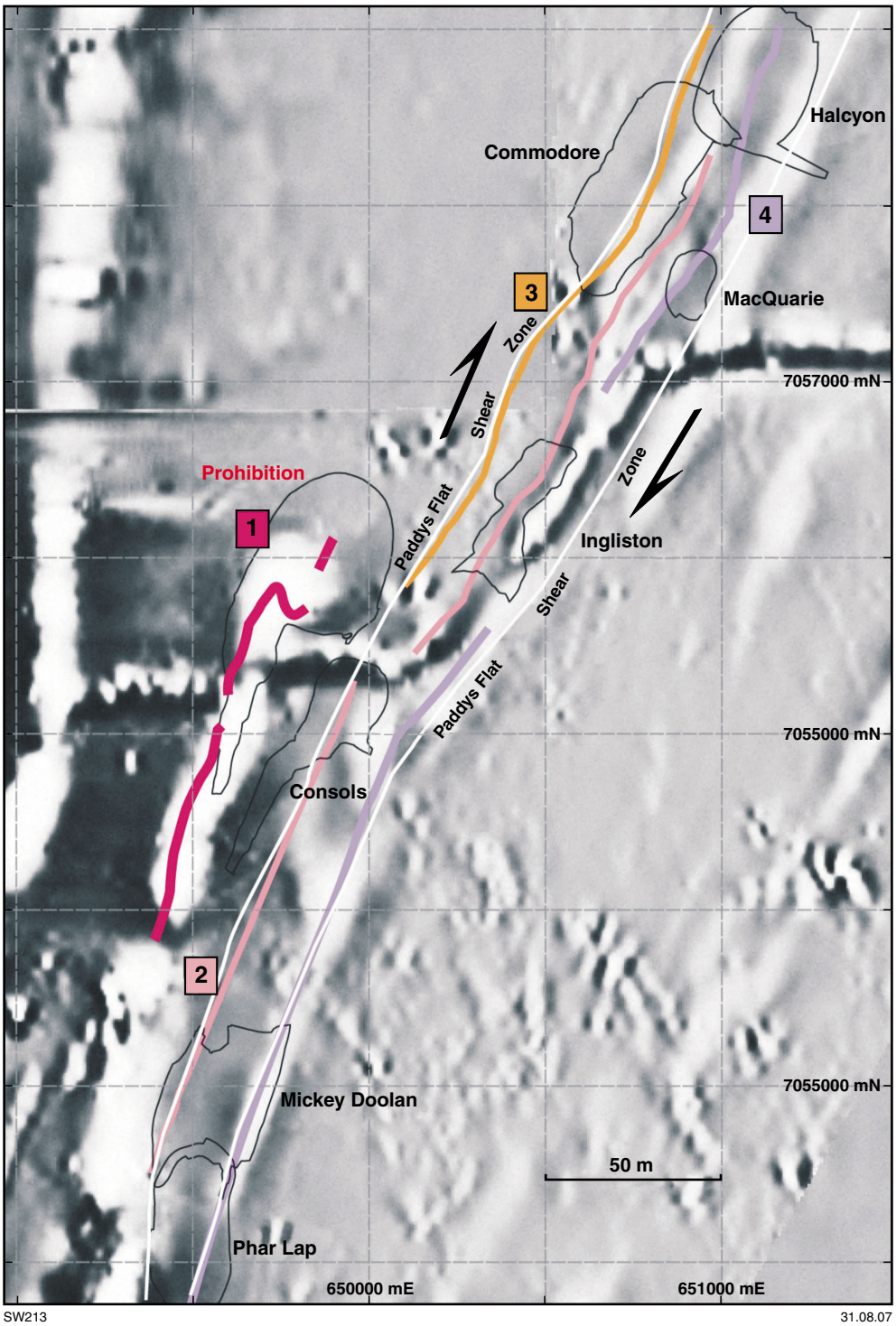

Figure 31. Various mineralization styles recognized at Paddys Flat. 1: Fe-rich chert hosted mineralization. 2: Porphyry and alteration halo hosted mineralization. 3: Undifferentiated felsic volcanic hosted mineralization. 4: Sheared ultramafic and or intermediate volcanic hosted mineralization. (Background: Second vertical derivative of the total magnetic intensity)

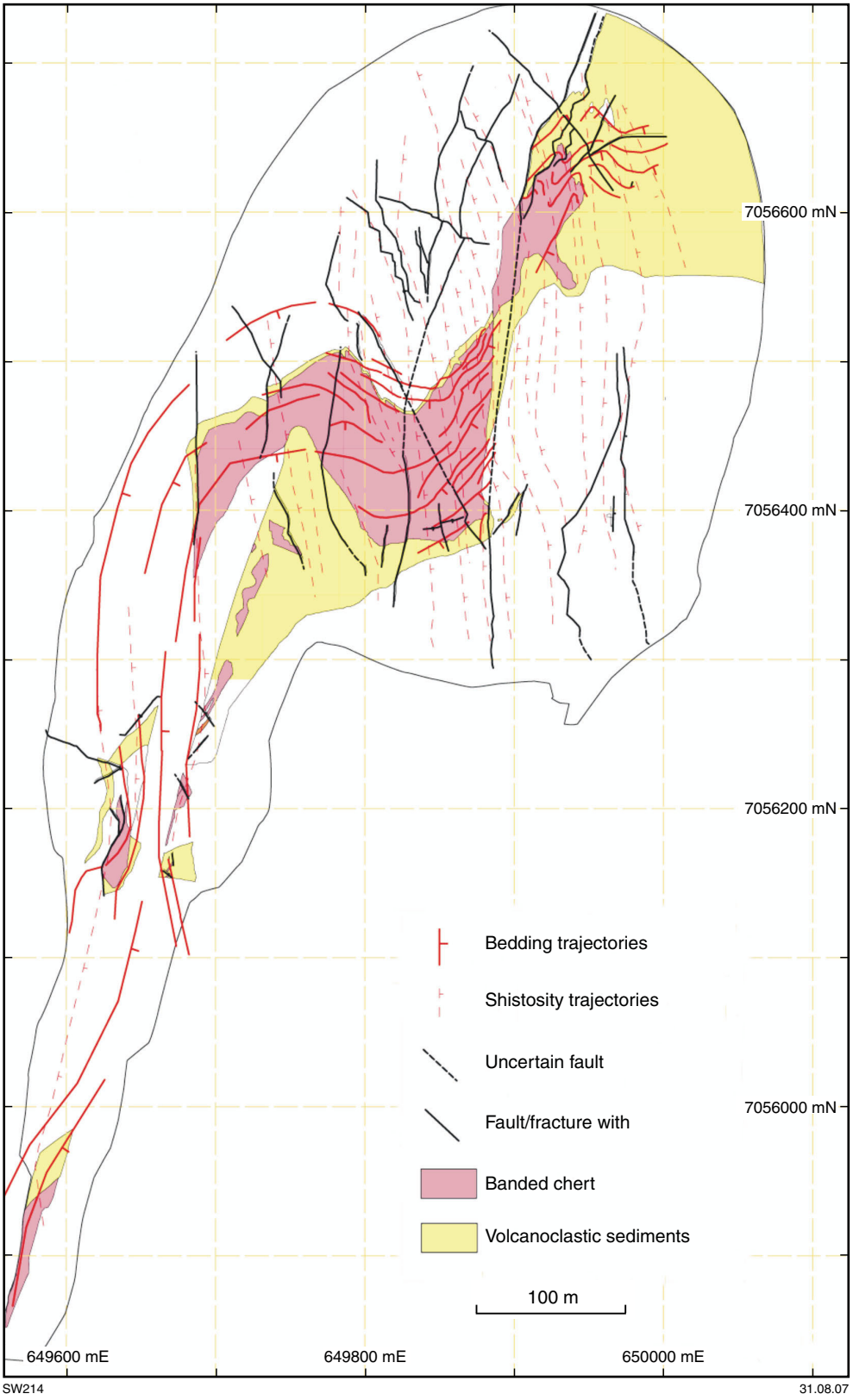

Figure 32. Geological interpretation sketch of the Prohibition pit

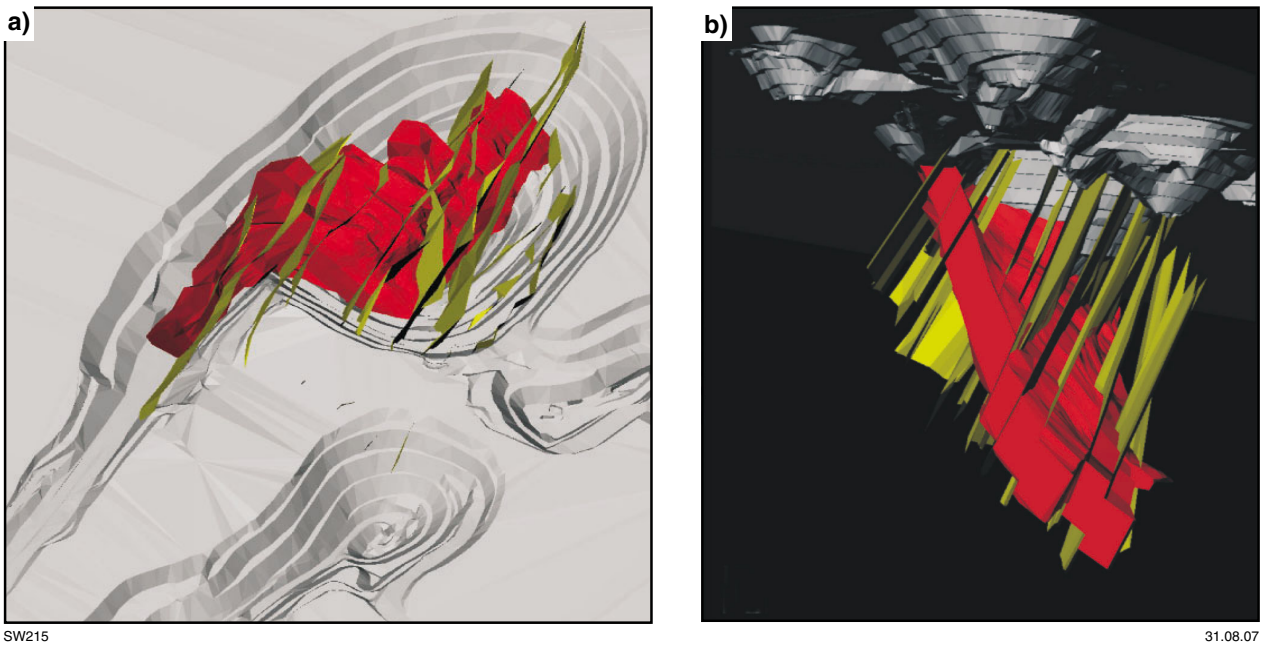

Figure 33. 3D geological model of the Prohibition deposit in a map view a) and looking north b). The red wireframes represent the banded ferruginous chert and the ochre wireframes represent the numerous westerly dipping faults that control the mineralization

This locality involves a short east to west traverse through a layered mafic–ultramafic intrusive unit that may have a strike extent of more than 40 km in the central part of the Abbotts greenstone belt.

At the start of the traverse, a small outcrop of felsic rock is one of the few examples of this unit exposed in the Abbotts greenstone belt. The felsic rocks are altered but probably andesitic in composition, with a pale green, very fine grained matrix containing phenocrysts of feldspar and subordinate amphibole. Altered plagioclase and K-feldspar phenocrysts (typically <3 mm) make up more than 10% of the rock, and are euhedral to subhedral, commonly with ragged edges to grains. Some grains appear broken. The pale green amphibole is finer, up to 1 mm, and less abundant. The rock also contains fine-grained mafic xenoliths that range in size from one to five centimetres. Although moderately altered, the presence of ragged and broken grains, and the range in grain size, and grain and clast type, in this rock suggest that it is volcaniclastic.

West of the felsic unit, a 50 m-wide metagabbro interval consists of coarse-grained amphibole (after pyroxene), biotite, and feldspar. In general, the gabbro becomes finer grained and less leucocratic to the west. Thin units of gabbronorite within the gabbro contain phenocrysts of altered orthopyroxene up to 15 mm long. The orthopyroxene is weathered brown and constitutes up to 30% of the rock. To the west, the gabbro grades into dolerite which is a finer grained (up to 1 mm) equivalent of the gabbro.

Farther west, the dolerite is in sharp contact with rubbly outcrops of red-brown, weathered ultramafic rock. This unit, which is up to 50 m wide and has a very high magnetic susceptibility, is a fine- to medium-grained peridotite with well-preserved (typically ortho- and meso-) cumulate textures. It consists principally of olivine (typically altered to serpentine and talc), pyroxene (commonly altered), and magnetite. The mafic–ultramafic succession described above is repeated to the west, but the overall differentiation trend does not give a clear indication of younging direction.

The mafic–ultramafic succession described above is repeated to the west. The extent and number of mafic–ultramafic bodies in the Abbotts greenstone belt is difficult to determine as the exposure to the east is limited. Aeromagnetic images show evidence of numerous highly magnetic rock packages to the east of the exposed Abbotts greenstone belt, and may indicate other intrusions, or multiple repetitions of the same intrusion. Similar mafic–ultramafic intrusions are not found in the Meekatharra–Wydgee greenstone belt, suggesting the two greenstone belts may have been deposited in separate basins.

All rocks along this traverse show evidence of retrograde metamorphism (e.g. talc and chlorite).

Locality 22: Chunderloo Shear Zone

by CJ Forbes

From Meekatharra, go 5.5 km along the Gascoyne Junction–Carnarvon Road. (From Locality 21, return to the main road, turn left and go 9.8 km then turn right at the first grid). At the first grid (MGA 643170E 7056745N), turn left (south) and follow the track on the east side of the fence for 4.6 km to a fence junction (MGA 643106E

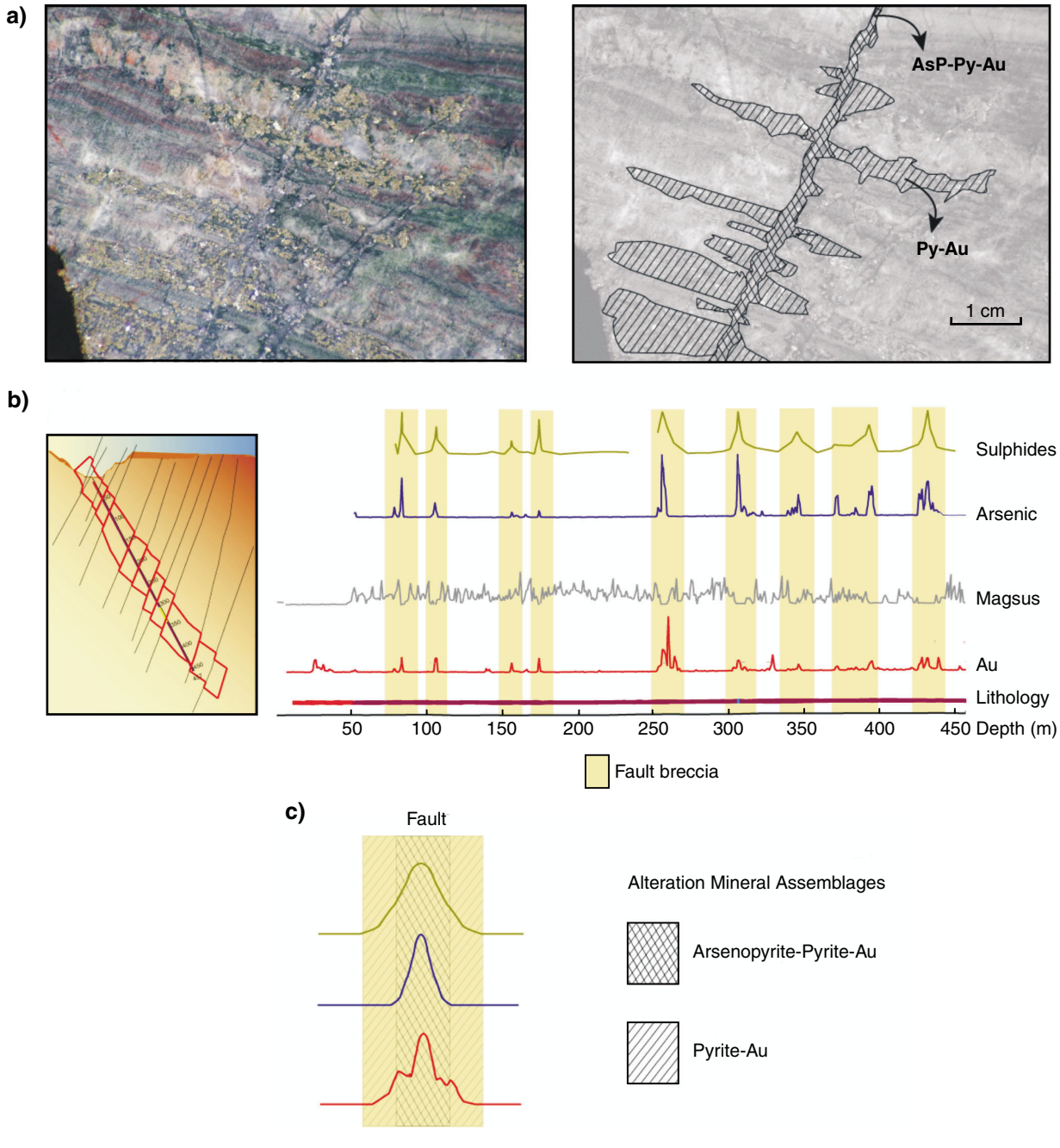

Figure 34. Distribution of the gold (Au) and sulfide in the mineralized sections: a) Photograph of a hand specimen showing the selective replacement of iron-rich layers by pyrite (Py) and arsenopyrite (AsP). Note the zonation in the distribution of both mineral phases with the arsenopyrite preferentially deposited on the rim of the veins and the pyrite halo extending along the original bedding; b) Evolution in the gold content versus the magnetic susceptibility, the concentration in arsenic (used as a proxy for arsenopyrite), and the sulfide content across the westerly dipping faults; c) Schematic diagram presenting the detail of the zonation of the mineral assemblages across brecciated areas

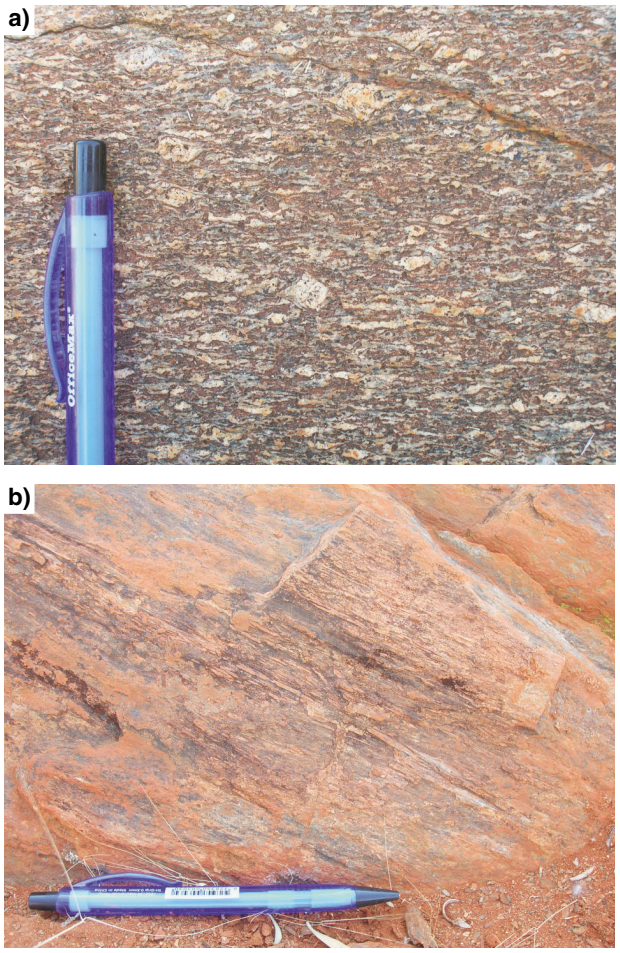

Figure 35. a) Sheared feldspar phenocrysts within granite showing dextral kinematics. Photo taken looking to the east, subparallel to the mineral lineation and perpendicular to the shear plane (C-plane); b) Mineral lineation defined by amphibole and feldspar on the dominant foliation plane of the high-strain amphibolites. North to the right of photo

7052128N). Turn right at the junction and go through the gap in the fence. Travel west along the track for 2.2 km (MGA 640813E 7052155N). Just before the creek, turn south-southwest and go off-road to the locality (MGA 640543E 7051839N).

The Chunderloo Shear Zone (Spaggiari, 2006) is a kilometre-scale, northeasterly trending structure that separates the Abbotts greenstone belt from the Meekatharra–Wydgee greenstone belt (Fig. 25). The shear zone is prominent in aeromagnetic and gravity images (Figs 20, 27), and traverses mostly granitic lithologies.

At Locality 22, the Chunderloo Shear Zone is exposed within granite and greenstone of the Meekatharra–Wydgee greenstone belt. The shear plane is developed pervasively in the granite (monzogranite to granodiorite). A well-developed mineral lineation, defined by elongate quartz and feldspar, is preserved on the C-plane, and plunges shallowly southwest. In other areas, the mineral lineation plunges shallowly northeast. Kinematic indicators such as S–C fabrics and asymmetric feldspar porphyroblasts are well preserved in the granite, and mainly show dextral movement (Fig. 35a).

To the east, the sheared granite is in contact with high-strain amphibolites. The shear fabric is mostly subparallel to the contact. However, where the contact is locally at an angle to the shear fabric, the shear fabric is continuous across the contact. Kinematic indicators such as S–C fabrics are difficult to see within the strongly foliated amphibolites, and have a well-developed, northeasterly plunging mineral lineation, defined by amphibole, on the foliation plane (Fig. 35b).

Although there is a change in the plunge of the mineral lineation between the granite (southwest) and the amphibolite (northeast) at this locality, the dominant foliation plane (shear plane) has a consistent orientation. South of here (see Locality 23), where the granite–greenstone contact is exposed outside the Chunderloo Shear Zone, the contact is often sheared, with shallow northeasterly plunging mineral lineations and dominantly dextral shear-sense indicators. The change in mineral lineation plunge direction in this area may be due to one or more of a number of possibilities: (1) the contrasting lithologies and folding; (2) the mineral lineations developed during different times of shear zone activity; and (3) the northeasterly plunging lineation in the greenstones developed during deformation along the granite–greenstone contact, whereas the southwesterly plunging mineral lineation in the granite is due to larger scale deformation in the Chunderloo Shear Zone.

Strongly foliated monzogranite from this locality has a SHRIMP U–Pb zircon age of 2660 ± 3 Ma (Wingate and Bodorkos, 2007f). This age is typical of that obtained for low-Ca granites throughout the Yilgarn Craton (e.g. Cassidy et al., 2002) but chemistry from this site is not yet available.

Locality 23: Sheared pillow basalts at contact with granite on the western Meekatharra–Wydgee greenstone belt

by CJ Forbes

From the Chunderloo Shear Zone locality, return to the track along the fence and head east back to the fence junction. Turn right at the junction and follow the track south on the west side of the fence. After 2.2 km (MGA 643090E 7049913N), follow the track right, diverging from the fence. After 900 m, cross a big track and proceed to the haul road (MGA 642440E 7049060N). Turn right onto the haul road, and follow it for 0.5 km to a junction marked by an upstanding piece of polypipe (MGA 642015E 7048740N). Turn off the haul road (right of the polypipe) and follow this track southwest for 180 m (MGA 641870E 7048630N). Turn right onto a track heading approximately northwest and go 240 m (MGA 641680E 7048790N). Take the left fork heading west that goes between two small mullock heaps. After 5.6 km, take the right fork in the track

(MGA 636836E 7046302N). Eight kilometres after this turnoff (past Wandary Well) turn left off the track (MGA 631320E 7043575N) and head east to the base of the hills (MGA 634508E 7043551N).

At Locality 23, sheared pillowed tholeiitic basalt (now amphibolite) is well exposed near the granite–greenstone contact. On subvertical faces, the pillow structures are well preserved, and some show a way-up direction to the west (MGA 634565E 7043526N). The pervasive shear fabric developed in the area cross-cuts the pillow structures. On horizontal surfaces, the metabasalt is clearly strongly sheared, and the pillow structures are not as apparent.

At this locality, the metamorphic grade of the metabasalt increases to the west and the rock gradually becomes more clearly amphibolitic. A shallow northeasterly plunging mineral lineation on the shear plane is also better developed to the west, where it is defined by the alignment of amphibole needles. Shear-sense indicators (S–C fabrics) consistently give a dextral sense of movement.

Although granite at the base of the ridge appears relatively undeformed, scattered outcrops of sheared granite farther west preserve a moderately to well developed shear fabric, a northeasterly plunging mineral lineation defined by quartz and feldspar, and dextral kinematic indicators.

Locality 24: Hornblende-rich granodiorite

by CJ Forbes

From Locality 23, head west back to the track and continue south for 1.5 km to Finger Post Bore (MGA 631315E 7042076N). Go through the gap in the fence next to the cattle run and travel cross-country for about 1.9 km in a southwesterly direction to the locality (MGA 629667E 7041124N).

Hornblende-rich granodiorite at Locality 24 contains coarse-grained hornblende, biotite, quartz and feldspar with minor epidote. Hornblende is the dominant mafic mineral and occurs as euhedral grains up to 10 mm, or as clots up to 30 mm.

The granite preserves evidence of heterogeneous strain distribution. In low-strain zones, the granite has a poorly to moderately developed foliation defined by the partial alignment of feldspar and mafic minerals. In higher strain areas, this foliation is much better developed, and evidence of shearing (S–C fabrics) is also preserved. Pegmatite veins are mainly subparallel to the shear plane, but locally cut across it. The veins vary in width from 3 cm to over 2 m.

This rock is a typical mafic granite of Cassidy et al. (2002), and its SHRIMP U–Pb zircon age of 2787 ± 3 Ma (Wingate and Bodorkos, 2007g) is consistent with the age of mafic granites in the Murchison Domain (Cassidy et al., 2002). However, the chemical data for this site are not yet available.

Return to Finger Post Bore (MGA 631315E 7042076N), head southeast for 5.5 km to the abandoned Norie Homestead. Take the left fork just past the homestead (MGA 634540E 7037831N), and continue for about 4 km to the Great Northern Highway. Turn right at the highway and travel south to Tuckanarra (MGA 607430E 6999770N). Turn west onto the Beebyn–Kambar Road and follow it to where it joins the sealed Cue–Beringarra Road near Glen Homestead. Turn right (northeast) onto the sealed road, and drive through the Weld Range to Jack Hills.

The Jack Hills greenstone belt, Narryer Terrane

by CV Spaggiari

Introduction

The Jack Hills greenstone belt is about 70 km long and is situated within the southern central part of the Narryer Terrane, in the northwest of the Yilgarn Craton (Fig. 2). Structural, lithological, and geochronological data from the belt show that it has undergone a long and complex depositional and deformational evolution from c. 3000 to 1075 Ma (Compston and Pidgeon, 1986; Wilde and Pidgeon, 1990; Dunn et al., 2005; Spaggiari, 2007a,b; Spaggiari et al., 2007). Both the Jack Hills greenstone belt and nearby Mount Narryer metasedimentary belt are well known for their siliciclastic sequences that contain detrital zircons that are 4.0 Ga and older (Froude et al., 1983b; Compston and Pidgeon, 1986). These zircons have ages up to 4.4 Ga (Wilde et al., 2001), are older than any known rocks on Earth, and provide a unique record of early Earth processes. They contain geochemical and isotopic evidence that has generated much debate about the conditions of early Earth (see Spaggiari, 2007a,b and references therein). The Jack Hills greenstone belt differs from the greenstone belts in the Murchison Domain of the Youanmi Terrane in that it includes a significant proportion of siliciclastic metasedimentary rocks. Siliciclastic metasedimentary rocks are also abundant in the Mount Narryer metasedimentary belt of the Narryer Terrane but, unlike in the Jack Hills greenstone belt, banded iron-formation, and mafic and ultramafic rocks are not abundant (see Williams and Myers, 1987). It is not clear to what extent a common geological history is shared by the Jack Hills greenstone belt, the Mount Narryer metasedimentary belt, and the greenstone belts of the Murchison Domain, or how they relate to each other.

Lithologies of the Jack Hills greenstone belt

The dominant lithologies of the Jack Hills greenstone belt (Fig. 36) are banded iron-formation, chert, quartzite, mafic and ultramafic rocks, and siliciclastic rocks including quartz–mica schist, andalusite schist, quartzite, metasandstone, and pebble metaconglomerate (Elias, 1982; Williams et al., 1983; Wilde and Pidgeon, 1990; Myers, 1997; Spaggiari, 2007a). These are surrounded by Archean granitic gneisses and granitic rocks. At least

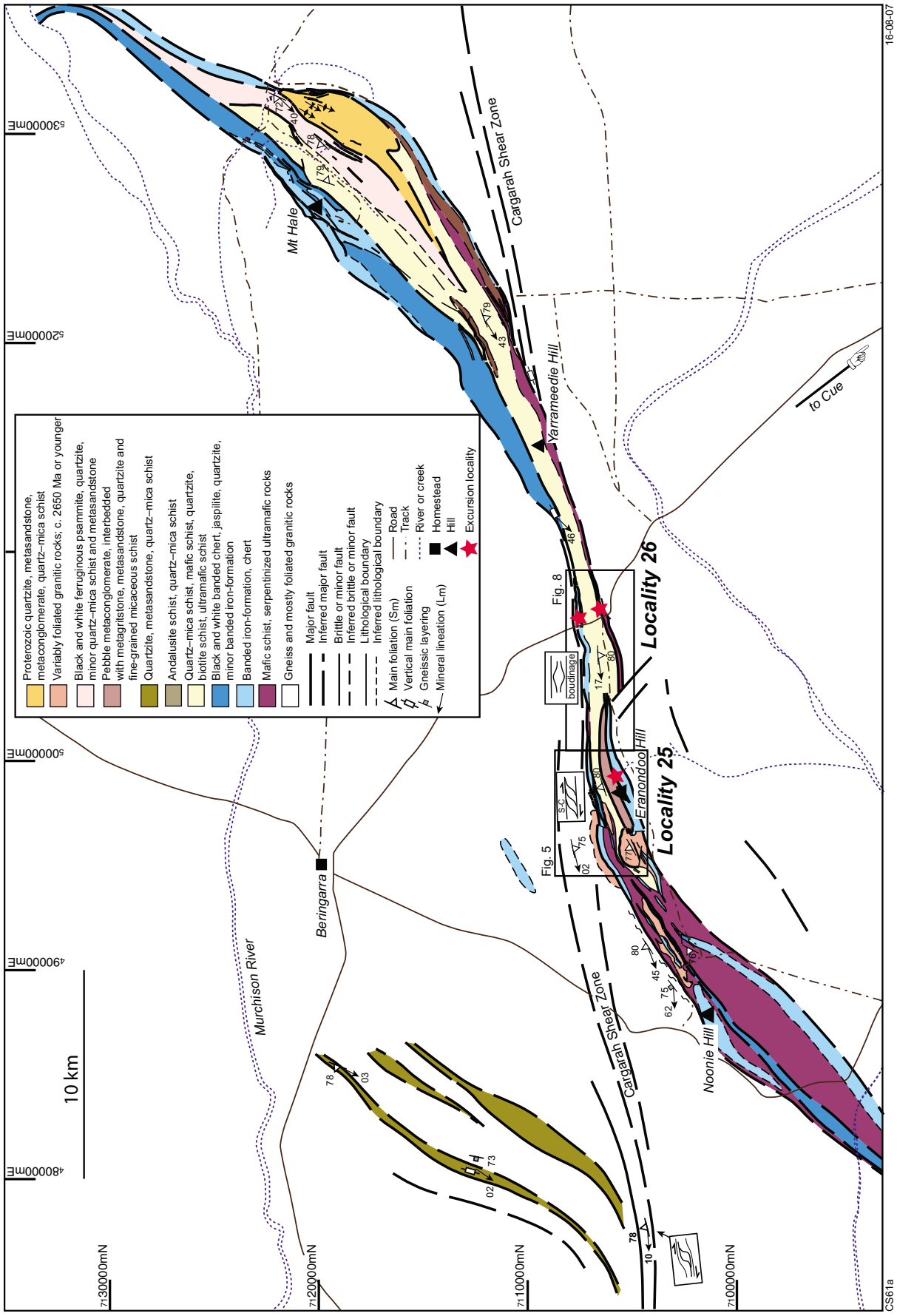

Figure 36. Simplified geological map of the Jack Hills greenstone belt showing field excursion localities (after Spaggiari, 2007a)

two, but possibly four, associations are present in the Jack Hills greenstone belt (Wilde and Pidgeon, 1990; Spaggiari, 2007a):

1. an older association of banded iron-formation, metachert, quartzite, quartz–mica schist, and mafic and ultramafic rocks;
2. an association of pelitic and semipelitic rocks, quartzite, and mafic schists;
3. a mature clastic association that hosts the majority of the 4.0 Ga-and-older detrital zircons;
4. a Proterozoic association of quartz–mica schist, quartzite, and metasandstone with local metaconglomerate.

The mature clastic rocks were interpreted by Wilde and Pidgeon (1990) to have been deposited as an alluvial fan, and are where the majority of 4.0 Ga-and-older detrital zircons have been found. Apart from the Proterozoic rocks of association 4, it is not clear whether the associations listed above were deposited at the same time, or whether they are unrelated successions juxtaposed by deformation (Wilde and Pidgeon, 1990; Spaggiari et al., 2007). Banded iron-formation, chert, some quartzite, mafic and ultramafic schist, and some pelitic and semipelitic rocks in the Jack Hills greenstone belt (association 1 and at least part of association 2) have been intruded by monzogranites, muscovite granite and pegmatite (Pidgeon and Wilde, 1998; Spaggiari, 2007a). The monzogranites have SHRIMP U–Pb zircon ages of 2654 ± 7 and 2643 ± 7 Ma (Pidgeon and Wilde, 1998). However, there are no clear intrusive relationships with the mature clastic rocks that host the 4.0 Ga-and-older detrital zircons and the depositional age of the clastic rocks is not well constrained (Spaggiari et al., 2007).

Until recently all rocks in the belt were thought to be Archean, but it is now evident that some metasedimentary rocks are Proterozoic (Cavosie et al., 2004; Dunn et al., 2005). The extent of the Proterozoic rocks is unknown. No attempt has been made to create a stratigraphy for the Jack Hills rocks because of difficulties in dividing lithologically similar, strongly deformed, and extensively recrystallized rocks.

The supracrustal rocks of the Jack Hills greenstone belt have undergone greenschist to amphibolite facies metamorphism. The presence of grunerite in banded iron-formation and the association of calcic plagioclase and hornblende in mafic schists are indicative of amphibolite-facies conditions (Wilde and Pidgeon, 1990). Hornblende in the mafic schists is commonly overprinted by actinolite, suggesting some retrogression to greenschist facies. The majority of pelitic rocks are semipelites that lack diagnostic mineral assemblages, other than andalusite. Quartz–biotite–cordierite assemblages in some siliciclastic rocks indicate upper greenschist-facies metamorphism (Wilde and Pidgeon, 1990).

Structural and tectonic history of the Jack Hills greenstone belt

The Jack Hills region has undergone a series of deformational and metamorphic events from at least 3.3 Ga, when amphibolite to granulite facies metamorphism produced granitic gneissic rocks that surround most of the belt (Table 3; Kinny et al., 1988;

Table 3. Summary of the regional geological events and their effects on the Jack Hills greenstone belt

Age (Ma)	*Orogenic or regional event*	*Effect on Jack Hills greenstone belt*
3000	Formation of granitic gneisses and intrusions of granitic rocks in the Narryer Terrane	Formation of basement
c. 3000	Probable time of formation of some greenstones in the Murchison Domain, Yilgarn Craton	Deposition of association 1 (BIF, chert, quartzite, pelitic and semipelitic rocks, mafic and ultramafic rocks) at c. 3000 Ma, or prior to 2750 Ma Deposition of mature clastic rocks at this time?
2750–2600	Intrusion of voluminous monzogranitic rocks across the Yilgarn Craton	Intrusion of monzogranite (e.g. the Blob) Deposition of mature clastic rocks after granite intrusion?
2005–1960	Glenburgh Orogeny	No recognized effects other than detritus in Proterozoic rocks
1830–1780	Capricorn Orogeny	Deposition of Proterozoic sequence, possibly in jogs during shearing. Some rocks may be younger Major dextral, transpressional shearing (Cargarah Shear Zone)
1680–1620	Mangaroon Orogeny	Reactivation of Cargarah Shear Zone at this time?
c. 1400–1350	No known event	Reactivation of Cargarah Shear Zone at this time?
1210	Marnda Moorn large igneous province	Intrusion of mafic dykes. Semibrittle faulting
1075	Warakurna large igneous province	Intrusion of mafic dykes

SOURCE: after Spaggiari (2007a)

Myers, 1988a; Nutman et al., 1991, 1993; Pidgeon and Wilde, 1998). The majority of supracrustal rocks in the belt are strongly deformed and dominated by a strong foliation that is subparallel to the trend of the belt (Fig. 37). Coplanar and coaxial overprinting relationships make it difficult to assign specific foliations to tectonic events, but the preservation of multiple foliations in some outcrops, and fold relationships preserved in the banded iron-formation sequence, have helped define a structural chronology (Table 4). The earliest deformation event to have affected the Jack Hills greenstone belt is recorded by the rare preservation of recumbent folds in the banded iron-formation sequence, and an early foliation in most rocks of associations 1 and 2, but not in association 3 (the mature clastic rocks). This event occurred prior to intrusion of the Neoarchean monzogranites, and may have been related to amalgamation of the Narryer Terrane to the Youanmi Terrane, which are stitched by these granites (Myers, 1990b; Nutman et al., 1991; Pidgeon and Wilde, 1998).

Early deformation and intrusion of Neoarchean granites was followed by upright to inclined folding, and predominantly dextral, transpressive shearing. The folds themselves are cut by shears but it is difficult to distinguish whether the folding pre-dated the shearing as a separate event, or formed in response to it, or contains elements of both. The main structural feature of the Jack Hills region is a major, east-trending shear zone (the Cargarah Shear Zone) that cuts the central part of the belt and has produced the present-day sigmoidal geometry (Figs 36, 37, 38). The southwestern and northeastern parts of the belt are interpreted to lie within fault splays from the main shear zone. This is well illustrated by ASTER satellite and aeromagnetic imagery (Figs 37, 38). This geometry, kinematic indicators, and shear-related structures indicate that it is a dextral transpressional zone (Spaggiari, 2007a,b). $^{40}Ar/^{39}Ar$ data, and structural and metamorphic similarities to the nearby Errabiddy Shear Zone, which marks the craton boundary with the Glenburgh Terrane (Occhipinti et al., 2004), suggest that the shear zone formed during the 1830 to 1780 Ma Capricorn Orogeny (Williams, 1986; Spaggiari, 2007a; Spaggiari et al., in prep.).

A total of 13 samples from the Jack Hills region have been dated by the $^{40}Ar/^{39}Ar$ technique, using both infrared and UV-laser techniques (Spaggiari, 2007a; Spaggiari et al., in prep.). The majority of white mica and biotite $^{40}Ar/^{39}Ar$ ages cluster between 1900 and 1700 Ma suggesting that the main phase of cooling through the white mica and biotite Ar closure temperatures (420–300°C (Lister and Baldwin, 1996) and 300 ± 50°C (Harrison, 1985) respectively) in the Jack Hills region was complete by c. 1700 Ma (Fig. 39). Cooling by c. 1700 Ma is interpreted to have followed the main phase of transpressive, dextral shearing along the Cargarah Shear Zone, as most foliations targeted in the dating were related to this. The spread in the ages is interpreted to be due to the long and complex deformation history of the belt, including variable movement and reactivation of the shear zone network over a substantial period of time, resulting in partial resetting of the $^{40}Ar/^{39}Ar$ ages during deformation or cooling, or both. This has produced heterogeneous distributions of radiogenic Ar both within individual grains and also from sample to sample (Spaggiari et al., in prep.). The majority of the shears in the belt are reworked and overprinted by widespread brittle and semibrittle faulting, and localized folding. The $^{40}Ar/^{39}Ar$ dating also indicates a younger, less intense deformation and cooling event at c. 1172 Ma (Spaggiari et al., in prep.).

Locality 25: 4.0 Ga-and-older detrital zircon site, west-central area

F*rom the Cue–Beringarra Road, turn onto a small track leading west (MGA 506680E 7107025N). You will come to a gate after about 300 m, and after about 2.5 km will pass between ridges of ultramafic rocks to the south, and ridges of banded iron-formation and chert to the north. Follow the track for 7.4 km to an intersection with another track heading north (MGA 499829E 7105096N). Follow this track up the gully as far as it goes (about 900 m) and park near the small creek.*

From this locality a traverse can be made through banded iron-formation, Proterozoic rocks, and mature clastic rocks that include outcrop W74, where most of the 4.0 Ga-and-older detrital zircons have come from. *Please refrain from sampling this outcrop* as it contains the greatest percentage of these zircons, which is only about 12%, and is of international significance. The sequence is well exposed and samples can be readily obtained along strike.

The west-central area of the Jack Hills greenstone belt (Fig. 40) contains most of outcrop of the mature clastic association. The unit is folded into tight southwest-plunging folds that are inclined towards the south. Outcrop W74 is interpreted to occur on the southern limb of an inclined syncline (Fig. 41a,b). The mature clastic association is fault bound by lenses of Proterozoic rocks, banded iron-formation, chert and quartzite to the south, and mafic, pelitic and semipelitic schists to the north.

An intrusion of late Archean monzogranite, known as the Blob, outcrops to the southwest (Fig. 40), but the nature of its contact with the mature clastic rocks is not clear. The granite contains lenses or rafts of metasedimentary rocks, but it is not clear which unit these belong to. The intrusive relationship of the granite to banded iron-formation and chert, and quartz–mica schist on the eastern side of the granite is evident (Fig. 42a), but the mature clastic rocks, which overlie the quartz–mica schist in this area, may be in faulted contact, or unconformable, or both. The granite is predominantly weakly foliated, but sheared and locally folded on its margins. The shears and strong foliation wrap around the granite, much like a large-scale porphyroclast. Strongly deformed, steeply dipping, mafic, pelitic and semipelitic schists outcrop to the north of the granite. Banded iron-formation, chert, quartzite strike ridges, and lenses of mafic and ultramafic rocks define the northern margin of the belt in this area, and are intruded by muscovite granite. The muscovite granite also intrudes granitic gneiss along the margin (e.g. MGA 495880E 7106770N).

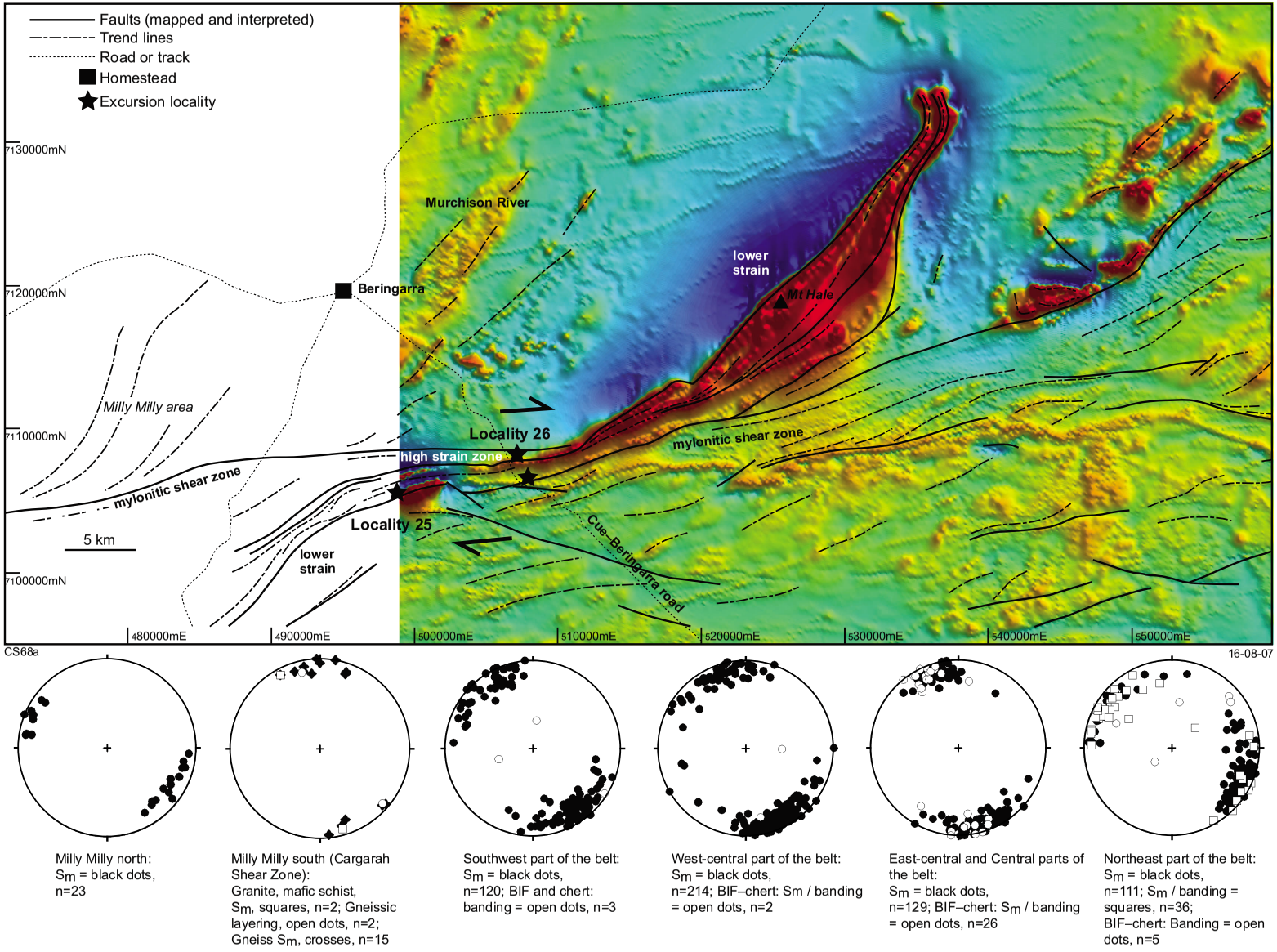

Figure 37. Annotated aeromagnetic image (TMI, reduced to pole) showing the continuation of the Cargarah Shear Zone to the east. Note that 400 m or less line-spacing aeromagnetic data is not available west of that shown (west of the BELELE sheet). Stereonets are equal angle. S_m refers to the main foliation (after Spaggiari, 2007a)

Table 4. Chronology of structures in the Jack Hills region

Rock units	*Main mineralogy and type of foliation; associated structure(s)*				
Gneiss and granitic rocks	Gneissic layering (probably pre-dates S_1 below; pre-3000 Ma); Tight inclined folding of gneissic layering (possibly pre-dates folding below)	Intrusion of monzogranite and pegmatite	Main foliation (S_m) ± S–C foliations: Qtz, ± Bt, ± white mica, ± feldspar; Shear zone and folds	Localized and minor crenulation cleavage: Qtz, white mica Upright open or kink folds	Localized low-grade small shears and brittle faults
Mafic and ultramafic rocks	S_1 foliation (mostly schistose or slaty): mafics = Hbl ± Act, Bt, ± Chl, ± Qtz, ± Ep ultramafics = Serp, ± talc Inclined to recumbent folds?	Localized crenulation cleavage: mafics = Act, Plag, ± Bt, ± Chl, ± Qtz, ± Ep, ultramafics = Serp, ± talc Upright folds?	Main foliation (S_m) ± S–C foliations: mafics = Act, Plag, ± Bt, ± Chl, ± Qtz, ± Ep ultramafics = Serp, ± talc; Shear zone and tight folds	Localized crenulation cleavage: mafics = Act, Plag, ± Chl, ± Qtz, ± Ep Ultramafics = Serp, ± talc? Kink folds, upright folds	Localized low-grade small shears and brittle faults
BIF, chert, and quartzite	S_1 foliation ± banding: Qtz, Fe-oxide, ± stilpnomelane Inclined to recumbent folds (F_1)	Crenulation cleavage ± banding: Qtz, Fe-oxide, ± stilpnomelane Axial planar to inclined to upright chevrons (F_2)	Main foliation (S_m) ± S–C foliations: Qtz, Fe-oxide, ± stilpnomelane; Shear zone and tight to isoclinal folds	Localized crenulation cleavage: Qtz, Fe-oxide, ± pressure solution Upright kink folds, open folds, conjugates	Localized low-grade small shears and brittle faults
Pelite and semipelite	S_1 foliation (mostly schistose or slaty): Qtz, white mica, ± Bt, andalusite, ± Chl Inclined to recumbent folds?	Axial planar to upright folds (F_2) crenulation cleavage: Qtz, white mica, ± Bt, ± Chl Axial planar to upright folds (F_2)	Main foliation (S_m) ± S–C foliations: Qtz, white mica, ± Bt, ± Chl; Shear zone and tight to isoclinal folds	Localized crenulation cleavage: Qtz, white mica or sericite, ± Chl, ± pressure solution Upright kink folds, open folds, conjugates	Localized low-grade small shears and brittle faults
Mature clastic rocks: (metaconglomerate, quartzite, metasandstone, Qtz–mica schist)		Spaced foliation (slaty or schistose in Qtz–mica schist): Qtz, white mica, ± Chl, ± andalusite Axial planar to inclined to upright folds (F_1)	Main foliation (S_m), may be spaced, ± S–C foliations: Qtz, white mica, ± Chl, ±andalusite; Shear zone and tight folds	Localized crenulation cleavage: Qtz, white mica or sericite, ± Chl, ± pressure solution Upright kink folds, open folds, conjugates	Localized low-grade small shears and brittle faults
Proterozoic siliciclastic rocks: sandstone, quartzite, Qtz–mica schist		Spaced foliation (slaty or schistose in Qtz–mica schist): Qtz, white mica, ± Chl, ± andalusite Axial planar to inclined to upright folds (F_1)	main foliation (S_m), may be spaced, ± S–C foliations: Qtz, white mica, ± Chl, ± andalusite Shear zone and tight folds	Localized crenulation cleavage: Qtz, white mica or sericite, ± Chl, ± pressure solution Upright kink folds, open folds, conjugates	Localized low-grade small shears and brittle faults
Mesoproterozoic mafic dykes					Intrusion of mafic dikes
TIME	3000 Ma	2650 Ma	c.1800 Ma	1210 Ma	1075 Ma

NOTES: Hbl = hornblende
Act =actinolite
Bt = biotite
Chl= chlorite
Qtz = quartz
Ep = epidote
Serp = Serpentinite
Plag = plagioclase

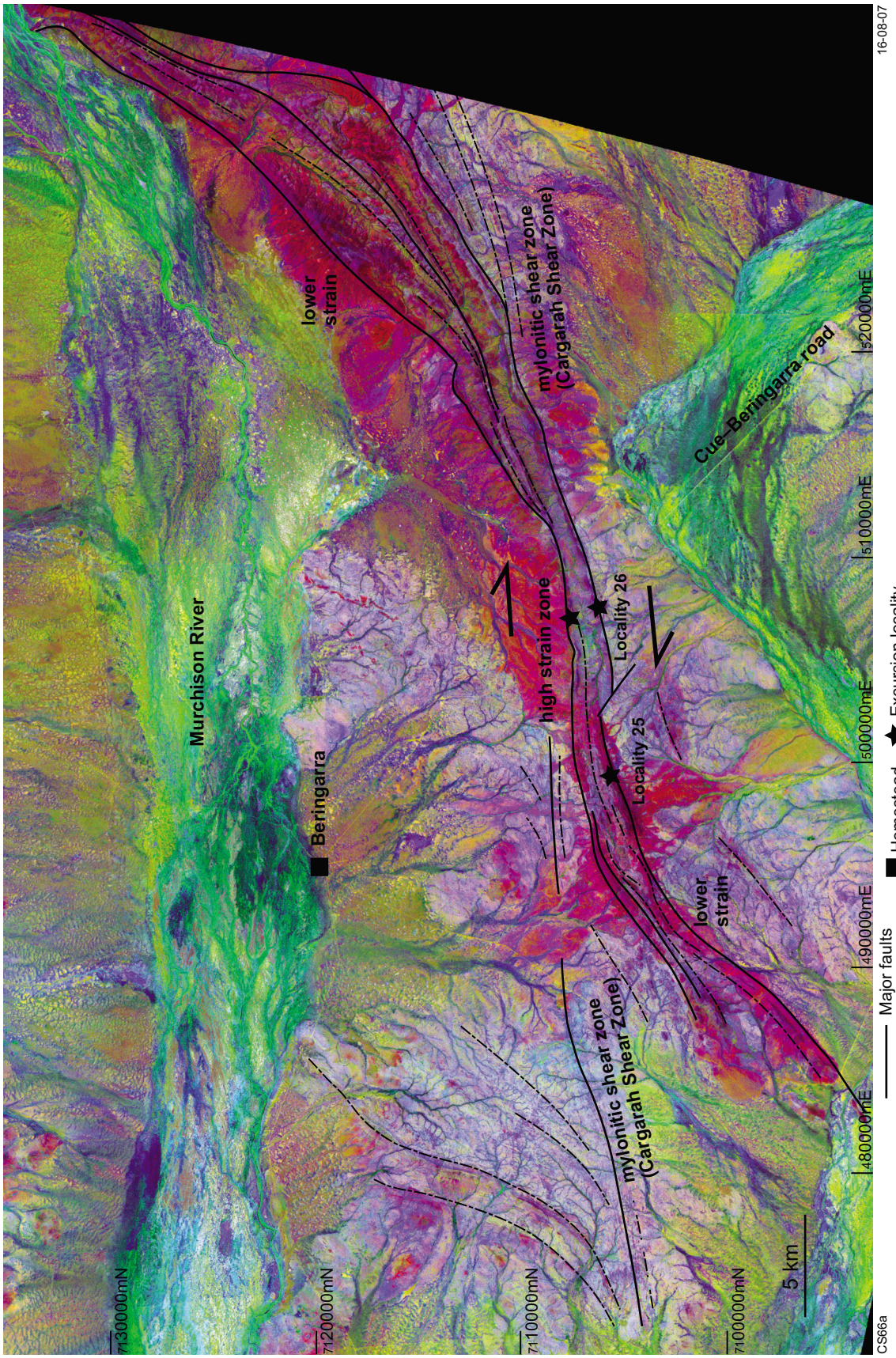

Figure 38. ASTER satellite image (decorrelation stretch of bands 2,3, and 1) of the Jack Hills greenstone belt. The annotation is based on both the image interpretation and field observations (after Spaggiari, 2007a)

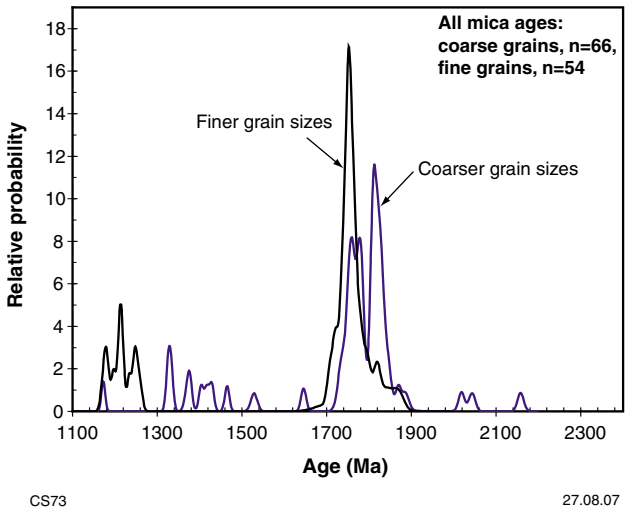

Figure 39. Probability density plot of $^{40}Ar/^{39}Ar$ ages from fine- (black line) versus coarse-grained (blue line) white mica and biotite to compare age differences (after Spaggiari et al., in prep.)

The Cargarah Shear Zone cuts through gneiss and granitic rocks north of the belt in this area, and is locally marked by mylonites, small-scale isoclinal folding, and large quartz veins. In this area the belt is part of the southwestern fault splay off the shear zone, and links to the shear zone to the east, in the central part of the belt. Mylonitization increases to the east (Fig. 42b), but local high-strain zones with predominantly dextral S–C foliations are common throughout. Small late-stage brittle faults cut all rocks, including the Proterozoic rocks.

The southern contact of the mature clastic rocks is complex, and is folded and faulted with banded iron-formation, chert, and quartzite. Two fault-bound lenses of Proterozoic quartz–mica schist and quartzite are mostly mylonitic (Fig. 42c) and contain slivers of ultramafic schist (e.g. MGA 497464E 7105183N). This unit contains sample sites 01JH63 and JH3, which contain Proterozoic detrital zircons (Fig. 41a; Cavosie et al., 2004; Dunn et al., 2005). It should be noted that the geographic coordinates for the JH3 sample locality given in Dunn et al. (2005) do not correspond to the location plotted on their map. The map position in this guide is assumed to be the correct position. Quartzite sample 01JH63 contained concordant (i.e. ≤10% discordant) late Archean grains (2736 ± 6, 2620 ± 10, and 2590 ± 30 Ma), two concordant Paleoproterozoic grains (1973 ± 11 and 1752 ± 22 Ma), and a single concordant grain at 1576 ± 22 Ma (Cavosie et al., 2004). This quartzite is interpreted as part of the Proterozoic unit of predominantly micaceous schist and quartz–mica schist, represented by sample JH3, which is indistinguishable from other quartz–mica schists in the belt. Sample JH3 contained concordant Paleoproterozoic grains ranging in age from c. 1981 to 1944 Ma, with a single youngest grain at 1791 ± 21 Ma. The sample also contained a significant proportion of concordant late Archean grains, a single concordant zircon with an age of 4113 ± 3 Ma, plus a few grains in the range 3500 to 3300 Ma (Dunn et al., 2005). This shows that a source of the 4.0 Ga-and-older zircons was still present and being eroded during the Proterozoic, or that these zircons were recycled from other younger sources. Neoarchean granites could have provided some of this detritus because they do locally contain xenocrysts of 4.0 Ga-and-older zircons (Nelson et al., 2000).

Near the W74 outcrop (Fig. 41), the faulted contact between the mature clastic rocks and the Proterozoic unit shows evidence of late-stage, brittle or semibrittle movement, such as a sharp irregular contact, small duplexes that suggest sinistral displacement, and quartz veins (Fig. 42d). $^{40}Ar/^{39}Ar$ dating (UV method) of sample JAW-03-03 produced three, evenly distributed age groups with weighted mean ages of 1250.7 ± 6.5, 1213.7 ± 5.6, and 1178.1 ± 6.5 Ma (95% confidence, MSWD = 1.19, 0.16 and 0.96 respectively; Spaggiari et al., in prep.). The sample was collected from within the fault zone and indicates it may be a relatively young structure, or a reactivated one.

A mafic dyke that trends west-northwest and roughly follows the creek leading from the car park cross-cuts all folding and the contact with the Proterozoic rocks. Based on petrographic criteria, this dyke has been correlated with east-trending mafic dykes east and south of the Jack Hills greenstone belt that have been dated at 1075 ± 10 Ma using combined SHRIMP U–Pb and paleomagnetic techniques (Wingate, MTD, 2004, written comm.; Wingate et al., 2004). These dykes are part of the 1075 Ma Warakurna large igneous province (Wingate et al., 2004).

The southern margin of the belt in the west-central area (Fig. 40) is a steeply dipping sheared contact between banded iron-formation and granitic rocks and granitic gneiss. Mylonite zones are exposed locally within granitic rocks and gneiss parallel to the belt. The banded iron-formation is internally folded with tight to isoclinal, mostly second-generation folds, which are locally refolded into tight folds, parallel to the trend of the belt (e.g. just north of MGA 496838E 7106498N, and MGA 496474E 7105003N).

Locality 26: Effects of the Cargarah Shear Zone in the central part of the belt

This locality is easily accessible along the Cue–Beringarra Road (MGA 507020E 7106300N). Park just off the road and walk east. From here a short traverse can be made across the southern margin of the belt. If time allows one can continue to the other side of the belt, approximately 1.5 km to the north.

This locality is situated within the central, predominantly high strain section of the belt (Figs 37, 38, 39). The central area (Fig. 43), from north to south, consists of boudinaged strike ridges of strongly deformed banded iron-formation, chert, and quartzite; a wide central zone of strongly deformed mafic and semipelitic schist; and strike ridges of predominantly mafic and ultramafic rocks along the southern contact with gneissic and granitic rocks. This

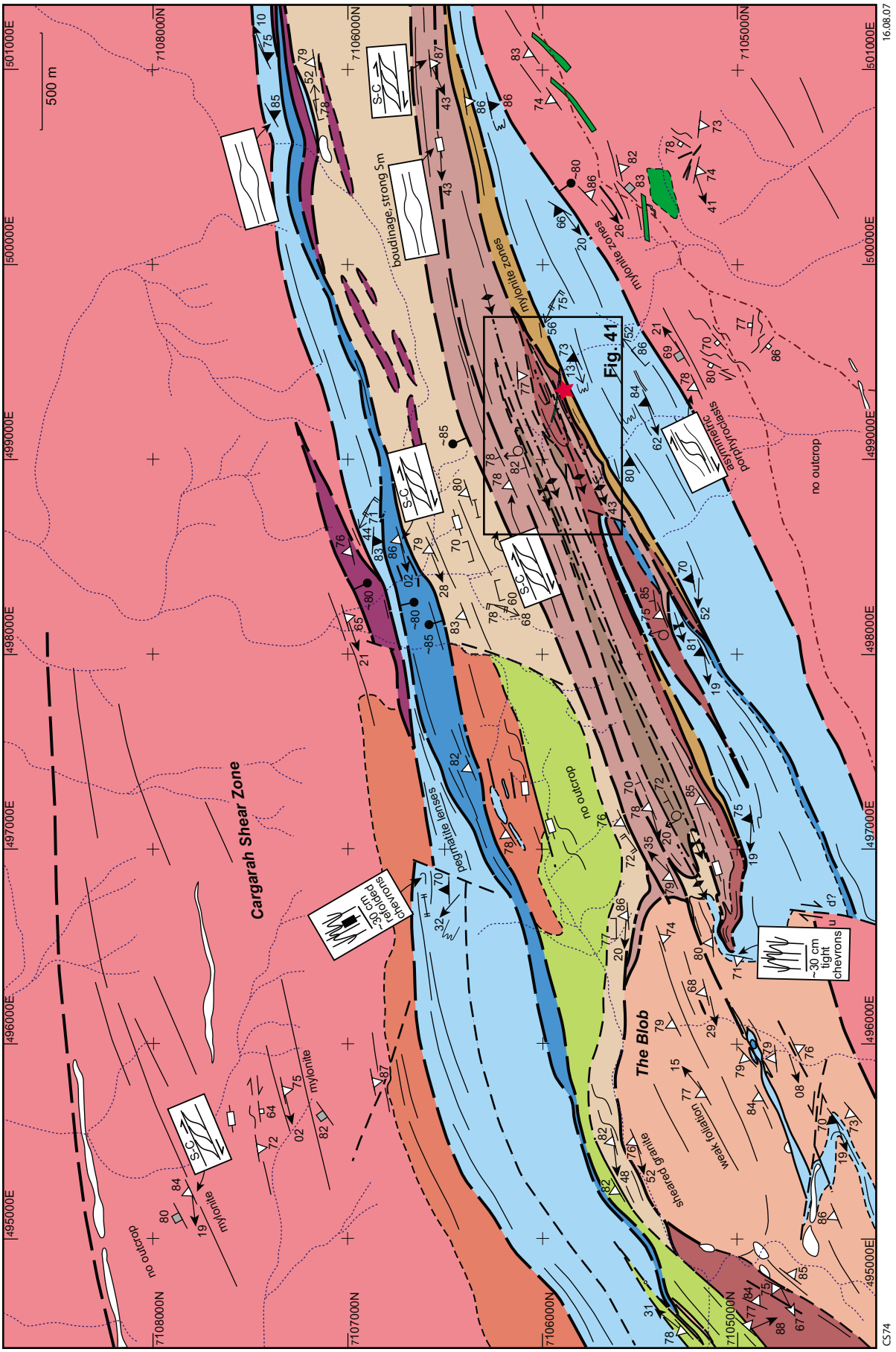
500 m
Cargarah Shear Zone
The Blob
Fig. 41
mylonite zones
boudinage, strong 5m
asymmetric porphyroclasts
no outcrop
pegmatite lenses
~30 cm tight chevrons
~30 cm isoclinal chevrons
mylonite
weak foliation
sheared granite
S-C
d?
16.08.07
CS74

Figure 40. Map of the west-central area of the Jack Hills greenstone belt (simplified from Plate 4, Spaggiari, 2007a)

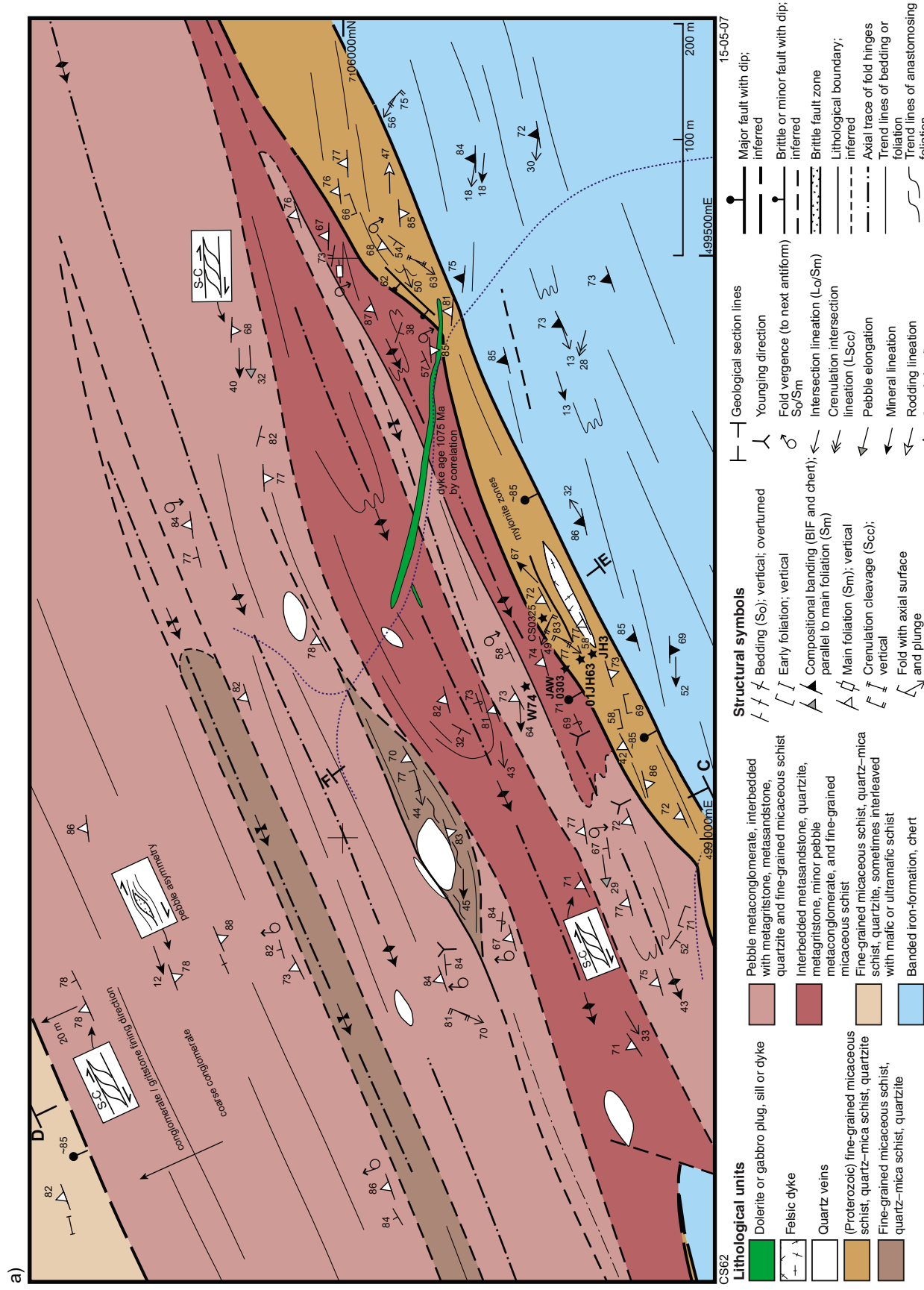
a)
CS62
15-05-07
7106000mN
499500mE
499000mE
100 m
200 m
dyke age 1075 Ma by correlation
mylonite zones
pebble asymmetry
conglomerate / gritstone fining direction
coarse conglomerate
20 m
Lithological units
Dolerite or gabbro plug, sill or dyke
Felsic dyke
Quartz veins
(Proterozoic) fine-grained micaceous schist, quartz–mica schist, quartzite
Fine-grained micaceous schist, quartz–mica schist, quartzite
Pebble metaconglomerate, interbedded with metagritstone, metasandstone, quartzite and fine-grained micaceous schist
Interbedded metasandstone, quartzite, metagritstone, minor pebble metaconglomerate, and fine-grained micaceous schist
Fine-grained micaceous schist, quartz–mica schist, quartzite, sometimes interleaved with mafic or ultramafic schist
Banded iron-formation, chert
Structural symbols
Bedding (S0); vertical; overturned
Early foliation; vertical
Compositional banding (BIF and chert); parallel to main foliation (Sm)
Main foliation (Sm); vertical
Crenulation cleavage (Scc); vertical
Fold with axial surface and plunge
Antiform; synform
Geological section lines
Younging direction
Fold vergence (to next antiform)
S0/Sm
Intersection lineation (L0/Sm)
Crenulation intersection lineation (LScc)
Pebble elongation
Mineral lineation
Rodding lineation
Sample locality
Creek
Major fault with dip; inferred
Brittle or minor fault with dip; inferred
Brittle fault zone
Lithological boundary; inferred
Axial trace of fold hinges
Trend lines of bedding or foliation
Trend lines of anastomosing foliation

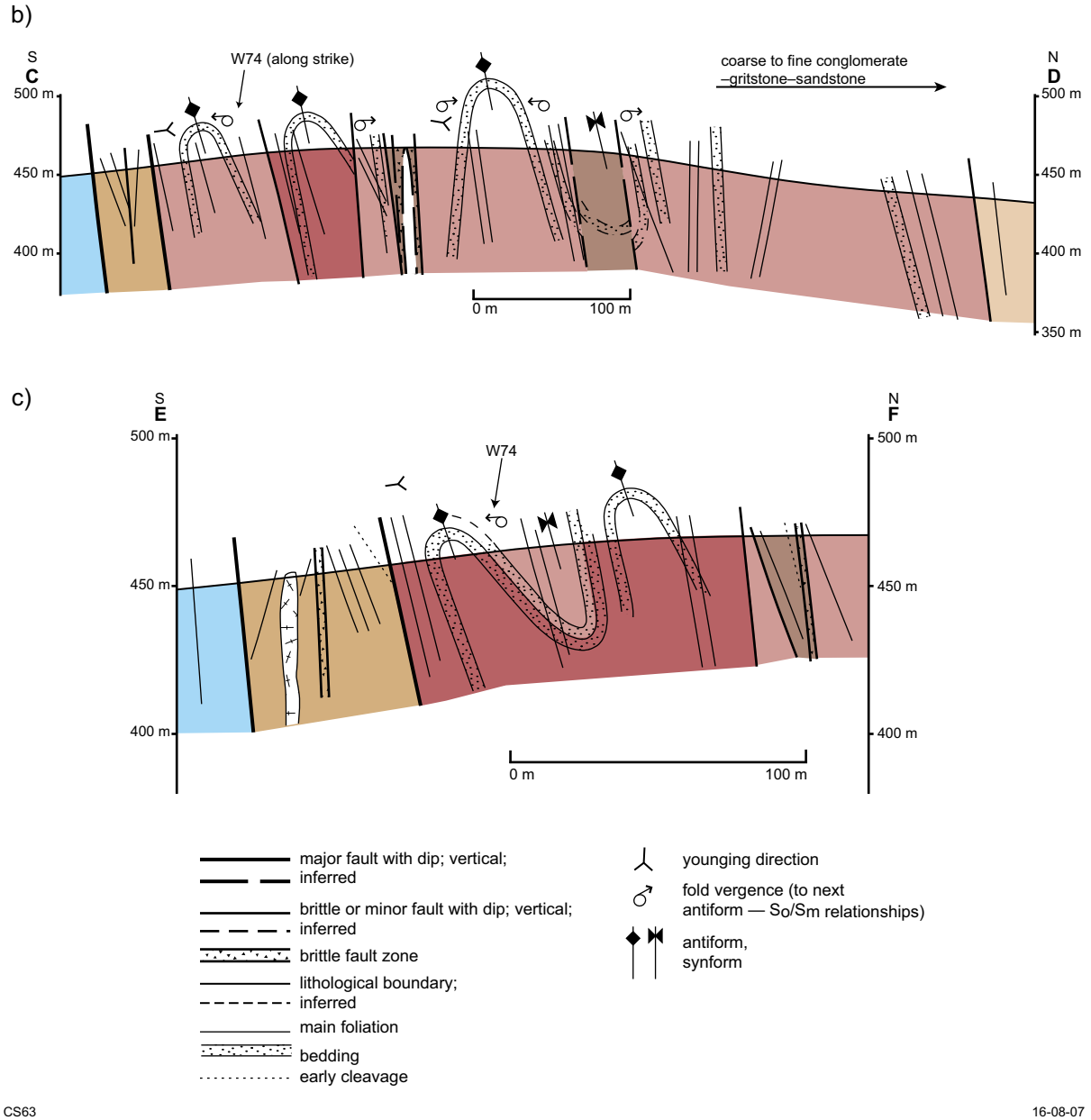

Figure 41. a) Detailed geological map of the area including the W74 site, from the west-central area (Fig. 40). Geochronological sample sites discussed in the text, and sites of cross sections C–D and E–F are shown; b) and c) Cross sections C–D and E–F showing structural and lithological relationships in the W74 area (after Spaggiari, 2007a)

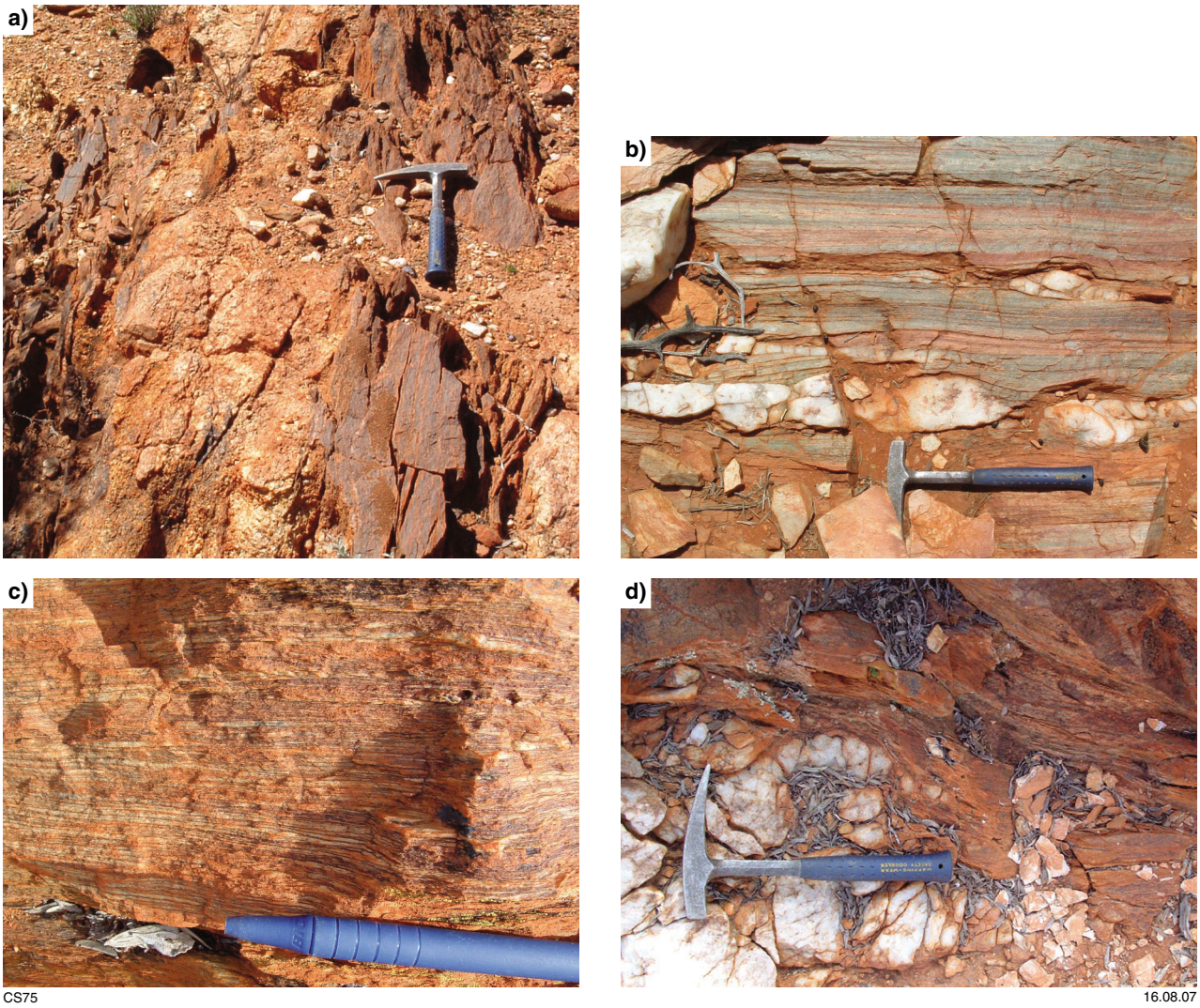

Figure 42. a) Quartz–mica schist intruded by granite near the eastern margin of the main granite body known as the Blob, from the west-central map area (Fig. 40); b) Mylonitic foliation (S_m) and boudinage in mature clastic rocks in the central part of the belt (see Fig. 43). This is where the mature clastic association pinches out within the Cargarah Shear Zone; c) Mylonitic Proterozoic quartz–mica schist from the west-central part of the belt (Fig. 40); d) Boudinaged quartz veins in Proterozoic quartz–mica schist, within the fault contact with the mature clastic association. This is also the $^{40}Ar/^{39}Ar$ sample locality of JAW-03-03 (MGA 499135E, 7105844N), from the west-central part of the belt (Figs 40, 41a)

part of the belt is coincident with the Cargarah Shear Zone, is steeply dipping, and dominated by high-strain, boudinage, tight to isoclinal folds, and predominantly dextral S–C foliations and kinematic indicators (Fig. 44a). Mylonite is locally developed, particularly in banded iron-formation, chert, and quartzite on the northern margin. The mineral lineation plunges shallowly to moderately, either to the east or west. The main foliation is locally folded by northeast-trending upright folds. In the western part of the area, strike ridges of strongly deformed, locally mylonitic mature clastic rocks, banded iron-formation, and chert pinch out within the narrowest part of the belt. This is interpreted to have been caused by stretching during shearing. Late-stage, northwest- and northeast-trending, steeply dipping brittle faults that cut the margins of the belt have a typical displacement of about 100 m, but displacements up to 1 km have been noted.

Near the southern margin of the belt, in the eastern part of the area, rafts of gneiss are preserved in monzogranite and pegmatite (Fig. 45; see also Pidgeon and Wilde, 1998). Relatively undeformed domes and tors of monzogranite flank the Cue–Beringarra road but, towards the southern contact, the granite and pegmatite are strongly deformed and sheared. A dolerite dyke outcrops just near the contact, trending parallel with the belt. This dyke appears to be undeformed, and is probably part of the 1075 Ma Warakurna Large Igneous Province mafic dyke suite (Wingate, MTD, 2004, written comm.; Wingate et al., 2004). The contact with mafic and ultramafic rocks is a steeply dipping shear zone with complex small-scale folds and both sinistral and dextral kinematic indicators. Stretched lenses of banded iron-formation and chert outcrop within mafic and ultramafic rocks near the contact.

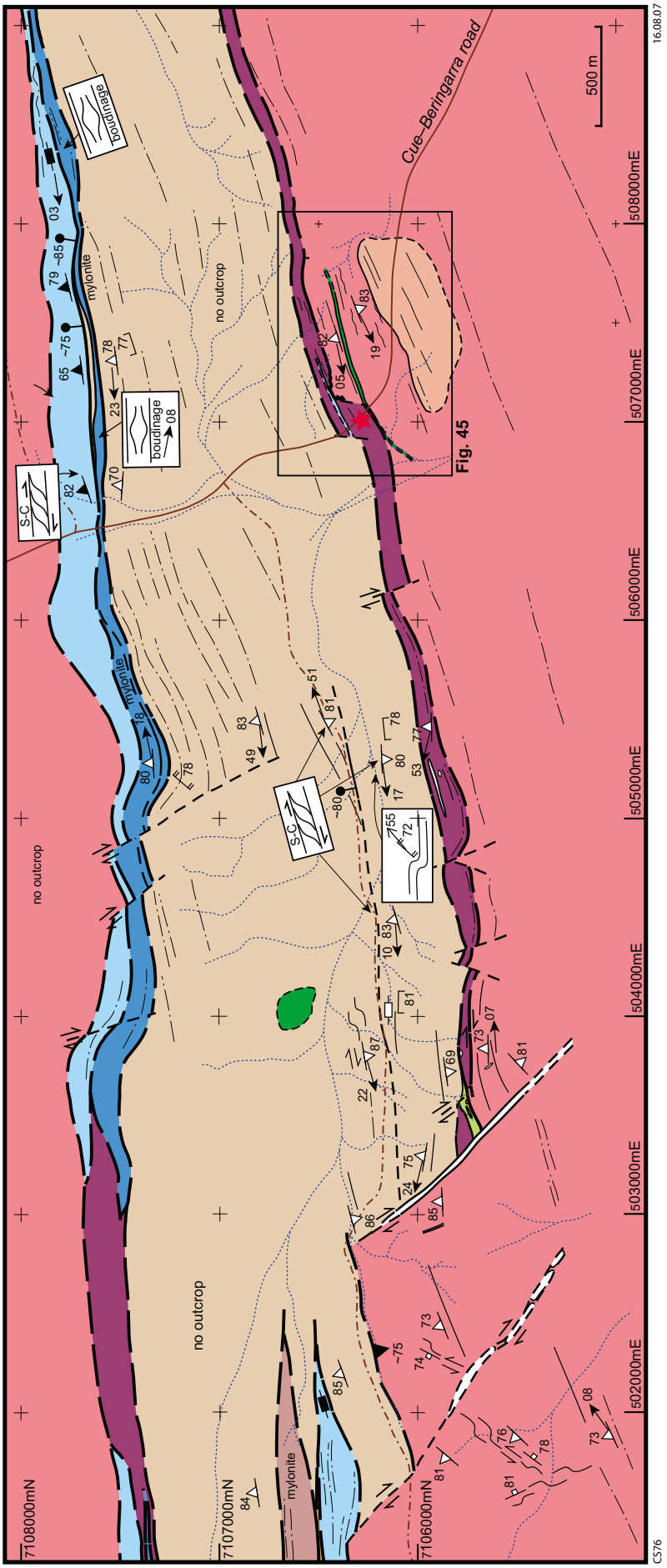

Figure 43. Map of the central area of the Jack Hills greenstone belt (simplified from Plate 3, Spaggiari, 2007a). Legend as per Figure 40

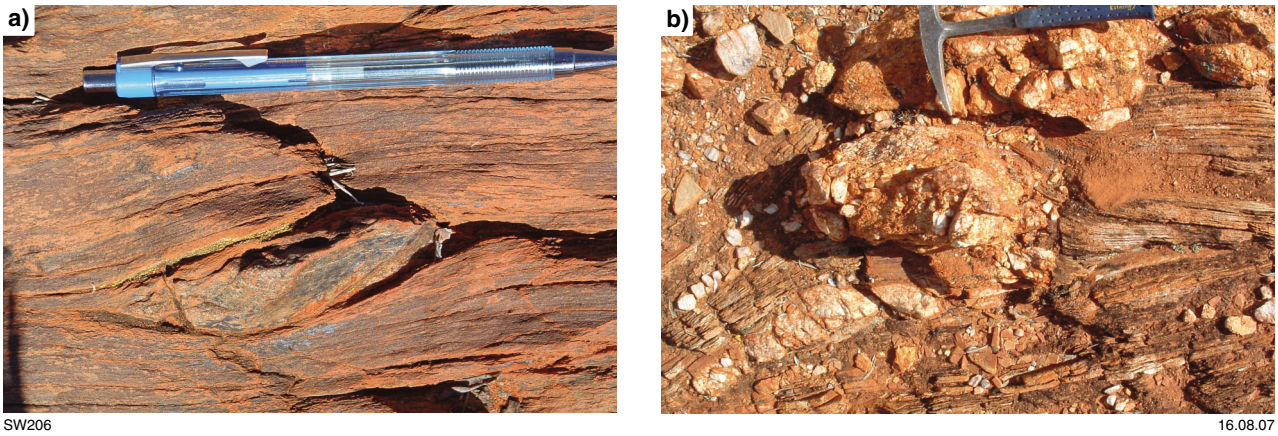

Figure 44. a) Dextral augen structure in quartz–mica schist in the central part of the belt (Fig. 43); b) Strongly deformed pegmatite and granitic gneiss in the central part of the belt, close to sample CS0392 site (see Fig. 45)

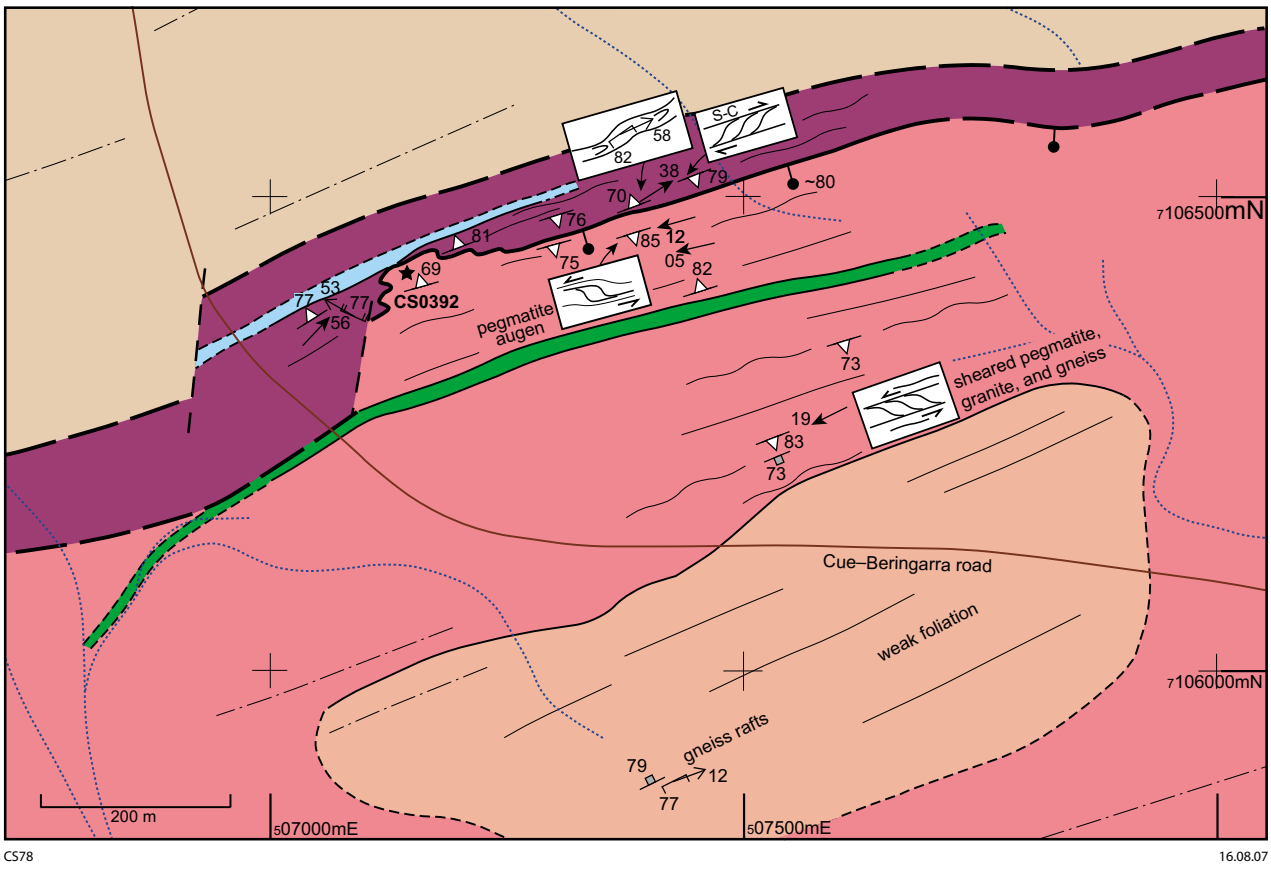

Figure 45. Detailed map of the southern part of the central area showing main excursion locality and $^{40}Ar/^{39}Ar$ sample site CS0392. Legend as per Figure 40

$^{40}Ar/^{39}Ar$ dating of two white mica grains from sheared pegmatite sample CS0392 at this locality (Figs 44b, 45) gave two groups of ages: an older group of three analyses with ages of 1809.8 ± 6.2, 1809.5 ± 6.9, and 1808.5 ± 6.2 Ma (1σ), and a younger group with a spread of ages between 1784–1761 Ma (Spaggiari et al., in prep.). These give weighted mean ages of 1809.3 ± 7.3 and 1776 ± 7 Ma (95% confidence, MSWD = 0.01 and 1.3) respectively. The two age groups may reflect partial resetting of the mica grains during cooling or deformation processes, or both.

References

Ahmat, AL, and Ruddock, I, 1990, Windimurra and Narndee Layered Complexes, *in* Geology and mineral resources of Western Australia: Geological Survey of Western Australia, Memoir 3, p. 119–126.

Alexander, P, Henley, RW, and Kavanagh, ME, 1991, Mineralization styles and geochemistry in the Paddy's Flat gold district, Meekatharra, Western Australia, Proceedings of the Second Pacific Rim Conference: Australasian Institute of Mining and Metallurgy, Gold Coast, Australia, p. 295–304.

Archibald, NJ, Bettenay, LF, Binns, RA, Groves, DI, and Gunthorpe, RJ, 1978, The evolution of Archaean greenstone terrains, Eastern Goldfields Province, Western Australia: Precambrian Research, v. 6, p. 103–131.

Barley, ME, Brown, SJA, Krapež, B, and Cas, RAF, 2002, Tectonostratigraphic analysis of the Eastern Yilgarn Craton: an improved geological framework for exploration in Archaean terranes: Amira International Limited, AMIRA Project no. P437A final report (unpublished).

Barley, ME, Brown, SJA, Cas, RAF, Cassidy, KF, Champion, DC, Gardoll, SJ, and Krapež, B, 2003, An integrated geological and metallogenic framework for the eastern Yilgarn Craton: developing geodynamic models of highly mineralised Archaean granite–greenstone terranes: Amira International Limited, AMIRA Project no. P624 final report (unpublished).

Barley, ME, Eisenlohr, BN, Groves, DI, Perring, CS, and Vearncombe, JR, 1989, Late Archaean convergent margin tectonics and gold mineralization: A new look at the Norseman–Wiluna Belt, Western Australia: Geology, v. 17, p. 826–829:

Barnes, SJ (editor), 2006, Nickel deposits of the Yilgarn Craton: geology, geochemistry, and geophysics applied to exploration: Society of Economic Geologists, Special Publication 13, 210p.

Bateman, R, Costa, S, Swe, T, and Lambert, D, 2001, Archaean mafic magmatism in the Kalgoorlie area of the Yilgarn Craton, Western Australia: a geochemical and Nd isotopic study of the petrogenetic and tectonic evolution of a greenstone belt: Precambrian Research, v. 108, p. 75–112.

Beeson, J, Groves, DI, and Ridley, JR, 1993, Controls on mineralization and tectonic development of the central part of the northern Yilgarn Craton: Minerals and Energy Research Institute of Western Australia, Report no. 109, 93p.

Blewett, RS, and Czarnota, K, in prep., Diversity of structurally controlled gold through time and space of the central Eastern Goldfields Superterrane — a field guide: Geological Survey of Western Australia, Record 2007/19.

Bloem, EJM, Dalstra, HJ, Groves, DI, and Ridley, JR, 1994, Metamorphic and structural setting of Archaean amphibolite-hosted gold deposits near Southern Cross, Southern Cross Province, Yilgarn Block, Western Australia: Ore Geology Reviews, v. 9, p. 183–208.

Binns, RA, Gunthorpe, RJ, and Groves, DI, 1976, Metamorphic patterns and development of greenstone belts in the eastern Yilgarn Block, Western Australia, *in* The early history of the Earth *edited by* BF Windley: John Wiley and Sons, London, p. 303–313.

Bodorkos, S, Love, GJ, Nelson, DR, and Wingate, MTD, 2006, 179239: porphyritic metadacite, Montague Well; Geochronology dataset 647, *in* Compilation of geochronology data, June 2007 update: Geological Survey of Western Australia.

Brown, SJA, Krapež, B, Beresford, SW, Cassidy, KF, Champion, DC, Barley, ME, and Cas, RAF, 2001, Archaean volcanic and sedimentary environments of the Eastern Goldfields Province, Western Australia — a field guide: Geological Survey of Western Australia, Record 2001/13, 66p.

Bunting, JA, and Macdonald, FA, 2004, The Yarrabubba Structure, Western Australia — clues to identifying impact events in deeply eroded ancient cratons: Geological Society of Australia, Abstracts v. 73, p. 227.

Campbell, IH, Griffiths, RW, and Hill, RI, 1989, Melting in an Archaean mantle plume: heads it's basalts, tails it's komatiites: Nature, v. 339, p. 697–699.

Campbell, IH, and Hill, RI, 1988, A two-stage model for the formation of the granite–greenstone terrains of the Kalgoorlie–Norseman area, Western Australia: Earth and Planetary Science Letters, v. 90, p. 11–25.

Cassidy, KF, Champion, DC, Krapež, B, Barley, ME, Brown, SJA, Blewett, RS, Groenewald, PB, and Tyler, IM, 2006, A revised geological framework for the Yilgarn Craton, Western Australia: Geological Survey of Western Australia, Record 2006/8, 8p.

Cassidy, KF, Champion, DC, McNaughton, NJ, Fletcher, IR, Whitaker, AJ, Bastrakova, IV, and Budd, AR, 2002, Characterization and metallogenic significance of Archaean granitoids of the Yilgarn Craton, Western Australia: Amira International Limited, AMIRA Project no. P482/MERIWA Project M281, Report no. 222 (unpublished).

Cavosie, AJ, Wilde, SA, Liu, D, Weiblen, PW, and Valley, JW, 2004, Internal zoning and U–Th–Pb chemistry of Jack Hills detrital zircons: a mineral record of early Archean to Mesoproterozoic (4348–1576 Ma) magmatism: Precambrian Research, v. 135, p. 251–279.

Champion, DC, 2004, Terrane, domain and fault system nomenclature, *in* 3D geological models of the eastern Yilgarn Craton *edited by* RS Blewett and AP Hitchman: Australia CSIRO, Predictive Mineral Discovery Cooperative Research Centre, Project no. Y2 (unpublished).

Champion, DC, and Sheraton, JW, 1997, Geochemistry and Nd isotope systematics of Archaean granites of the Eastern Goldfields, Yilgarn Craton, Australia: implications for crustal growth processes: Precambrian Research, v. 83, p. 109–132.

Chen, SF, 2005, Geology of the Atley, Rays Rocks, and southern Sandstone 1:100 000 sheets: Geological Survey of Western Australia, 1:100 000 Geological Series Explanatory Notes, 42p.

Chen, SF, Libby, JW, Greenfield, JE, Wyche, S, and Riganti, A, 2001, Geometry and kinematics of large arcuate structures formed by impingement of rigid granitoids into greenstone belts during progressive shortening: Geology, v. 29, p. 283–286.

Chen, SF, Libby, JW, Wyche, S, and Riganti, A, 2004, Kinematic nature and origin of regional-scale ductile shear zones in the central Yilgarn Craton, Western Australia: Tectonophysics, v. 394, p. 139–153.

Chen, SF, Morris, PA, and Pirajno, F, 2005, Occurrence of komatiites in the Sandstone greenstone belt, north-central Yilgarn Craton: Australian Journal of Earth Sciences, v. 52, p. 959–963.

Chen, SF, Riganti, A, Wyche, S, Greenfield, JE, and Nelson, DR, 2003, Lithostratigraphy and tectonic evolution of contrasting greenstone successions in the central Yilgarn Craton, Western Australia: Precambrian Research, v. 127, p. 249–266.

Chen, SF, Wyche, S, and Doyle, MG, 2006, Youno Downs, WA Sheet 2743: Geological Survey of Western Australia, 1:100 000 Geological Series.

Chin, RJ, and Smith, RA, 1983, Jackson, WA: Geological Survey of Western Australia, 1:250 000 Geological Series Explanatory Notes, 30p.

Claoué–Long, JC, Compston, W, and Cowden, A, 1988, The age of the Kambalda greenstones resolved by ion-microprobe — implications for Archaean dating methods: Earth and Planetary Science Letters, v. 89, p. 239–259.

Compston, W, and Pidgeon, RT, 1986, Jack Hills, evidence of more very old detrital zircons in Western Australia: Nature, v. 321, p. 766–769.

Cooper, RW, and Flint, DJ, 2007, Iron ore deposits of the Yilgarn Craton — 2007 (1:1 500 000 scale): Geological Survey of Western Australia.

Dalstra, HJ, Ridley, JR, Bloem, EJM, and Groves, DI, 1999, Metamorphic evolution of the central Southern Cross Province, Yilgarn Craton, Western Australia: Australian Journal of Earth Sciences, v. 46, p. 765–784.

Davis, BK, and Maidens, E, 2003, Archaean orogen-parallel extension: evidence from the northern Eastern Goldfields Province, Yilgarn Craton: Precambrian Research, v. 127, p. 229–248.

Dunn, SJ, Nemchin, AA, Cawood, PA, and Pidgeon, RT, 2005, Provenance record of the Jack Hills metasedimentary belt: Source of the Earth's oldest zircons: Precambrian Research, v. 138, p. 235–254.

Ellis, P, 2006, Geology and mineralisation of the Jaguar copper–zinc deposit, Western Australia, in Copper–zinc massive sulphide deposits *in* Western Australia *edited by* TF McConachy and BIA McInnes: CSIRO Explores 2, p. 39–46.

Elias, M, Belele, WA, 1982, (1st edition): Geological Survey of Western Australia, 1:250 000 Geological Series Explanatory Notes, 22p.

Froude, DO, Compston, W, and Williams, IS, 1983a, Early Archaean zircon analyses from the central Yilgarn Block: Australian National University, Canberra, Research School of Earth Sciences (RSES), Annual Report 1983, p. 124–126.

Froude, DO, Ireland, TR, Kinny, PD, Williams, IS, Compston, W, Williams, IR, and Myers, JS, 1983b, Ion microprobe identification of 4100–4200 Myr-old terrestrial zircons: Nature, v. 304, p. 616–618.

Gee, RD, 1982, Southern Cross, WA: Geological Survey of Western Australia, 1:250 000 Geological Series Explanatory Notes, 25p.

Gee, RD, Baxter, JL, Wilde, SA, and Williams, IR , 1981, Crustal development in the Yilgarn Block, *in* Archaean geology *edited by* JE Glover and DI Groves: International Archaean Symposium, 2nd, Perth, WA, 1980, Proceedings: Western Australia Geological Society of Australia, Special Publication, no. 7, p. 43–56.

Geological Survey of Western Australia, 2006, Murchison geological exploration package. February 2006 update: Geological Survey of Western Australia, Record 2006/2.

Geological Survey of Western Australia, 2007a, Compilation of geochronology data, June 2007 update: Geological Survey of Western Australia.

Geological Survey of Western Australia, 2007b, Central Yilgarn Geological Information Series, June 2007 update: Geological Survey of Western Australia.

Geological Survey of Western Australia, 2007c, Murchison Geological Information Series, June 2007 update: Geological Survey of Western Australia.

Gole, MJ, and Hill, RET, 1989, The Walter Williams Formation: the result of a regionally extensive single komatiite eruptive event, Yilgarn Block, Western Australia: Geological Society of Finland, Bulletin, v. 61, p. 24.

Gole, MJ, and Hill, RET, 1990, The refinement of extrusive models for the genesis of nickel deposits: implications from case studies at Honeymoon Well and the Walter Williams Formation: Minerals and Energy Research Institute of Western Australia, Report 68, 93p.

Griffin, WL, Belousova, EA, Shee, SR, Pearson, NJ, and O'Reilly, SYO, 2004, Archean crustal evolution in the northern Yilgarn Craton: U–Pb and Hf-isotope evidence from detrital zircons: Precambrian Research, v. 131, p. 231–282.

Hagemann, SG, Neumayr, P, and Witt, WK (editors), 2001, World-class gold camps and deposits in the eastern Yilgarn Craton, Western Australia, with special emphasis on the Eastern Goldfields Province: Geological Survey of Western Australia, Record 2001/17, 216p.

Hallberg, JA, 2000, Hallberg Murchison 1:25 000 geology dataset, 1989–1994 (including GSWA Record 2000/20: Geological Survey of Western Australia.

Hallberg, JA, Johnston, C, and Bye, SM, 1976, The Archaean Marda igneous complex, Western Australia: Precambrian Research, v. 3, p. 111–136.

Hallberg, JA, and Thompson, JFH, 1985, Geological setting of the Teutonic Bore massive sulfide deposit, Archean Yilgarn Block, Western Australia: Economic Geology, v. 80, p. 1953–1964.

Harrison, TM, 1985, Diffusion of ^{40}Ar in biotite: Temperature, pressure and compositional effects: Geochimica et Cosmochimica Acta, v. 49, p. 2461–2468.

Hill, RET, Barnes, SJ, and Dowling, SE, 2001, Komatiites of the Norseman–Wiluna Greenstone Belt, Western Australia — a field guide: Geological Survey of Western Australia, Record 2001/10, 71p.

Hill, RET, Barnes, SJ, Gole, MJ, and Dowling, SJ, 1995, The volcanology of komatiites as deduced from field relationships in the Norseman–Wiluna greenstone belt, Western Australia: Lithos, v. 34, p. 159–188.

Kinny, PD, and Nutman, AP, 1996, Zirconology of the Meeberrie Gneiss, Yilgarn Craton, Western Australia: an early Archaean migmatite: Precambrian Research, v. 78, p. 165–178.

Kinny, PD, Wijbrans, JR, Froude, DO, Williams, IS, and Compston, W, 1990, Age constraints on the geological evolution of the Narryer Gneiss Complex, Western Australia: Australian Journal of Earth Sciences, v. 37, p. 51–69.

Kinny, PD, Williams, IS, Froude, DO, Ireland, TR , and Compston, W, 1988, Early Archaean zircon ages from orthogneisses and anorthosites at Mount Narryer, Western Australia: Precambrian Research, v. 38, p. 325–341.

Krapež, B, Brown, SJA, Hand, J, Barley, ME, and Cas, RAF, 2000, Age constraints on recycled crustal and supracrustal sources of Archaean metasedimentary sequences, Eastern Goldfields Province, Western Australia: evidence from SHRIMP zircon dating: Tectonophysics, v. 322, p. 89–133.

Lister, GS, and Baldwin, SL, 1996, Modelling the effect of arbitrary P–T–t histories on argon diffusion in minerals using the MacArgon program for the Apple Macintosh: Tectonophysics, v. 253, p. 83–109.

Maas, R, and McCulloch, MT, 1991, The provenance of Archean clastic metasediments in the Narryer Gneiss Complex, Western Australia: trace element geochemistry, Nd isotopes, and U–Pb ages for detrital zircons: Geochimica and Cosmochimica Acta, v. 55, p. 1914–1932.

MacDonald, FA, Bunting, JA, and Cina, CE, 2003, Yarrabubba — a large, deeply eroded impact structure in the Yilgarn Craton, Western Australia: Earth and Planetary Sciences Letters, v. 213, p. 235–247.

Marston, RJ, 1979, Copper mineralization in Western Australia: Geological Survey of Western Australia, Mineral Resources Bulletin 13, 208p.

Marston, RJ, 1984, Nickel mineralization in Western Australia: Geological Survey of Western Australia, Mineral Resources Bulletin 14, 271p.

Mathison, CI, Perring, RJ, Vogt, JH, Parks, J, Hill, RET, and Ahmat, AL, 1991, The Windimurra Complex *in* Mafic–ultramafic complexes of Western Australia: Sixth International Platinum Symposium, Guidebook for the post-symposium excursion *edited by* SJ Barnes and RET Hill: Geological Society of Australia (WA Division), Excursion Guidebook No. 3, p. 45–76.

McDonough, WF, and Sun, SS, 1995, The composition of the earth: Chemical Geology, v. 120, p 223–253.

Midwest Corporation Ltd, 2007, Midwest Corporation Ltd, viewed 3 July 2007, <http://www.midwestcorp.com.au/WeldRange.html>.

Mikucki, EJ, and Roberts, FI, 2004, Metamorphic petrography of the Kalgoorlie region, Eastern Goldfields Granite–Greenstone Terrane: METPET database: Geological Survey of Western Australia, Record 2003/12, 40p.

Mueller, AG, Campbell, IH, Sciøtte, L, Sevigny, JH, and Layer, PW, 1996, Constraints on the age of granitoid emplacement, metamorphism, gold mineralization, and subsequent cooling of the Archean greenstone terrane at Big Bell, Western Australia: Economic Geology, v. 91, p. 896–915.

Murchison Metals Ltd, 2007, Murchison Metals Ltd, viewed 3 July 2007, <http://www.mml.net.au>.

Myers, JS, 1988a, Early Archaean Narryer Gneiss Complex, Yilgarn Craton, Western Australia: Precambrian Research, v. 38, p. 297–307.

Myers, JS, 1988b, Oldest known terrestrial anorthosite at Mount Narryer, Western Australia: Precambrian Research, v. 38, p. 309–323.

Myers, JS, 1990a, Precambrian tectonic evolution of part of Gondwana, southwestern Australia: Geology, v. 18, p. 537–540.

Myers, JS, 1990b, Western Gneiss Terrane, *in* Geology and mineral resources of Western Australia: Geological Survey of Western Australia, Memoir 3, p. 13–31.

Myers, JS, 1993, Precambrian history of the West Australian Craton and adjacent orogens: Annual Review of Earth and Planetary Sciences, v. 21, p. 453–485.

Myers, JS, 1995, The generation and assembly of an Archaean supercontinent: evidence from the Yilgarn Craton, Western Australia, *in* Early Precambrian processes *edited by* MP Coward and AC Ries: The Geological Society of London, Special Publication no. 95, p. 143–154.

Myers, JS, 1997, Byro, WA Sheet SG 50-10 (2nd edition): Geological Survey of Western Australia, 1:250 000 Geological Series.

Myers, JS, and Williams, IR, 1985, Early Precambrian crustal evolution at Mount Narryer, Western Australia: Precambrian Research, v. 27, p. 153–163.

Nelson, DR, 1997, Evolution of the Archaean granite–greenstone terranes of the Eastern Goldfields, Western Australia: SHRIMP U–Pb zircon constraints: Precambrian Research, v. 83, p. 57–81.

Nelson, DR, 2001, 169003: vesicular rhyolite, Carron Hill; Geochronology dataset 170, in Compilation of geochronology data, June 2007 update: Geological Survey of Western Australia.

Nelson, DR, 2002a, 169067: quartz-chlorite schist, Pincher Well; Geochronology dataset 105, *in* Compilation of geochronology data, June 2007 update: Geological Survey of Western Australia.

Nelson, DR, 2002b, 169074: quartzite, Kohler Bore; geochronology dataset 110, *in* Compilation of geochronology data, June 2007 update: Geological Survey of Western Australia.

Nelson, DR, 2002c, 169070: foliated biotite granodiorite, Coomb Bore; Geochronology dataset 108, *in* Compilation of geochronology data, June 2007 update: Geological Survey of Western Australia.

Nelson, DR, 2004a, 165364: quartz–feldspar porphyry, Bulchina; Geochronology dataset 57, *in* Compilation of geochronology data, June 2007 update: Geological Survey of Western Australia.

Nelson, DR, 2004b, 165365: foliated biotite granodiorite, Coomb Bore; Geochronology dataset 218, *in* Compilation of geochronology data, June 2007 update: Geological Survey of Western Australia.

Nelson, DR, 2005a, 169075: quartzite, Kohler Bore; geochronology dataset 578, *in* Compilation of geochronology data, June 2007 update: Geological Survey of Western Australia.

Nelson, DR, 2005b, 178064: coarse sandstone, The Stock Well; geochronology dataset 591, *in* Compilation of geochronology data, June 2007 update: Geological Survey of Western Australia.

Nelson, DR, 2005c, 165364: quartz–feldspar porphyry, Bulchina; Geochronology dataset 532, *in* Compilation of geochronology data, June 2007 update: Geological Survey of Western Australia.

Nelson, DR, 2005d, 178056: foliated hornblende monzogranite, Coomb Bore; Geochronology dataset 583, *in* Compilation of geochronology data, June 2007 update: Geological Survey of Western Australia.

Nelson, DR, Robinson, BW, and Myers, JS, 2000, Complex geological histories extending for ≥4.0 Ga deciphered from xenocryst zircon microstructures: Earth and Planetary Science Letters, v. 181, p. 89–102.

Nesbitt, RW , Sun, SS, and Purvis, AC, 1979, Komatiites: geochemistry and genesis: Canadian Mineralogist, v. 17, p. 165–186.

Nutman, AP, Bennett, VC, Kinny, PD, and Price, R , 1993, Large-scale crustal structure of the northwestern Yilgarn Craton, Western Australia: evidence from Nd isotopic data and zircon geochronology: Tectonics, v. 12, p. 971–981.

Nutman, AP, Kinny, PD, Compston, W, and Williams, IS, 1991, SHRIMP U–Pb zircon geochronology of the Narryer Gneiss Complex, Western Australia: Precambrian Research, v. 52, p. 275–300.

Occhipinti, SA, Sheppard, S, Passchier, C, Tyler, IM, and Nelson, DR , 2004, Palaeoproterozoic crustal accretion and collision in the southern Capricorn Orogen: the Glenburgh Orogeny: Precambrian Research, v. 128, p. 237–255.

Passchier, CW, 1994, Structural geology across a proposed Archaean terrane boundary in the eastern Yilgarn Craton, Western Australia: Precambrian Research, v. 68, p. 43–64.

Perring, CS, Barnes, SJ, and Hill, RET, 1996, Geochemistry of komatiites from Forrestania, Southern Cross Province, Western Australia: Evidence for crustal contamination: Lithos, v. 37, p. 181–197.

Pidgeon, RT, and Hallberg, JA, 2000, Age relationships in supracrustal sequences in the northern part of the Murchison Terrane, Archaean Yilgarn Craton, Western Australia: a combined field and zircon U–Pb study: Australian Journal of Earth Sciences, v. 47, p. 153–165.

Pidgeon, RT, and Wilde, SA, 1990, The distribution of 3.0 Ga and 2.7 Ga volcanic episodes in the Yilgarn Craton of Western Australia: Precambrian Research, v. 48, p. 309–325.

Pidgeon, RT, and Wilde, SA, 1998, The interpretation of complex zircon U–Pb systems in Archaean granitoids and gneisses from the Jack Hills, Narryer Gneiss Terrane, Western Australia: Precambrian Research, v. 91, p. 309–332.

Pirajno, F, 2005, Hydrothermal processes associated with meteorite impact structures: evidence from three Australian examples and implications for economic resources: Australian Journal of Earth Sciences, v. 52, p. 587–605.

Rattenbury, MS, 1993, Stop 5. Copperfield granite, *in* Kalgoorlie 93 — an international conference on crustal evolution, metallogeny and exploration in the Eastern Goldfields, Excursion Guide *compiled by* PR Williams and JA Haldane: Australian Geological Survey Organisation, Record 1993/53, p. 43.

Reed Resources Ltd, 2007, Reed Resources Ltd, Australia, viewed 5 May 2007, <http://www.reedresources.com>.

Riganti, A, 2003, Geology of the Everett Creek 1:100 000 sheet: Geological Survey of Western Australia, 1:100 000 Geological Series Explanatory Notes, 39p.

Schiøtte, L, and Campbell, IH, 1996, Chronology of Mount Magnet granite–greenstone terrain, Yilgarn Craton, Western Australia: implications for field based predictions of the relative timing of granitoid emplacement: Precambrian Research, v. 78, p. 237–260.

Sharpe, R, and Gemmell, JB, 2002, The Archean Cu–Zn magnetite-rich Gossan Hill volcanic-hosted massive sulfide deposit, Western

Australia: genesis of a multistage hydrothermal system: Economic Geology, v. 97, p. 517–539.

Spaggiari, CV, 2006, Interpreted bedrock geology of the northern Murchison Domain, Youanmi Terrane, Yilgarn Craton: Geological Survey of Western Australia, Record 2006/10, 19p.

Spaggiari, CV, 2007a, Structural and lithological evolution of the Jack Hills greenstone belt, Narryer Terrane, Yilgarn Craton, Western Australia: Geological Survey of Western Australia, Record 2007/3.

Spaggiari, CV, 2007b, The Jack Hills greenstone belt, Western Australia, Part 1: Structural and tectonic evolution over >1.5 Ga: Precambrian Research, v. 155, p. 204–228.

Spaggiari, CV, Pidgeon, RT, and Wilde, SA, 2007, The Jack Hills greenstone belt, Western Australia, Part 2: Lithological relationships and implications for the deposition of >4.0 Ga detrital zircons: Precambrian Research, v. 155, p. 261–286.

Spaggiari, CV, Wartho, J-A, Wilde, SA, and Bodorkos, S, in prep., Proterozoic development of the northwestern margin of the Archean Yilgarn Craton: Precambrian Research.

Sproule, RA, Lesher, CM , Ayer, JA , Thurston, PC, and Herzberg, CT, 2002, Spatial and temporal variations in the geochemistry of komatiites and komatiitic basalts in the Abitibi greenstone belt: Precambrian Research, v. 115, p. 153–186.

Stewart, AJ, Williams, IR, and Elias, M, 1983, Youanmi, WA: Australia BMR and Geological Survey of Western Australia, 1:250 000 Geological Series Explanatory Notes, 58p.

Swager, CP, 1990, Locality 32, Ghost Rocks, basalt and komatiite, *in* Third International Archaean Symposium, Excursion Guidebook *edited by* SE Ho, JE Glover, JS Myers, and JR Muhling: Geology Department and University Extension, University of Western Australia, Publication no. 21, p. 287–288.

Swager, CP, 1994, Geology of the Menzies 1:100 000 sheet (and adjacent Ghost Rocks area): Geological Survey of Western Australia, 1:100 000 Geological Series Explanatory Notes, 31p.

Swager, CP, 1997, Tectono-stratigraphy of late Archaean greenstone terranes in the southern Eastern Goldfields, Western Australia: Precambrian Research, v. 83, p. 11–42.

Swager, CP, Goleby, BR, Drummond, BJ, Rattenbury, MS, and Williams, PR, 1997, Crustal structure of granite–greenstone terranes in the Eastern Goldfields, Yilgarn Craton, as revealed by seismic profiling: Precambrian Research, v. 83, p. 43–56.

Swager, CP, Griffin, TJ, Witt, WK, Wyche, S, Ahmat, AL, Hunter, WM, and McGoldrick, PJ, 1995, Geology of the Archaean Kalgoorlie Terrane — an explanatory note: Geological Survey of Western Australia, Report 48, 26p.

Timms, N, 2006, Geological Mapping Report: Yaloginda Area: Mercator Gold Australia Pty Ltd, 91p (unpublished).

Tingey, RJ, 1985, Sandstone, WA: Australia BMR and Geological Survey of Western Australia, 1:250 000 Geological Series Explanatory Notes, 37p.

Troy Resources NL, 2007, Troy Resources NL viewed 6 June 2007 <http://www.try.com.au>.

Tyler, IM, and Hocking, RM, 2001, Tectonic units of Western Australia (scale 1:2 500 000): Geological Survey of Western Australia.

Wang, Q, Beeson, J, and Campbell, IH, 1998a, Granite–greenstone zircon U–Pb chronology of the Gum Creek greenstone belt, Southern Cross Province, Yilgarn Craton: Tectonic Implications, *in* Structure and evolution of the Australian continent *edited by* J Braun, JC Dooley, BR Goleby, RD Van Der Hilst, and CT Klootwijk: American Geophysical Union, Geodynamics Series, v. 26, p. 175–186.

Wang, Q, Schiøtte, L, and Campbell, IH, 1998b, Geochronology of supracrustal rocks from the Golden Grove area, Murchison Province, Yilgarn Craton, Western Australia: Australian Journal of Earth Sciences, v. 45, p. 571–577.

Ward, HJ, 1975, Barrambie iron–titanium–vanadium deposit, *in* Economic geology of Australia and Papua New Guinea, Volume I. Metals *edited by* CL Knight: Australasian Institute of Mining and Metallurgy, Monograph 5, p. 201–207.

Watkins, KP, and Hickman, AH, 1990, Geological evolution and mineralization of the Murchison Province Western Australia: Geological Survey of Western Australia, Bulletin 137, 267p.

Weinberg, RF, Moresi, L, and Van Der Borgh, P, 2003, Timing of deformation in the Norseman–Wiluna Belt, Yilgarn Craton, Western Australia: Precambrian Research, v. 120, p. 219–239.

Wiedenbeck, M, and Watkins, KP, 1993, A time scale for granitoid emplacement in the Archean Murchison Province, Western Australia, by single zircon geochronology: Precambrian Research, v. 61, p. 1–26.

Wilde, SA, Middleton, MF, and Evans, BJ, 1996, Terrane accretion in the southwest Yilgarn Craton: evidence from a deep seismic crustal profile: Precambrian Research, v. 78, p. 179–196.

Wilde, SA, and Pidgeon, RT, 1990, Geology of the Jack Hills metasedimentary rocks, *in* Third International Archaean Symposium, Perth, Excursion Guidebook *edited by* SE Ho, JE Glover, JS Myers, and JR Muhling: The University of Western Australia, Geology Department and University Extension, Publication 21, p. 82–95.

Wilde, SA, Valley, JW, Peck, WH, and Graham, CM, 2001, Evidence from detrital zircons for the existence of continental crust and oceans on Earth 4.4 Gyr ago: Nature, v. 409, p. 175–178.

Williams. IR, and Myers, JS, 1987, Archaean geology of the Mount Narryer region, Western Australia: Geological Survey of Western Australia, Report 22, 32p.

Williams, IR, Walker, IM, Hocking, RM, and Williams, SJ, 1983, Byro, WA (1st edition): Geological Survey of Western Australia, 1:250 000 Geological Series Explanatory Notes, 27p.

Williams, PR, and Currie, KL, 1993, Character and regional implications of the sheared Archaean granite–greenstone contact near Leonora, Western Australia: Precambrian Research, v. 62, p. 343–367.

Williams, PR, Rattenbury, MS, and Witt, WK (compilers), 1993, A field guide to the felsic igneous rocks of the northeast Eastern Goldfields Province, Western Australia: core complexes, batholiths, plutons and supracrustals, *in* Kalgoorlie 93 — an international conference on crustal evolution, metallogeny and exploration in the Eastern Goldfields, Excursion Guide *compiled by* PR Williams and JA Haldane: Australian Geological Survey Organisation, Record 1993/53, p. 23–74.

Williams, SJ, 1986, Geology of the Gascoyne Province Western Australia: Geological Survey of Western Australia, Report 15, 85p.

Wingate, MTD, and Bodorkos, S, 2007a, 184112: volcaniclastic sandstone, Ram Bore; Geochronology dataset 702, *in* Compilation of geochronology data: Geological Survey of Western Australia.

Wingate, MTD, and Bodorkos, S, 2007b, 183921: volcaniclastic sandstone, Lordy Bore; Geochronology dataset 710, *in* Compilation of geochronology data: Geological Survey of Western Australia.

Wingate, MTD, and Bodorkos, S, 2007c, 178105: porphyritic andesite, Woolgra Bore; Geochronology dataset 708, *in* Compilation of geochronology data: Geological Survey of Western Australia.

Wingate, MTD, and Bodorkos, S, 2007d, 184107: metamorphosed quartz sandstone, Christmas Bore; Geochronology dataset 678, *in* Compilation of geochronology data: Geological Survey of Western Australia.

Wingate, MTD, and Bodorkos, S, 2007e, 178113: gabbro sill, Kurrajong Bore; Geochronology dataset 779, *in* Compilation of geochronology data: Geological Survey of Western Australia.

Wingate, MTD, and Bodorkos, S, 2007f, 178101: biotite monzogranite, Chunderloo Bore; Geochronology dataset 704, *in* Compilation of geochronology data: Geological Survey of Western Australia.

Wingate, MTD, and Bodorkos, S, 2007g, 178102: biotite–hornblende tonalite, Finger Post Bore; Geochronology dataset 705, *in* Compilation of geochronology data: Geological Survey of Western Australia.

Wingate, MTD, and Compston, W, 2000, Crystal orientation effects during ion microprobe U–Pb analysis of baddeleyite: Chemical Geology, v. 168, p. 75–97.

Wingate, MTD, Pirajno, F, and Morris, PA, 2004, Warakurna large igneous province: a new Mesoproterozoic large igneous province in west-central Australia: Geology, v. 32, p. 105–108.

Winnal, NJ, Hibberd, TJ, Thynne, DS, and Wahdan, E, 1998, Some gold deposits of the Bluebird, Nannine and Cuddingwarra goldfields, Murchison district, *in* Geology of Australian and Papua New Guinean Mineral Deposits *edited by* DA Berkman and DH Mackenzie: The Australasian Institute of Mining and Metallurgy, Melbourne, p. 111–118.

Witt, WK, 1994, Geology of the Bardoc 1:100 000 sheet, Geological Survey of Western Australia, 1:100 000 Geological Series Explanatory Notes, 50p.

Witt, WK, 1998, Geology and mineral resources of the Ravensthorpe and Cocanarup 1:100 000 sheets: Geological Survey of Western Australia, Report 54, 152p.

Witt, WK, 1999, The Archaean Ravensthorpe Terrane, Western Australia: synvolcanic Cu–Au mineralization in a deformed island arc complex: Precambrian Research, v. 96, p. 143–181.

Wyche, S, 1999, Geology of the Mulline and Riverina 1:100 000 sheets: Geological Survey of Western Australia, 1:100 000 Geological Series Explanatory Notes, 28p.

Wyche, S, 2003, Menzies, WA (2nd edition): Geological Survey of Western Australia, 1:250 000 Geological Series Explanatory Notes, 38p.

Wyche, S, in prep., Evidence of pre-3100 Ma crust in the Youanmi and Southwest Terranes, and Eastern Goldfields Superterrane, of the Yilgarn Craton, *in* Earth's Oldest Rocks *edited by* MJ Van Kranendonk, RH Smithies, and VC Bennett: Elsevier BV, Developments in Precambrian Geology, v. 15.

Wyche, S, Nelson, DR, and Riganti, A, 2004, 4350–3130 Ma detrital zircons in the Southern Cross Granite–Greenstone Terrane, Western Australia: implications for the early evolution of the Yilgarn Craton: Australian Journal of Earth Sciences, v. 51, p. 31–45.

Yeats, CJ, McNaughton, NJ, and Groves, DI, 1996, SHRIMP U–Pb geochronological constraints on Archean volcanic-hosted massive sulfide and lode gold mineralization at Mount Gibson, Yilgarn Craton, Western Australia: Economic Geology, v. 91, p. 1354–1371.

WYCHE ET AL.

A Geological traverse across the northern Yilgarn Craton — a field guide

RECORD 2007/20

This Record is published in digital format (PDF) and is available online at: www.doir.wa.gov.au/GSWA/publications. Laser-printed copies can be ordered from the Information Centre for the cost of printing and binding.

Further details of geological publications and maps produced by the Geological Survey of Western Australia can be obtained by contacting:

Information Centre
Department of Industry and Resources
100 Plain Street
East Perth WA 6004
Phone: (08) 9222 3459 Fax: (08) 9222 3444

www.doir.wa.gov.au/GSWA/publications